KONINKLIJKE NEDERLANDSE AKADEMIE VAN WETENSCHAPPEN

PROCEEDINGS

SERIES B

PHYSICAL SCIENCES

VOLUME LXIV - No. 3

NORTH-HOLLAND PUBLISHING COMPANY - AMSTERDAM - 1961

JOURNAL DE PHYSIQUE
10, Rue Vauquelin
PARIS V

24 OCT 1961

The complete Proceedings consist of three Series, viz.:

SERIES A: MATHEMATICAL SCIENCES

SERIES B: PHYSICAL SCIENCES

SERIES C: BIOLOGICAL AND MEDICAL SCIENCES

Articles for these Series cannot be accepted unless formally communicated for publication by one of the members of the Royal Neth. Academy of Sciences.

TECTONICS OF A METAGABBRO LACCOLITH IN THE ADIRONDACK MTS., AND ITS SIGNIFICANCE IN DETERMINING TOP AND BOTTOM OF A METAMORPHIC SERIES

BY

D. DE WAARD

(Communicated at the meeting of February 25, 1961)

ABSTRACT

A series of high-grade metamorphic, metasedimentary, Precambrian rocks in the southwestern Adirondack Mountains is folded to a closed, overturned 'downfold'. The determination of whether the downfold represents a syncline or the plunging front of an anticline depends on the determination of the direction of top and bottom in the folded rock series. One small metagabbro mass has the plano-convex shape of a laccolith; its shape enables determination of top and bottom of the intruded series prior to the folding and indicates that the nature of the downfold is a syncline.

A tectonic analysis is given of the laccolith and its contact relations. Using the axial symmetry of a laccolithic mass a composite section is constructed normal to the foliation to illustrate the possible shape and the position of the gabbro laccolith in the metamorphic series.

Introduction

The object of this note is to demonstrate the use of a laccolithic structure in the determination of top and bottom in a folded series of metamorphic rocks. The series in question consists of a succession of sheets of various gneisses, marbles and amphibolites, with sills and small bodies of metadiabase and metagabbro. The series is folded, almost isoclinally, into an overturned fold with an axial plane dipping about 35° N. Detailed mapping revealed a structure which can be described as a "down fold" or a "synform" [1]); depending on top and bottom direction in the sheets the structure is either a syncline, the simplest interpretation, or the plunging front of an anticiline, a not uncommon type of structure in Alpine tectonics. Too little is known of the geologic relations in this region to indicate which of the two types of structure might be expected; the synclinal or anticlinal nature of the down fold can be determined only by ascertaining the top and bottom directions in the rock series.

In metamorphic rocks, features which indicate top and bottom of a series are mainly limited to the inherited structures of sedimentary and

1) J. G. Ramsay, Superimposed folding at Loch Monar, Inverness-shire and Ross-shire, Q. J. Geol. Soc. London, 113, 1958, 271–307.

igneous origin. SHROCK [1]) lists a number of such palimpsest structures, none of which were observed in this area of high-grade metamorphism. Not mentioned by SHROCK is the shape of an intrusive body as a possible indication for top and bottom of the intruded series.

Most of the intrusive bodies in the area in question are diabase sills; metagabbro occurs in thicker sills, in lenticular structures, and in one body which has a short and thick, plano-convex shape with concordant contacts, located in the north limb of the down fold. Absence of orientation in the blastophytic texture of the metadiabase and metagabbro, except

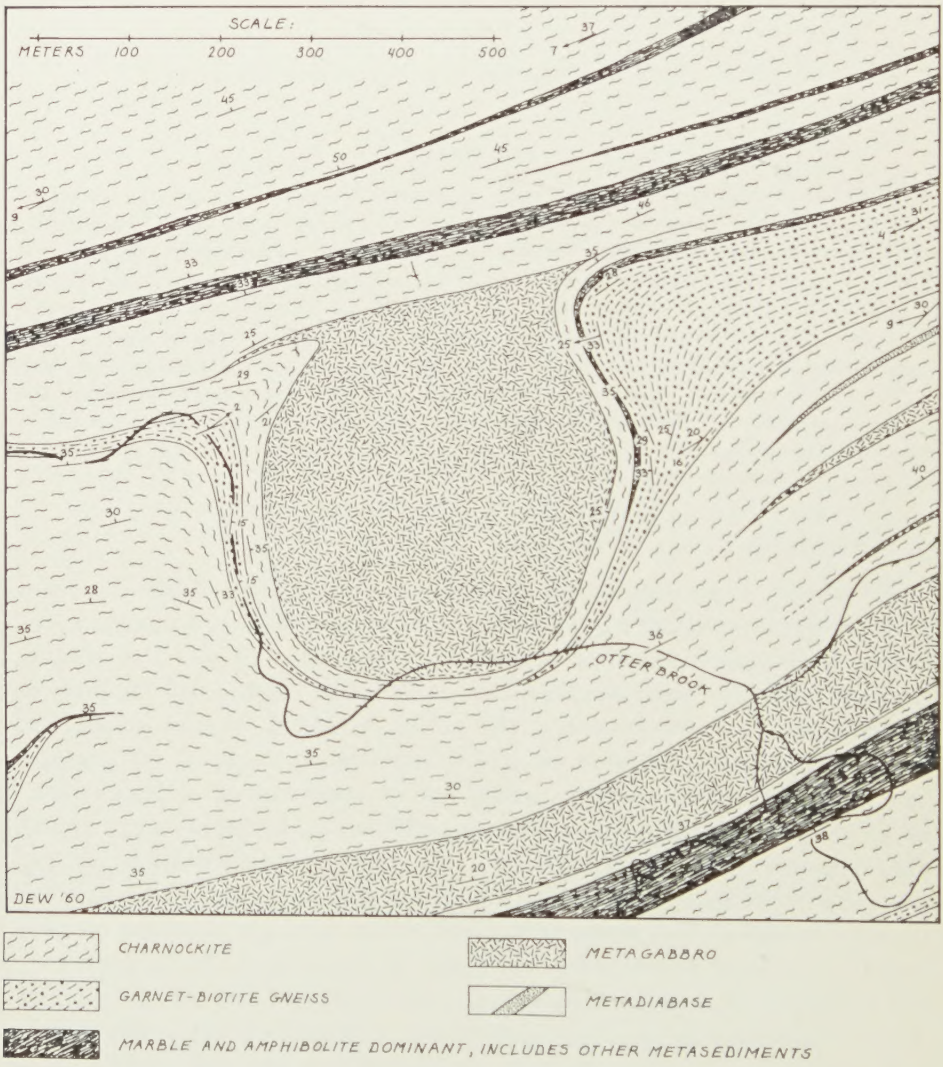

Fig. 1. Geologic map of the metagabbro laccolith. The topography of this area is shown in map, fig. 2. Strike and dip symbols indicate the orientation of foliation planes; arrows refer to linear mineral parallelism.

[1]) R. R. SHROCK, Sequence in layered rocks, McGraw-Hill, New York, 1948.

locally such as along contacts, indicates that little internal deformation took place in the rock during metamorphism, and that the original shape of the intrusions largely has been preserved. Assuming (1) that the plano-convex gabbro intrusion is a true laccolith, and (2) that the convex side of a laccolith always represents the top of the intrusion, then the position of this structure indicates top and bottom directions in the series which, in turn, enables the determination of the synclinal or anticlinal nature of the down fold.

The laccolith

The gabbro laccolith is located at 43° 38′ 29″ N, 74° 41′ 25″ W, in the Adirondack Mountains, West Canada Lakes quadrangle, New York. Topographically, the outcrop of gabbro stands out conspicuously as a round hill amidst a strongly linear topography controlled by the northward dipping series of gneisses.

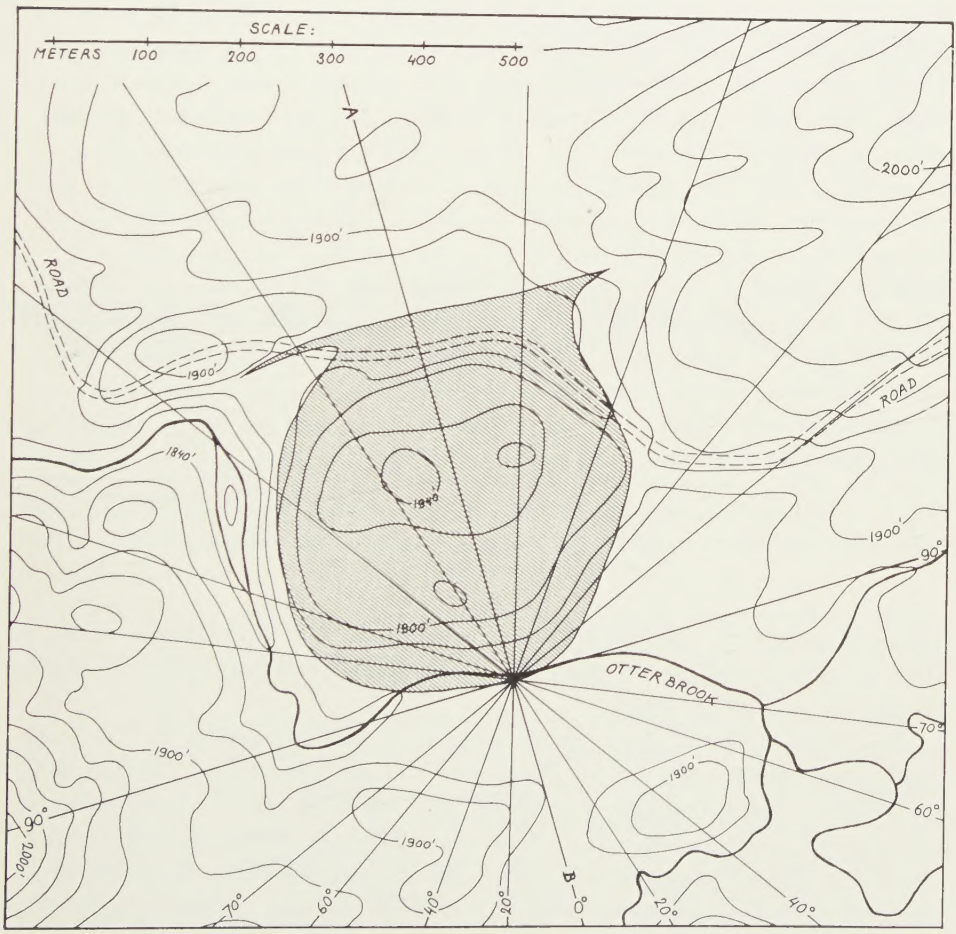

Fig. 2. Topographic expression of the metagabbro laccolith (shaded area). Radial lines indicate the location of sections used to construct composite section, fig. 6; section A–B is shown in fig. 3.

A detailed geologic map (fig. 1) illustrates the structural relations of the rocks in this area. The foliation planes of the rocks NW of the gabbro body appear little or not affected by the presence of the intrusion; anywhere else the foliation tends to conform to the orientation of the gabbro contact, and to diverge from the general trend of the foliation in the area. Except for the NW contact the foliation planes of the gneisses near the gabbro border dip between 25° and 35° towards the center of the intrusion, which suggests the shape of the gabbro mass approximates a segment of a sphere. The NW contact is straight and parallel to the foliation of the gneiss, which indicates a flat contact plane dipping about 35° N. Section, fig. 3, illustrates the shape of the remaining segment of

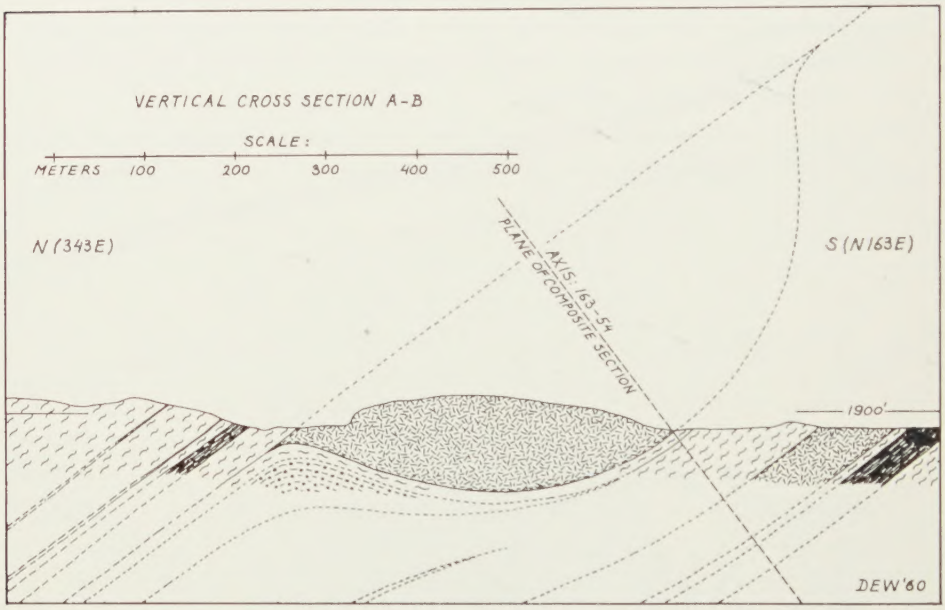

Fig. 3. Section A–B across the laccolith. Orientation and location of the symmetry axis was determined to construct a composite section (fig. 6) perpendicular to this section and containing the axis.

this plano-convex gabbro mass as based upon the contact relations in the outcrop; a possible reconstruction of the removed part of the laccolith is shown in broken lines.

Intrusion occurred prior to the period of metamorphism in the area, and, most likely, prior to the folding of the intruded beds. The shape of a laccolith is most simply explained by a doming-up of overlying beds during the intrusion at a time that the intruded strata were in normal, probably flat-lying position [1]). Since the convex side of a laccolith is in contact with the overlying beds, the present position of the metagabbro

[1]) G. K. Gilbert, Report on the geology of the Henry Mountains, U.S. Geographical and Geological Survey of the Rocky Mountains region, Washington, 1877.

mass is overturned in the northern limb of the down fold, and the downfold, therefore, is a syncline.

Tectonic analysis

Diagrams, fig. 4 and 5, illustrate the effect of the convex contact of the laccolith on the orientation of adjacent foliation planes. Poles of unaffected foliation planes (dots) are concentrated around an average of 253–36; poles of foliation planes from near the convex contact (circles) are scattered, towards and around the center of the diagram. Similarly, unaffected lineations (crosses) are grouped together while those found near the gabbro contact (asterisks) deviate to various degrees from the average.

Diagram, fig. 5, attempts to elucidate the deviation of linear and planar structures as shown in fig. 4. From the average orientation of unaffected foliation planes, S, rotation occurs radially; small circles show the degree of rotation, and arrows indicate the sense of rotation of the poles of foliation planes. The axes of rotation are situated in the great circle normal to S, which is the average foliation plane, and to the flat base of the laccolith. Lineations, being lines in foliation planes, rotate with the foliation from the average, B, in paths along small circles, some of which are shown and marked a, b, c, d, e, and f, corresponding to the similarly marked planes and axes of rotation of the foliation. A dashed line indicates the effect of 60° rotation of B along various paths.

The dispersion of poles as shown in fig. 4 corresponds to the shaded area in diagram, fig. 5. The restriction of the rotation to this area is, of course, due to the fact that data are obtained from the present outcrop which is only one section of the laccolith. Other sections would show different degrees and other directions of rotation. In the present section a maximum of rotation is observed of 55° (c, d, and e) about rotation axes oriented between NE–SW and E–W. There is a corresponding rotation of linear structures.

Composite section

Construction of composite sections is based upon the symmetry of the structure, and on the assumption that this symmetry persists throughout the structure. Composite sections serve to give a more complete picture of the structure by projecting the observed surface data on the plane of the section in accordance with the symmetry properties of the structure in question. The symmetry of the gabbro body as observed at the surface in the shape of the contact and contact relations point to the axial symmetry of a laccolith, the principle of which is shown in diagram, fig. 5. Transfer of surface data to the plane of the composite section is based upon the symmetry property that all sections which contain the axis of symmetry are identical. Since contact relations are concordant this also holds largely for the adjacent wall rock.

Fig. 4. Pole diagram illustrating the observed effect of the proximity of the convex contact on the orientation of foliation planes and mineral lineations in the area. Poles of unaffected foliation planes (dots) and lineations (crosses) are found in groups; poles of foliation planes from localities near the contact (circles), and the lineations from those localities (asterisks) are dispersed by rotation. (Equal area projection on the lower hemisphere).

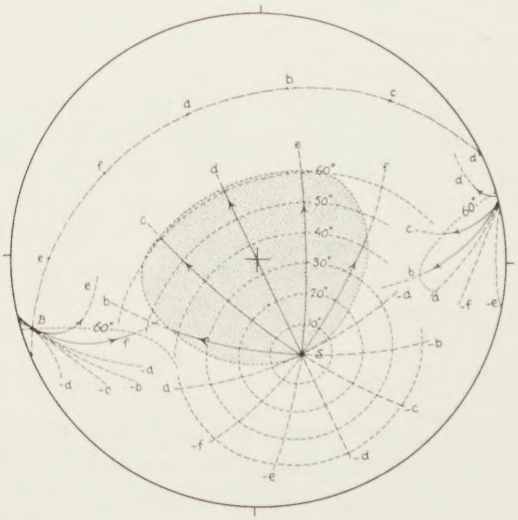

Fig. 5. Analysis of diagram, fig. 4. Foliation planes near the convex contact of the laccolith are rotated from the unaffected average, S, about axes of rotation situated in the plane normal to S, along paths radiating from S, in a sense indicated by arrows, and to the amount shown by small circles. Similarly, lineations in the foliation plane rotate along paths radiating from the unaffected average, B; an amount of 60° is indicated by the intersecting dashed line. Due to the restriction of data to the present surface (which is one section through the laccolith), the sense and the degree of rotation which can be observed is restricted to the shaded area in the diagram, and is indicated by full-drawn lines and arrows. The observed maximum deviation of 55° means that a maximum angle of 55° is found between a contact on the convex side and the floor of the laccolith.

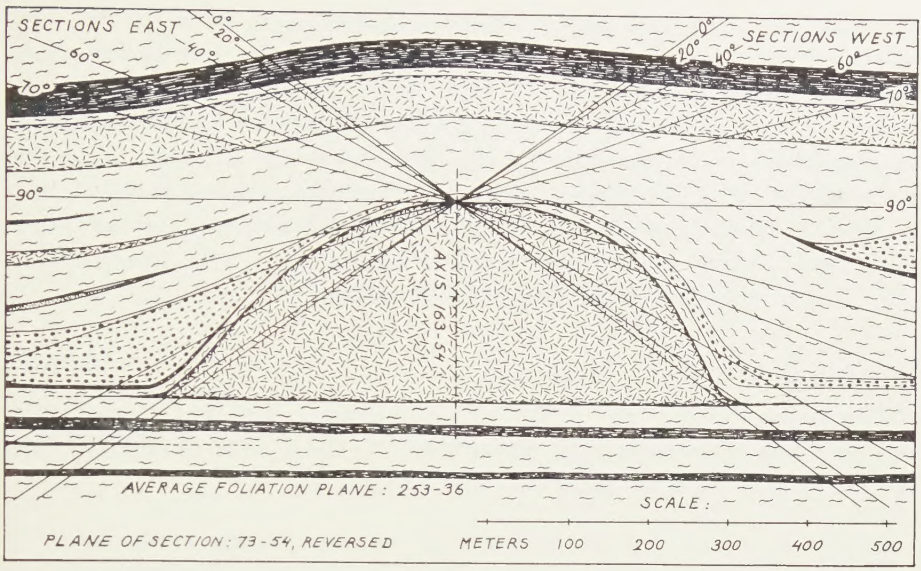

Fig. 6. Composite section across the laccolith. Surface data along sections (locations shown in map, fig. 2) which contain the axis of symmetry are projected by rotation on the plane of the composite section which is perpendicular to the average foliation plane with a strike parallel to that of the foliation. The section is inverted to demonstrate the constructed shape and the contact relations of the laccolith in the position of intrusion.

The location of the symmetry axis was found by using the orientations of foliation planes near the contacts to determine the radii and centers of circular sections through the laccolith at right angles to the axis. The surface geology of each section shown by lines radiating from the symmetry axis in map, fig. 2, are combined in fig. 6, and sketched in full to a composite section which, in restored position, illustrates the possible shape of the laccolith, and its position in the series of metamorphic rocks.

The section demonstrates the different plastic behavior of the various rock kinds during metamorphism and deformation. The laccolith, apparently, stood out rigidly during deformation, pushing away the more mobile material in the layers above it. Particularly the biotite-garnet gneiss appears to have the tendency to be squeezed out near the top of the laccolith and to accumulate alongside the gabbro mass.

Geologic history

The sequence of events in the area can be summarized as follows:

1. Sedimentation of alternating beds of various chemical composition corresponding largely to that of charnockite, biotite-garnet gneiss, marble, and amphibolite.

2. Intrusion during the period of sedimentation of the gabbro laccolith, lenticular gabbro masses, and diabase sills.

3. Period of metamorphism and orogeny. Metamorphism of sediments

to charnockite, biotite-garnet gneiss, marble, and amphibolite, and metamorphism of the basic intrusives to metagabbro and metadiabase. Synmetamorphic folding of the rock series; development of foliation parallel to the stratification, formation of a mineral lineation parallel to the fold axis of the syncline. A rigid structural behavior of larger metagabbro and metadiabase masses; development of mineral orientation in smaller masses, and locally along shear zones and contacts of larger intrusions. During folding the laccolith rotated 144° with the northern limb of the syncline to an overturned position.

Acknowledgment

This paper forms part of the results of tectonic-petrologic research in the southwestern Adirondack Mountains; the project is financially supported by the National Science Foundation.

Department of Geology,
Syracuse University, Syracuse, N.Y.

FROSTING OF QUARTZ GRAINS

BY

PH. H. KUENEN [1]) AND W. G. PERDOK [2])

(Communicated at the meeting of March 25, 1961)

Abstract

It is shown that the frosted appearance of many quartz grains is not produced by circular impact markings of a few microns, but by diffraction of light on minute irregularities. Impact cones on rounded quartz grains are much larger, nearly one tenth of the grain diameter. Wind action gives coarse frosting on protruding parts of a grain, but this is subdued by the action of dew or under water. Aqueous transportation can also frost protruding parts. Reaction solution (etching) tends to produce frosting, as does alternate wetting and drying by dew. Non-reaction solution (physical solution) tends to round and de-frost, and immersion in a saturated solution can also cause de-frosting by regrowth.

Introduction

Most grains of quartz sand are frosted, if only slightly, and in the desert the surface of the particles is usually as opaque as ground glass. Most authors have attributed this surface finish to mechanical attack, by scour under water and more especially to eolian impacting. However, SORBY (1880), RUSSELL (1939), TRICART (1958) and others have quoted cases in which chemical corrosion must have been responsible. Polishing is generally believed to result from mechanical rubbing under water. In earlier papers one of us has pointed out that experimental frosting in a wind tunnel produces a coarser finish than natural frost and that it is possible to polish sand by rolling in dry condition, but that under variable conditions of rolling under water grains remain opaque (KUENEN, 1959, 1960). The conclusion was drawn that both frosting and de-frosting must be attributed mainly to chemical causes.

This surmise was confirmed by noting the distribution of the surface finish over irregular or very small particles. Experimental mechanical polish or frost are both restricted to convexities of the surface, while hollow and even flat parts are left unchanged. In contrast, natural frost covers the entire grain uniformly, even in deep depressions. Besides, grains in the process of becoming de-frosted attain the same degree of transparency in concavities as on bulges. A weighty argument was found

[1]) Geological Institute, University of Groningen.

[2]) Institute for Crystal Physics, University of Groningen.

in the frosted surface of very small, entirely angular particles of $^1/_{20}$ millimetre occurring in many desert sands, for these have not undergone any detectable impact-abrasion. Alternate wetting by dew and drying was suggested as the cause of desert frosting, solution and deposition by under- and oversaturated ground water or river water can account for aqueous frosting as well as polishing.

In the present paper the nature of frosting is examined and its causes are dealt with briefly. A more extensive treatment will be given elsewhere.

Optical nature of frosting

Cailleux (1942), led by his conviction that frost is due to wind action, claimed that under powerful magnification the surface is seen to consist of minute impact scars of circular or linear shape of 5 to 10 microns diameter. For several reasons this view cannot be upheld.

In the first place slight etching of quartz by HF produces a frost that presents the same picture under the microscope. In the second place the minute angular desert chips likewise show this circular pattern. In the third place in deep pits the frost is also visible as a circular marking. In the fourth place electron micrographs of frosted grains show complicated irregularities of 1 micron or less, but fail to reveal any circular shapes of a few microns diameter. In the fifth place obvious impact cones are found on many rounded river grains (probably with an earlier eolian history), but these are much larger and their size is related to the dimensions of the particle, just as with pebbles, namely roughly one tenth of the diameter.

The true cause of the circular pattern shown by frosted grains is the diffraction of the light by small surface irregularaties. It becomes even more marked when the surface is coated with a strongly reflecting bright film of aluminium.

Two kinds of solution

To understand the non mechanical origin of frosting and de-frosting it is necessary to realize that two entirely different processes are designated by the term "solution". One can be called *reaction solution* (etching or corrosion). It consists of a chemical reaction between a solid and a liquid, like the solution of $CaCO_3$ in HCl or quartz in HF. Evaporation will not cause the original solid to be reformed. The other process can be indicated by *non-reaction solution* (physical solution). It does not involve a chemical reaction and evaporation will cause the original solid to crystallize again (provided no complications are introduced).

The present authors claim that reaction solution tends to attack the solid over its entire surface especially at points where imperfections in the crystal lattice occur. Because of the exothermal nature of most such reactions, the local production of heat will favour attack in concavities. This should counteract to some extent lack of renewal of the solvent in

surface depressions [1]). On the other hand non-reaction solution will favour assault on angularities and crystallographic edges because here the faces of greatest solution velocity are potentially present, while in concavities the endothermal nature of the solution process as well as lack of renewal tend to decrease the rate of solution.

As a result of this difference, reaction solution will usually frost the surface of a grain, for instance in a weathering process, whereas non-reaction solution will tend to round and smooth a particle, for instance a grain of quartz in water undersaturated in silica, e.g. sea water.

In a saturated solution showing slight temperature variations, such as many rivers, sharp angularities will tend to dissolve while narrow cracks and indentures will tend to fill up because there is less renewal of the liquid in the latter.

In the case of dew the solution will round off the angularities and re-deposition will tend to fill in cracks and hollows thus softening the eolian mechanical roughness. But evidently it leaves a finely granulated (hence frosted) surface owing to the evaporation.

These various contentions were verified experimentally in a preliminary fashion, but a full confirmation will require a much more extensive treatment.

That physical solution can round a crystal is easily demonstrated and that industrial etching is usually attained by reaction solution is well known. The writers have shown that a mechanically frosted crystal of alum is smoothed and becomes transparent again by immersion in a saturated solution for a few hours.

The present authors have investigations under way on the quantitative significance of solution for the rounding of quartz grains, on the chemical and physical nature of quartz solution, and on the surface finish caused by various kinds of solution and deposition.

REFERENCES

Cailleux, A., Les actions éoliennes périglaciaires en Europe. Mém. Soc. géol. France, **46**, 1–176 (1942).

Kuenen, Ph. H., Sand — its origin, transportation, abrasion and accumulation. Geol. Soc. South Africa, du Toit Mem. Lect., **6**, 33 pp. (1959).

————, Experimental abrasion. 4: Eolian action. Journ. of Geol., **68**, 427–449 (1960).

Russell, R. D., Effects of transportation on sedimentary particles. Recent Marine Sediments, a symposium. Amer. Assoc. Petrol. Geol., 32–47 (1939).

Sorby, H. C., On the structure and origin of non-calcareous stratified rocks. Quart. Journ. Geol. Soc. London, **36**, Proc., 46–92 (1880).

Tricart, J., Méthode améliorée pour l'étude des sables. Rev. Géom. Dyn., **9**, 43–54 (1958).

[1]) A powerful attack of HF on quartz is apt to produce an etching pattern, a weak one a typical frosting.

STRESS RELEASE IN PLASTICALLY DEFORMED SILVERCHLORIDE BY ANNEALING

BY

R. G. DE LANGE [1]) AND W. G. BURGERS

(Communicated at the meeting of March 25, 1961)

Summary

It is shown that the reduction of the internal stresses in the individual crystallites of a strained silverchloride testpiece on annealing takes place at a different rate. Single crystals recover at a faster rate than polycrystalline testpieces.

1. *Introduction*

The glide mechanism of silverchloride crystals and the character and pattern of the internal stresses produced by plastic deformation was studied by NYE (1949) by means of the photoelastic effect. Recrystallized polycrystalline plates of silverchloride, deformed by simple extension, show birefringent bands in individual grains. By combining their direction with the orientation of the crystal lattice (deduced from a Laue photograph), NYE found that glide took place in ⟨110⟩ directions, the glide plane being not always a crystallographic plane, lying somewhere between {221} and {111}. This was interpreted as pointing to so-called "pencil glide" [2]).

Analysis of the pattern of birefringence led to the conclusion that the glide packets were bent about axes lying in the glide planes and contained a set of dislocations having either all the same sign or at least an excess of them.

Annealing of the deformed plates at a temperature of about 350–400° C brought about a general reduction of the birefringence, without altering its general distribution. As NYE points out, this might occur by a (partial) straightening-out of the glide-packets, involving a removal of the dislocations to their edges. While this is considered possible in deformed single crystals, it is thought that in a polycrystalline aggregate, where each grain is embedded by surrounding grains, such a process could not occur without setting up stresses in neighbouring grains, which would require definite atomic re-arrangements.

[1]) At present at the Metal Research Institute T.N.O.-Delft.

[2]) According to a recent paper by CARNAHAN, JOHNSTON, STOKES and LI (1961) pencil glide occurs only at relatively high temperatures (26° C and −72° C); at −196° C, however, deformation apparently takes place on fewer slip systems.

PLATE I

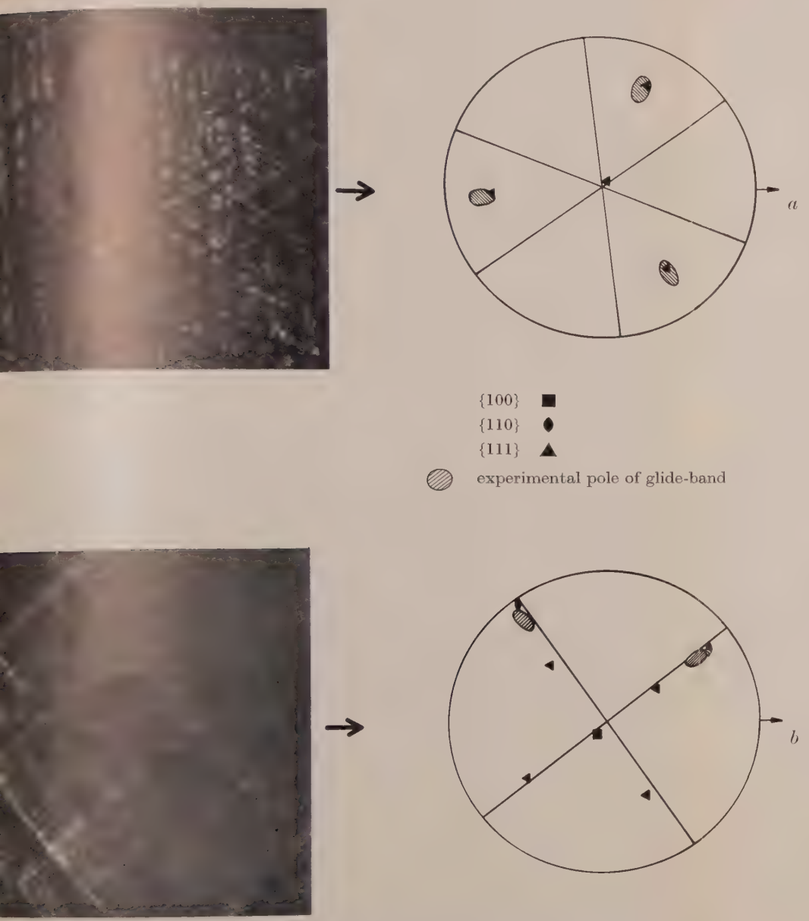

Fig. 1. Birefringent bands in plate-shaped silverchloride crystals after 6 % extension; crossed nicols. Direction of extension → (× 170).
a: normal to plate ∼ // ⟨111⟩: poles of glide-bands near {111}
b: normal to plate ∼ // ⟨100⟩: poles of glide-bands near {110}

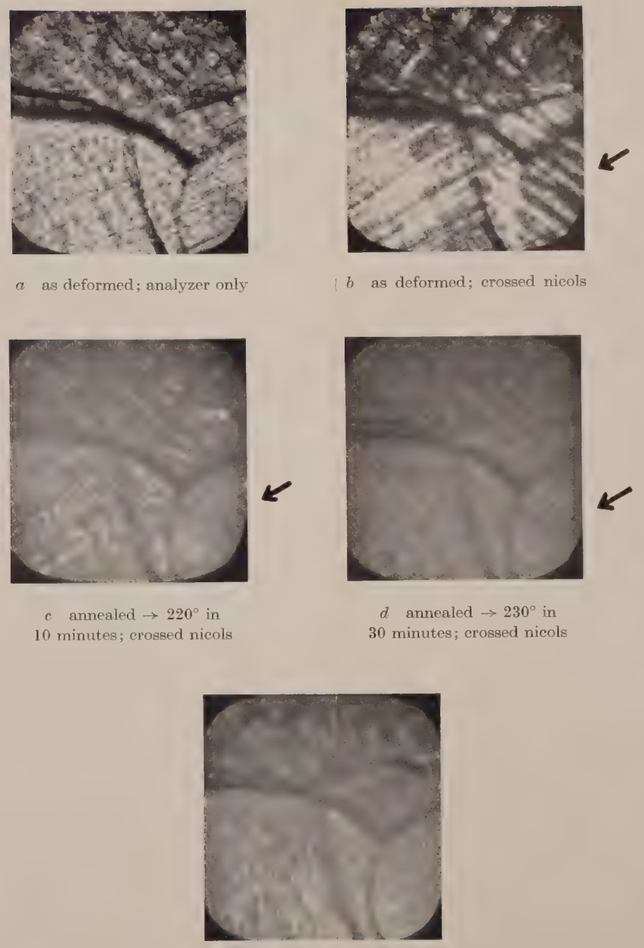

a as deformed; analyzer only

b as deformed; crossed nicols

c annealed → 220° in 10 minutes; crossed nicols

d annealed → 230° in 30 minutes; crossed nicols

e annealed → 350° in 75 minutes; crossed nicols

Fig. 2. Reduction of birefringence in plastically deformed silverchloride by annealing at increasing temperature. The reduction is different for individual crystallites: most pronounced for the crystallyte marked by the arrow. (∼ 80 ×).

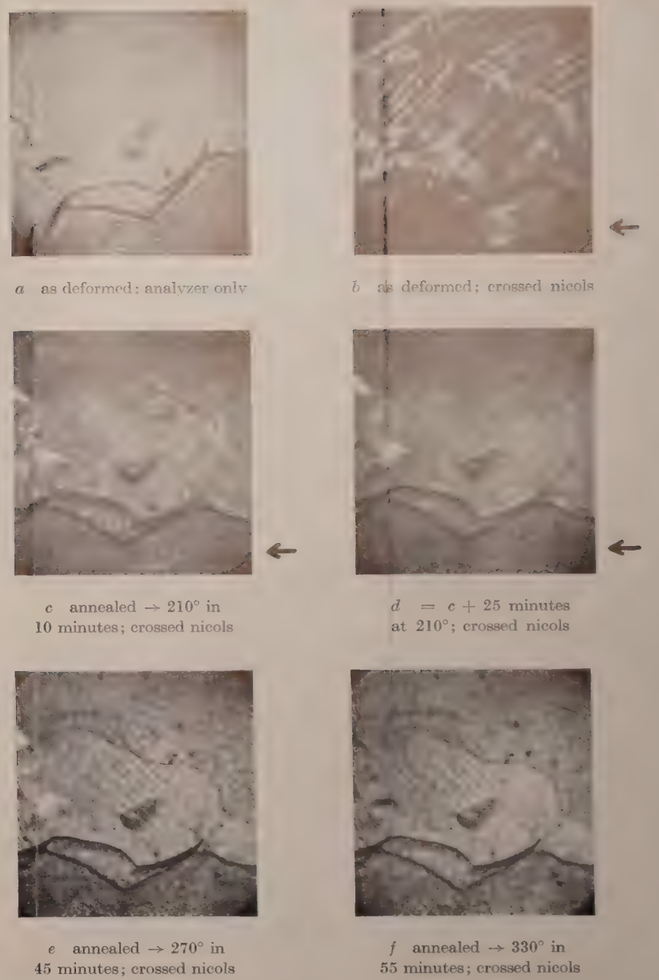

a as deformed; analyzer only

b as deformed; crossed nicols

c annealed → 210° in 10 minutes; crossed nicols

d = *c* + 25 minutes at 210°; crossed nicols

e annealed → 270° in 45 minutes; crossed nicols

f annealed → 330° in 55 minutes; crossed nicols

Fig. 3. Same as Fig. 2, other test-piece. (∼ 80 ×). (The white spots at the left on the photographs of Fig. 3 and at the bottom of those of Fig. 4 are due to a damaging effect of the tweezers used in handling the test-piece).

PLATE IV

a as deformed: analyzer only

b as deformed: crossed nicols

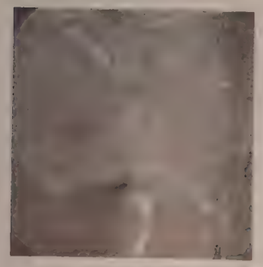

c annealed [illegible]
10 minutes; crossed nicols

d annealed [illegible]
20 minutes; crossed nicols

annealed [illegible]
minutes [illegible]

Fig. 4. Same test-piece as Fig. 3, for [illegible]
(Position in microscop[illegible])

PLATE V

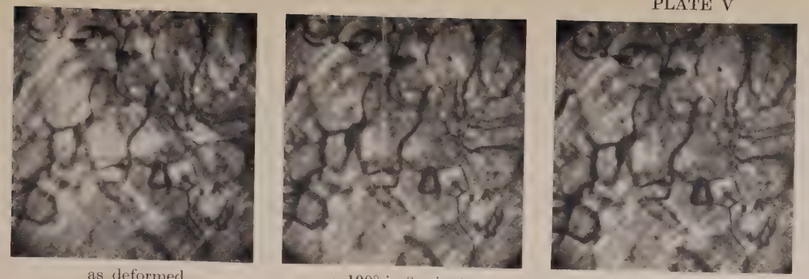

a
as deformed
→ 190° in 8 minutes
→ 200° in 11 minutes

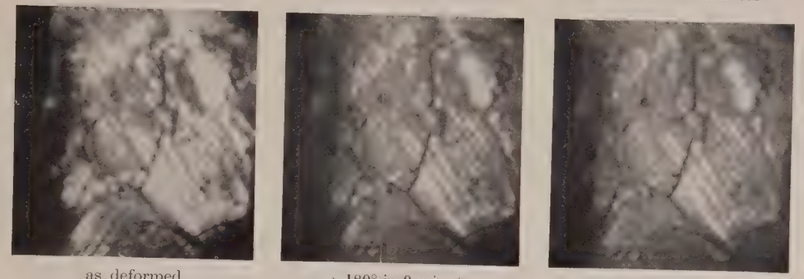

b
as deformed
→ 180° in 9 minutes
→ 200° in 15 minutes

c
as deformed
→ 170° in 4 minutes
→ 200° in 10 minutes

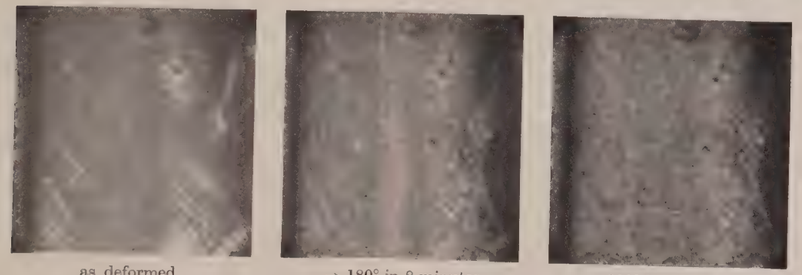

d
as deformed
→ 180° in 8 minutes
→ 200° in 11 minutes

Fig. 5. Influence of crystalsize on the reduction of stress birefringence in strained silverchloride due to annealing: the reduction increases with grainsize (∼ 80 ×).

PLATE V

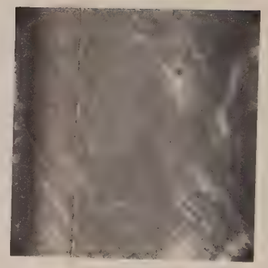

a
as deformed
→ 180° in 8 minutes
→ 200° in 11 minu

b
as deformed
→ 180° in 13 minutes
→ 200° in 21 minut

Fig. 6. Difference in rate of stress-reduction for two deformed silverchloride single crystals on annealing: crystal *b* is "slower" than crystal *a* (= crystal *d* of Fig. 5). (∼ 80 ×).

Nye's remark suggests the possibility that individual crystallites in a strained polycrystalline testpiece "straighten out" at a different rate, depending on the lattice conditions existing at their boundaries, which, in their turn, depend on the orientation relationship existing between adjacent grains. If this were so, one might expect a difference in rate of reduction of stress birefringence for individual crystallites on annealing a strained polycrystalline silverchloride testpiece. Moreover it might be anticipated that for comparable conditions of annealing, the stress reduction would be faster in a single crystal than in a polycrystalline testpiece.

The present investigation was primarily undertaken to find out to what extent these suppositions came true. As for some of the larger crystals the direction and position of the glide-bands could be determined with reasonable accuracy, the results obtained regarding this point are also given. They confirm on the main the conclusions already reached by NYE concerning the geometry of the glide process in silverchloride.

Experimental

Plates of silverchloride, measuring about $30 \times 7 \times 0{,}25$ cm, varying in crystalsize from polycrystalline (with about 20 crystallites) to nearly monocrystalline (some plates actually consisted of only one crystal) were prepared by recrystallization of rolled silverchloride plates. The method used was similar to that applied by BURGERS and TAN KOEN HIOK (1946) and by NYE (1949). In the present research the original plate of 1 mm thickness (obtained from Harshaw Company) was rolled to the final thickness of 0,25 mm, annealed at 270° C for $1\frac{1}{2}$ hour (to produce a fine-grained material), then strained by 4 % and finally recrystallized at 400° C for 2 hours.

In order to produce birefringence, the testpieces were extended by approximately 6 %. Distinct birefringent bands became visible in most crystals, either in one, two or three parallel sets. Figure 1*a* and *b* give two examples. Following NYE's method, for some of the larger crystals both the direction of the bands and the angle of tilt of the testpiece at which the bands became sharpest (in this position one views the glide-planes edge-on) were measured under the polarization microscope. Combining these data with the lattice orientation as deducted from a Laue-photograph gives the crystallographic character of the corresponding glide-planes. As pointed out by NYE, this method can only be applied if the glide-plane is not too far inclined to the normal of the crystal plate.

In five cases, for which unambiguous results could be obtained, the pole of the glide-band was close (within 5°) to the pole of a {111}-plane, the accuracy being insufficient to state with certainty whether this deviation was real or not. In four of these cases, if {111} was considered to be the glide-plane, the value of the applied shear stress was maximal for the ⟨110⟩-direction within this plane which enclosed an angle with the crystal plate close to 45°. In one crystal (fig. 1*b*), the normal to the

plate was close to a ⟨100⟩-direction. The poles of the two perpendicular systems of birefringent glide-bands lay in this case intermediate between {111} and {110}, although closest to the latter. In the position of the crystal both these planes contain ⟨110⟩-directions, making an angle with the direction of extension within 10° from 45°.

The above results agree mainly with those found by Nye. Concerning the possibility of glide along {110}, it is remarked in his paper that for a crystal, extended parallel to ⟨100⟩, the resolved shear stress would be maximal for glide in a {110} plane in a ⟨110⟩-direction. This was found by Stepanow (1934) under such conditions. Our crystal 2 lies close to such an orientation.

Annealing experiments

For the annealing experiments the (Leitz–Panphot) microscope was provided with a small furnace mounted on the specimen table, so that the testpieces could be viewed while heated. This limited their maximal dimensions to approximately 5 mm. In part of the experiments (figs. 2–4) deformation was brought about by a slight torsion and stretching with the aid of a pair of tweezers. In another series (figs. 5–6) the testpieces were extended by means of a small extension apparatus.

Figs. 2–4 refer to testpieces with fairly large crystallites. They clearly show that differences exist in the rate of stress reduction between individual grains. In all three cases it is fastest for the crystallite indicated by the arrow. For these crystallites the birefringent bands have already practically vanished after heating up to 190–220° in about 10 minutes, whereas in other crystallites in the same testpieces the birefringence is then still distinctly visible and disappears only after heating up to considerably higher temperatures (270–350° C).

Fig. 5 shows the effect of annealing testpieces of varying grainsize, increasing from "polycrystalline" in *a* to a single crystal with one small inclusion in *d*. The heat treatments are, although not identical, approximately the same.

Comparison of the four series of photographs shows that the stress reduction is faster in the coarse-grained testpieces *c* and *d* as compared with the polycrystalline pieces *a* and *b*. Whereas in *c* and *d* the birefringence has practically disappeared after annealing up to 200° in 10 minutes, it is then still clearly visible in the polycrystalline pieces *a* and *b*.

To make the birefringence disappear in these testpieces, heating up to 250–300° C in 30–40 minutes was required. This result fits in with Nye's observation that the stresses in the testpieces used by him were still visible at 350° C and only disappeared after a further period of heating at 415° C.

It must be remarked, however, that even two "single" crystals may show a marked difference in rate of stress annealing as is clear from

fig. 6. This is not strange, as one would expect dependence on the direction of the applied stress relative to the lattice orientation, causing a difference in internal mode of deformation (for example as to the number of active glide-planes involved, the occurrence of cross-glide etc.).

Oriented polygonization

The process of "straightening-out" of glide-lamellae, considered by NYE, involves a displacement of dislocations to some extent akin to what is supposed to take place during polygonization: in this latter case dislocations move, by glide and climb, to the two-dimensional layers between the individual "polygons". This analogy would support the view that also the capacity for polygonization for individual crystallites in a deformed polycrystalline testpiece would depend on their state of deformation and on their "surroundings" in the deformed testpiece. If so, polygonization would be "orientation dependent" in the sense that definite oriented lattice regions could polygonize "sooner" than others.

As to the state of deformation, for aluminium it has been experimentally shown (BURGERS, LIU and TIEDEMA (1951)) by studying the "break-up" of the asterism of the elongated spots on Laue-photographs of deformed single crystals, that the degree of polygonization due to a definite annealing treatment depends on the direction of the applied stress: it is much faster for extension parallel to a ⟨100⟩-direction than parallel to a ⟨110⟩-direction.

This conclusion is of interest in connection with current ideas on the process of recrystallization in cold-worked metals. The view has been advanced ((BECK (1949; CAHN (1950); BURGERS and TIEDEMA 1950)) that the "nucleus" of a new grain is a polygonized lattice region capable to grow at the expense of its neighbours. It has been suggested ((vide for example BURGERS (1961)) that in definite metals the above selection might lead to the preferred growth of lattice regions with a definite orientation with regard to the surrounding matrix and so to the formation of a recrystallization texture [1]).

On the basis of this point of view it would be of interest to extend the purely qualitative results of this investigation to a more quantitative study of the stress-annealing effect in deformed silverchloride, in the hope to establish a definite relation, if any, between the orientation of a

---

[1]) It is well known that apart from this conception other possible causes have (een advanced for this phenomenon; in particular selection by oriented growth bBECK (1953) (1954) (1961)), and a martensitic type of nucleus formation ((BURGERS and VERBRAAK (1957), VERBRAAK (1960), BURGERS (1961)). It seems unlikely that poe and the same nucleation mechanism holds for all metals. Various factors, in narticular the presence or absence of stacking faults and the energetic possibility of definite dislocation-reactions might play an important part as regards the precise mechanism of such processes.

crystallite, with regard to both the direction of the applied stress and the orientations of the surrounding crystallites, and its rate of annealing.

Delft, Laboratorium voor Fysische Scheikunde
der Technische Hogeschool
March 1961

One of the authors (R. G. de L.) wishes to express his thanks for a grant received from the Delfts Hogeschoolfonds.

LITERATURE

Beck, P. A., J. Appl. Physics **20**, 633 (1949).
——, Acta Met. **1**, 230 (1953); Advances in Physics **3**, 245 (1954); Z. Metallk. **52**, 13 (1961).
Burgers, W. G., Z. Metallk. **52**, 19 (1961).
—— and Tan Koen Hiok, Physica **11**, 353 (1946).
—— and T. J. Tiedema, Proc. Kon. Ned. Akad. v. Wetensch. Amsterdam **53**, 1525 (1950).
——, Y. H. Liu and T. J. Tiedema, Proc. Kon. Ned. Akad. v. Wetensch. Amsterdam **B 54**, 459 (1951).
—— and C. A. Verbraak, Acta Met. **5**, 765 (1957).
Cahn, R. W., Proc. Phys. Soc. London, **63**, 323 (1950).
Carnahan, R. D., T. L. Johnston, R. J. Stokes and C. H. Li, Trans. Metall. Soc. AIME **221**, 45 (1961).
Nye, J. F., Proc. Roy. Soc. London **A 198**, 190 (1949); **A 200**, 47 (1949).
Stepanow, A. W., Physik. Z. Sowj. Un. **6**, 312 (1934); **8**, 25 (1935).
Verbraak, C. A., Z. Metallk. **51**, 646 (1960).

ON THE DIFFRACTION OF SOUND WAVES IN A HEAT-CONDUCTING VISCOUS MEDIUM

BY

J. B. ALBLAS

Technological University of Eindhoven

(Communicated by Prof. C. J. BOUWKAMP at the meeting of January 28, 1961)

1. *Introduction*

The solution of the problem of the sound diffraction by a screen, first given by SOMMERFELD [1], is based on a number of simplifications. The screen has been taken to be infinitely thin and the medium is non-viscous and non-heat-conductive. As a consequence of these simplifications, the velocity at the edge of the screen has a singularity. It is now well known that the problem formulated by Sommerfeld has not a unique solution. BOUWKAMP [2] and MEIXNER [3] have pointed out that, to guarantee uniqueness of the solution, we have to prescribe the singularities in the form of "edge conditions", which are given by the physics of the problem. In Sommerfeld's solution the natural condition, that the field energy remains finite, is satisfied and the form of the singularities can be determined.

In a previous paper [4] we have investigated the (generalized) Sommerfeld problem for sound waves in a viscous medium, without consideration of the heat-conduction. One of the results of that paper is that, even for an infinitely thin screen a solution exists with finite velocities everywhere. This solution is not unique, but it can be made unique by prescribing suitable edge conditions.

In a review of the paper [4], LIGHTHILL [5] pointed out that the inclusion of finite heat-conductivity is imperative, if one wants to get quantitative results, as for gases the influences of viscosity and heat-conductivity on the propagation of sound waves are of the same order of magnitude. Now it is known [6] that the two phenomena can easily be combined for the problem of the undisturbed sound propagation. But, as was first pointed out to us by CARRIER [7], the combination of finite viscosity and finite heat-conductivity in the diffraction problem leads to a rather complicated mathematical problem.

It is the purpose of this paper to complete the previous one [4] by deriving a method for the evaluation of the unique exact solution of this problem. We restrict ourselves to give a simple approximate solution, which remains finite everywhere and which can be considered to give a

close description of the velocity and temperature distributions. This solution may be of some interest for the study of higher approximations in acoustics, as the methods of LIGHTHILL [8] and KUO [9], based on a first approximation with singularities, sometimes give rise to great difficulties, as has been pointed out by TSIEN [10].

The mathematical treatment given in this paper is based on the dual-integral method, given by NOBLE in his book on the Wiener-Hopf technique [11].

2. *Mathematical formulation of the problem*

We consider the diffraction of a sound wave, which propagates in a gas of finite viscosity and heat-conductivity, by an infinitely thin screen, occupying the half-plane $y=0$, $x<0$. The screen has an infinite heat-conductivity and the gas obeys the ideal-gas law. We restrict our considerations to the case of two dimensions and normal incidence.

The equations which describe the sound propagation are

$$
(1)\qquad \left\{\begin{aligned}
&\frac{\partial \varrho}{\partial t} + \operatorname{div}(\varrho \mathbf{v}) = 0,\\
&\varrho \frac{\partial \mathbf{v}}{\partial t} + \varrho\left(v_x \frac{\partial \mathbf{v}}{\partial x} + v_y \frac{\partial \mathbf{v}}{\partial y} + v_z \frac{\partial \mathbf{v}}{\partial z}\right)\\
&\qquad = -\operatorname{grad} p + \mu \Delta \mathbf{v} + \left(\frac{\mu}{3} + \mu'\right) \operatorname{grad} \operatorname{div} \mathbf{v},\\
&\varrho c_v \frac{\partial T}{\partial t} + \varrho c_v (\mathbf{v} \cdot \operatorname{grad} T) + p \operatorname{div} \mathbf{v} = \lambda \Delta T - \chi,\\
&p = R \varrho T.
\end{aligned}\right.
$$

where the following notations are used:

t is the time, x, y, z are the Cartesian coordinates, ϱ is the density, $\mathbf{v}$ the velocity, p the pressure and T the temperature. The coefficients of shear viscosity and bulk viscosity are μ and μ', the heat-conductivity is λ, the specific heat at constant volume is c_v, R is the gas constant and χ is the dissipation heat.

The system (1) is a non-linear system of equations, which is hard to solve. The physical conditions, however, often allow a linearization of this system, which can be performed by expanding the physical variables into series in powers of a small parameter.

Such a parameter is

$$\varepsilon = \frac{b\omega}{c},$$

where ω is the frequency of the incident steady-state wave (cf. eq. 11), b an amplitude and c the velocity of sound. We assume very small

disturbances, which assumption is expressed by $\alpha \ll 1$. We then have the expansions

$$\left.\begin{aligned} \varrho &= \varrho_0 + \alpha\varrho_1 + \alpha^2\varrho_2 + \ldots, \\ p &= p_0 + \alpha p_1 + \alpha^2 p_2 + \ldots, \\ T &= T_0 + \alpha T_1 + \alpha^2 T_2 + \ldots. \end{aligned}\right\}$$

$$\left.\begin{aligned} \mathbf{v} &= \alpha\mathbf{v}_1 + \alpha^2\mathbf{v}_2 \quad \ldots. \end{aligned}\right\}$$

from which we derive

$$p_0 = R\varrho_0 T_0,$$

and

$$c^2 = \gamma R T_0,$$

with

$$\gamma = c_p/c_v,$$

where c_p is the specific heat at constant pressure.

We restrict ourselves in this paper to the first-order approximation and we find

$$(2)\qquad \left\{\begin{aligned} &\frac{\partial\varrho_1}{\partial t} + \varrho_0 \operatorname{div}\mathbf{v}_1 = 0, \\ &\varrho_0\frac{\partial\mathbf{v}_1}{\partial t} = -\operatorname{grad} p_1 + \mu\Delta\mathbf{v}_1 + \left(\frac{\mu}{3}+\mu'\right)\operatorname{grad}\operatorname{div}\mathbf{v}_1, \\ &\varrho_0 c_v\frac{\partial T_1}{\partial t} + p_0\operatorname{div}\mathbf{v}_1 = \lambda\Delta T_1, \\ &p_1 = R\varrho_0 T_1 + RT_0\varrho_1. \end{aligned}\right.$$

We always can pose $\mathbf{v}_1$ in the form

$$(3)\qquad \mathbf{v}_1 = \operatorname{grad}\varphi - \operatorname{rot}\boldsymbol{\psi},$$

with

$$(4)\qquad \operatorname{div}\boldsymbol{\psi} = 0,$$

by which the equations (2) become

$$(5)\qquad \left\{\begin{aligned} &\frac{\partial\varrho_1}{\partial t} + \varrho_0\Delta\varphi = 0, \\ &\varrho_0\frac{\partial}{\partial t}\operatorname{grad}\varphi - \varrho_0\frac{\partial}{\partial t}\operatorname{rot}\boldsymbol{\psi} = -\operatorname{grad} p_1 \\ &\qquad + \mu\operatorname{grad}\Delta\varphi + \mu\operatorname{rot}\operatorname{rot}\operatorname{rot}\boldsymbol{\psi} + \left(\frac{\mu}{3}+\mu'\right)\operatorname{grad}\Delta\varphi, \\ &\varrho_0 c_v\frac{\partial T_1}{\partial t} + p_0\Delta\varphi = \lambda\Delta T_1, \end{aligned}\right.$$

where we have made use of

$$(6)\qquad \Delta\mathbf{v}_1 = \operatorname{grad}\operatorname{div}\mathbf{v}_1 - \operatorname{rot}\operatorname{rot}\mathbf{v}_1.$$

From these equations we derive

$$\Delta\left(\varrho_0\frac{\partial\varphi}{\partial t}+p_1-\left(\frac{4}{3}\mu+\mu'\right)\Delta\varphi\right)=0, \tag{7}$$

$$\operatorname{rot}\operatorname{rot}\left(\varrho_0\frac{\partial\boldsymbol{\psi}}{\partial t}+\mu\operatorname{rot}\operatorname{rot}\boldsymbol{\psi}\right)=0, \tag{8}$$

or, using (4) and (6)

$$\Delta\left(\varrho_0\frac{\partial\boldsymbol{\psi}}{\partial t}+\mu\operatorname{rot}\operatorname{rot}\boldsymbol{\psi}\right)=0. \tag{9}$$

The solutions of (7) and (9) are

$$\varrho_0\frac{\partial\varphi}{\partial t}=-p_1+\left(\frac{4}{3}\mu+\mu'\right)\Delta\varphi+f,$$

$$\varrho_0\frac{\partial\boldsymbol{\psi}}{\partial t}=-\mu\operatorname{rot}\operatorname{rot}\boldsymbol{\psi}+\mathbf{g},$$

with

$$\Delta f=0,\ \Delta\mathbf{g}=0.$$

We can take

$$f=0,\ \mathbf{g}=0,$$

as it is possible to incorporate f and $\mathbf{g}$ into φ and $\boldsymbol{\psi}$, respectively.

The complete system of equations becomes

$$\left\{\begin{aligned}
&\frac{\partial\varrho_1}{\partial t}+\varrho_0\Delta\varphi=0,\\
&\varrho_0\frac{\partial\varphi}{\partial t}=-p_1+\left(\frac{4}{3}\mu+\mu'\right)\Delta\varphi,\\
&\varrho_0\frac{\partial\boldsymbol{\psi}}{\partial t}=-\mu\operatorname{rot}\operatorname{rot}\boldsymbol{\psi},\\
&\varrho_0 c_v\frac{\partial T_1}{\partial t}+p_0\Delta\varphi=\lambda\Delta T_1,\\
&p_1=\varrho_0 RT_1+R\varrho_1 T_0.
\end{aligned}\right. \tag{10}$$

In a two-dimensional problem we only have one component of the vector $\boldsymbol{\psi}$,

$$\boldsymbol{\psi}=\psi\cdot\mathbf{e}_z,$$

where $\mathbf{e}_z$ is the unit vector along the z-axis.

We restrict the considerations to the steady-state wave solution with the time dependence

$$\mathrm{e}^{-i\omega t}, \tag{11}$$

The equations for the amplitudes of T_1 and φ, which will be indicated by the same notation, become

$$\Delta T_1 + \frac{i\omega\varrho_0 c_v}{\lambda} T_1 = \frac{\varrho_0 c^2}{\gamma\lambda}\Delta\varphi,$$

$$\Delta\varphi\left(1 - \frac{i\omega(4/3\mu + \mu')\gamma}{\varrho_0 c^2}\right) = -\frac{\gamma\omega^2}{c^2}\varphi - i\omega\frac{R\gamma}{c^2}T_1,$$

from which we derive

$$\Delta\varphi + \frac{\gamma\omega^2/c^2}{1 - \frac{i\omega(4/3\mu+\mu')\gamma}{\varrho_0 c^2}}\varphi = -\frac{i\omega R\gamma}{c^2 - \frac{i\omega(4/3\mu+\mu')\gamma}{\varrho_0}}T_1,$$

$$\Delta T_1 + \frac{i\omega\varrho_0 c_v}{\lambda}\left(1 + \frac{\gamma - 1}{1 - \frac{i\omega(4/3\mu+\mu')\gamma}{\varrho_0 c^2}}\right)T_1 = -\frac{\varrho_0\omega^2}{\lambda\left(1 - \frac{i\omega(4/3\mu+\mu')\gamma}{\varrho_0 c^2}\right)}\varphi.$$

We introduce the abbreviations

$$A = \frac{1}{1 - \frac{i\omega(4/3\mu+\mu')\gamma}{\varrho_0 c^2}}, \quad \varkappa = \frac{\lambda}{\varrho_0 c_v}, \quad k_0 = \omega/c$$

and the equations become

$$\Delta\varphi + k_0^2 A\gamma\varphi = -\frac{i\omega R\gamma}{c^2}AT_1, \tag{12}$$

$$\Delta T_1 + \frac{i\omega}{\varkappa}(1 + (\gamma - 1)A)T_1 = -\frac{\omega^2}{\varkappa c_v}A\varphi. \tag{13}$$

Equation (12) is important for the formulation of the boundary condition for T_1 at $y=0$, $x<0$. We eliminate T_1 from (12) and (13) and find

$$\Delta\Delta\varphi + \Delta\varphi\left[k_0^2\gamma A + \frac{i\omega\gamma}{\varkappa}A + \frac{i\omega}{\varkappa}(1-A)\right] + \frac{i\omega^3 A\gamma}{\varkappa c^2}\varphi = 0. \tag{14}$$

Equation (14) can be written as

$$(\Delta + k^2)(\Delta + m^2)\varphi = 0,$$

where the coefficients k^2 and m^2 are given by

$$k^2 + m^2 = \frac{i\omega\gamma}{\varkappa}A + k_0^2\gamma A + \frac{i\omega}{\varkappa}(1-A), \quad k^2 m^2 = \frac{i\omega^3 A\gamma}{\varkappa c^2}.$$

For small viscosity and heat conductivity (of the same order of magnitude) we have the expansions

$$k^2 = Ak_0^2 + \frac{i\gamma A\varkappa k_0^2}{4\omega} - \frac{i\omega(1-A)^2}{2\varkappa\gamma A} + \ldots,$$

$$m^2 = \frac{i\omega\gamma A}{\varkappa} - k_0^2(1-\gamma A) + \ldots.$$

Every solution of (15) can be written in the form

$$\varphi = \varphi_1 + \varphi_2, \tag{16}$$

and the problem is reduced to

$$\Delta\varphi_1 + k^2\varphi_1 = 0, \tag{17}$$

$$\Delta\varphi_2 + m^2\varphi_2 = 0, \tag{18}$$

$$\Delta\psi + l^2\psi = 0, \tag{19}$$

with $l^2 = i\omega\varrho_0/\mu$.

The parameters k, l, m are all complex. We define the square roots of k^2, l^2, m^2 by

$$\operatorname{Im} k > 0, \quad \operatorname{Im} l > 0, \quad \operatorname{Im} m > 0.$$

The auxiliary conditions are

(a) the functions φ_1, φ_2 and ψ have to be continuously differentiable in the region under consideration;

(b) the tangential velocity u vanishes along the screen:

$$u = \frac{\partial\varphi}{\partial x} - \frac{\partial\psi}{\partial y} = 0, \qquad y = 0, \; x < 0;$$

(c) the same holds for the normal velocity v:

$$v = \frac{\partial\varphi}{\partial y} + \frac{\partial\psi}{\partial x} = 0, \qquad y = 0, \; x < 0.$$

(d) at the screen the temperature T_1 is zero. According to (12), this condition is formulated as

$$\Delta\varphi + k_0^2\gamma A\varphi = 0,$$

which after introduction of (16), (17), (18) reduces to

$$a\varphi_1 + \varphi_2 = 0, \qquad y = 0, \; x < 0,$$

where the parameter a is defined by

$$a = \frac{k_0^2\gamma A - k^2}{k_0^2\gamma A - m^2};$$

(e) the incident wave is

$$\varphi_i = \mathrm{e}^{-ikx};$$

(f) near the edge we assume the temperature to be bounded.

3. *The formal solution*

The solution of the problem is found by means of the method of dual integral equations. We introduce the abbreviations γ_1, γ_2, γ_3, by

$$\gamma_1 = \sqrt{\lambda^2 - k^2}, \tag{20}$$

$$\gamma_2 = \sqrt{\lambda^2 - m^2}, \tag{21}$$

$$\gamma_3 = \sqrt{\lambda^2 - l^2}, \tag{22}$$

and write the unknown functions in the following form

$$\varphi_1 = e^{-iky} + \frac{1}{\sqrt{2\pi}} \int_{-\infty+ic}^{\infty+ic} A(\lambda)\, e^{-i\lambda x} e^{-\gamma_1 y}\, d\lambda, \qquad y > 0, \tag{23}$$

$$\varphi_1 = e^{-iky} + \frac{1}{\sqrt{2\pi}} \int_{-\infty+ic}^{\infty+ic} B(\lambda)\, e^{-i\lambda x} e^{\gamma_1 y}\, d\lambda, \qquad y < 0, \tag{24}$$

$$\varphi_2 = \frac{1}{\sqrt{2\pi}} \int_{-\infty+ic}^{\infty+ic} C(\lambda)\, e^{-i\lambda x} e^{-\gamma_2 y}\, d\lambda, \qquad y > 0, \tag{25}$$

$$\varphi_2 = \frac{1}{\sqrt{2\pi}} \int_{-\infty+ic}^{\infty+ic} D(\lambda)\, e^{-i\lambda x} e^{\gamma_2 y}\, d\lambda, \qquad y < 0, \tag{26}$$

$$\psi = \frac{1}{\sqrt{2\pi}} \int_{-\infty+ic}^{\infty+ic} E(\lambda)\, e^{-i\lambda x} e^{-\gamma_3 y}\, d\lambda, \qquad y > 0, \tag{27}$$

$$\psi = \frac{1}{\sqrt{2\pi}} \int_{-\infty+ic}^{\infty+ic} F(\lambda)\, e^{-i\lambda x} e^{\gamma_3 y}\, d\lambda, \qquad y < 0. \tag{28}$$

The square roots (20), (21), (22) are defined in the λ-plane, cut from k to $k+i\infty$, $-k$ to $-k-i\infty$, etc., such that

$$\operatorname{Re}(\sqrt{\lambda^2-k^2}) > 0, \quad \operatorname{Re}(\sqrt{\lambda^2-l^2}) > 0, \quad \operatorname{Re}(\sqrt{\lambda^2-m^2}) > 0,$$

along the path of integration $-\infty+ic$ to $\infty+ic$.

For $\lambda=0$, we find

$$\gamma_1 = -ik, \quad \gamma_2 = -im, \quad \gamma_3 = -il.$$

The constant c will be determined later. We have

$$\operatorname{Im} c < 0.$$

The continuity of the functions φ_1, φ_2 and ψ at $y=0$, $x>0$ leads to the equations

$$\int_{-\infty+ic}^{\infty+ic} e^{-i\lambda x}\, d\lambda\, \{A(\lambda) - B(\lambda)\} = 0, \qquad x > 0, \tag{29}$$

$$\int_{-\infty+ic}^{\infty+ic} e^{-i\lambda x}\, d\lambda\, \{C(\lambda) - D(\lambda)\} = 0, \qquad x > 0, \tag{30}$$

$$\int_{-\infty+ic}^{\infty+ic} e^{-i\lambda x}\, d\lambda\, \{E(\lambda) - F(\lambda)\} = 0, \qquad x > 0, \tag{31}$$

and the continuity of $\frac{\partial\varphi_1}{\partial y}$, $\frac{\partial\varphi_2}{\partial y}$, $\frac{\partial\psi}{\partial y}$ at $y=0$, $x>0$ to

$$\int_{-\infty+ic}^{\infty+ic} e^{-i\lambda x}\, d\lambda\, \gamma_1\{A(\lambda) + B(\lambda)\} = 0, \quad x > 0, \tag{32}$$

$$\int_{-\infty+ic}^{\infty+ic} e^{-i\lambda x}\, d\lambda\, \gamma_2\{C(\lambda) + D(\lambda)\} = 0, \quad x > 0, \tag{33}$$

$$\int_{-\infty+ic}^{\infty+ic} e^{-i\lambda x}\, d\lambda\, \gamma_3\{E(\lambda) + F(\lambda)\} = 0, \quad x > 0. \tag{34}$$

The condition $u=0$ for $y=\pm 0,\ x<0$ gives

$$\int_{-\infty+ic}^{\infty+ic} e^{-i\lambda x}\,d\lambda\,\{i\lambda A(\lambda)+i\lambda C(\lambda)-\gamma_3 E(\lambda)\}=0, \qquad x<0, \tag{35}$$

$$\int_{-\infty+ic}^{\infty+ic} e^{-i\lambda x}\,d\lambda\,\{i\lambda B(\lambda)+i\lambda D(\lambda)+\gamma_3 F(\lambda)\}=0, \qquad x<0. \tag{36}$$

The condition $v=0$ for $y=\pm 0,\ x<0$ gives

$$ik+\frac{1}{\sqrt{2\pi}}\int_{-\infty+ic}^{\infty+ic} e^{-i\lambda x}\,d\lambda\,\{\gamma_1 A(\lambda)+\gamma_2 C(\lambda)+i\lambda E(\lambda)\}=0, \qquad x<0, \tag{37}$$

$$-ik+\frac{1}{\sqrt{2\pi}}\int_{-\infty+ic}^{\infty+ic} e^{-i\lambda x}\,d\lambda\,\{\gamma_1 B(\lambda)+\gamma_2 D(\lambda)-i\lambda F(\lambda)\}=0, \qquad x<0, \tag{38}$$

while we derive from the condition $T_1=0$ for $y=\pm 0,\ x<0$

$$a+\frac{1}{\sqrt{2\pi}}\int_{-\infty+ic}^{\infty+ic} e^{-i\lambda x}\,d\lambda\,\{aA(\lambda)+C(\lambda)\}=0, \qquad x<0, \tag{39}$$

$$a+\frac{1}{\sqrt{2\pi}}\int_{-\infty+ic}^{\infty+ic} e^{-i\lambda x}\,d\lambda\,\{aB(\lambda)+D(\lambda)\}=0, \qquad x<0. \tag{40}$$

We proceed with the introduction of the functions

$$\left\{\begin{aligned} P_1(\lambda) &= A(\lambda)-B(\lambda),\\ P_2(\lambda) &= A(\lambda)+B(\lambda),\\ P_3(\lambda) &= C(\lambda)-D(\lambda),\\ P_4(\lambda) &= C(\lambda)+D(\lambda),\\ P_5(\lambda) &= E(\lambda)-F(\lambda),\\ P_6(\lambda) &= E(\lambda)+F(\lambda), \end{aligned}\right. \tag{41}$$

and we add or subtract the equations (35), (36); (37), (38) and (39), (40). The system (29) to (40) of 12 equations is in this way separated into two systems of six equations each. The first system for P_1, P_3 and P_6 is

$$\int_{-\infty+ic}^{\infty+ic} P_1(\lambda)\,e^{-i\lambda x}\,d\lambda=0, \qquad x>0, \tag{42}$$

$$\int_{-\infty+ic}^{\infty+ic} P_3(\lambda)\,e^{-i\lambda x}\,d\lambda=0, \qquad x>0. \tag{43}$$

$$\int_{-\infty+ic}^{\infty+ic} e^{-i\lambda x}\,d\lambda\,\{i\lambda P_1(\lambda)+i\lambda P_3(\lambda)-\gamma_3 P_6(\lambda)\}=0, \qquad x<0, \tag{44}$$

$$\int_{-\infty+ic}^{\infty+ic} P_6(\lambda)\,\gamma_3\,e^{-i\lambda x}\,d\lambda=0, \qquad x>0, \tag{45}$$

$$\frac{1}{\sqrt{2\pi}}\int_{-\infty+ic}^{\infty+ic} e^{-i\lambda x}\,d\lambda\,\{\gamma_1 P_1(\lambda)+\gamma_2 P_3(\lambda)+i\lambda P_6(\lambda)\}=-2ik, \qquad x<0, \tag{46}$$

$$\int_{-\infty+ic}^{\infty+ic} e^{-i\lambda x}\,d\lambda\,\{aP_1(\lambda)+P_3(\lambda)\}=0, \qquad x<0. \tag{47}$$

The second system consists of P_2, P_4, P_5. We find

$$\int_{-\infty+ic}^{\infty+ic} \gamma_1 P_2(\lambda)\, e^{-i\lambda x}\, d\lambda = 0, \qquad x > 0, \tag{48}$$

$$\int_{-\infty+ic}^{\infty+ic} \gamma_2 P_4(\lambda)\, e^{-i\lambda x}\, d\lambda = 0, \qquad x > 0, \tag{49}$$

$$\int_{-\infty+ic}^{\infty+ic} P_5(\lambda)\, e^{-i\lambda x}\, d\lambda = 0, \qquad x > 0, \tag{50}$$

$$\int_{-\infty+ic}^{\infty+ic} e^{-i\lambda x}\, d\lambda \{i\lambda P_2(\lambda) + i\lambda P_4(\lambda) - \gamma_3 P_5(\lambda)\} = 0, \qquad x < 0, \tag{51}$$

$$\int_{-\infty+ic}^{\infty+ic} e^{-i\lambda x}\, d\lambda \{\gamma_1 P_2(\lambda) + \gamma_2 P_4(\lambda) + i\lambda P_5(\lambda)\} = 0, \qquad x < 0, \tag{52}$$

$$\frac{1}{\sqrt{2\pi}} \int_{-\infty+ic}^{\infty+ic} e^{-i\lambda x}\, d\lambda \{a P_2(\lambda) + P_4(\lambda)\} = -2a, \qquad x < 0. \tag{53}$$

We consider the first system. From (42), (43), (44), (45) we obtain

$$i\lambda P_1(\lambda) + i\lambda P_3(\lambda) - \gamma_3 P_6(\lambda) = 0, \tag{54}$$

and from (42), (43) and (47) we find

$$P_3(\lambda) + a P_1(\lambda) = 0. \tag{55}$$

From (54) and (55) we can express $P_3(\lambda)$ and $P_6(\lambda)$ in terms of $P_1(\lambda)$. We obtain

$$\begin{cases} P_3(\lambda) = -a P_1(\lambda), \\ P_6(\lambda) = \dfrac{i\lambda}{\gamma_3}(1-a) P_1(\lambda), \end{cases} \tag{56}$$

and we have for $P_1(\lambda)$ the equations

$$\frac{1}{\sqrt{2\pi}} \int_{-\infty+ic}^{\infty+ic} P_1(\lambda)\, e^{-i\lambda x}\, d\lambda = 0, \qquad x > 0, \tag{57}$$

$$\frac{1}{\sqrt{2\pi}} \int_{-\infty+ic}^{\infty+ic} \gamma_1 P_1(\lambda) K(\lambda)\, e^{-i\lambda x}\, d\lambda = -2ik, \qquad x < 0, \tag{58}$$

where $K(\lambda)$ is defined by

$$K(\lambda) = 1 - \frac{a\gamma_2}{\gamma_1} - \frac{(1-a)\lambda^2}{\gamma_1 \gamma_3}. \tag{59}$$

An important property of the function $K(\lambda)$ is

$$\lim K(\lambda) = 0, \ (|\lambda| \to \infty).$$

The second system for P_2, P_4 and P_5 can also be reduced. From (48), (49), (50), (52) we find

$$\gamma_1 P_2(\lambda) + \gamma_2 P_4(\lambda) + i\lambda P_5(\lambda) = 0, \tag{60}$$

from which we derive after the introduction of

$$Q_1 = \gamma_1 P_2(\lambda), \quad Q_2 = \gamma_2 P_4(\lambda)$$

the relation

$$P_5(\lambda) = \frac{i}{\lambda}(Q_1 + Q_2).$$

For the functions $Q_1(\lambda)$ and $Q_2(\lambda)$ we obtain the equations

$$\frac{1}{\sqrt{2\pi}} \int_{-\infty+ic}^{\infty+ic} Q_1(\lambda)\, e^{-i\lambda x}\, d\lambda = 0, \qquad x > 0, \tag{61}$$

$$\frac{1}{\sqrt{2\pi}} \int_{-\infty+ic}^{\infty+ic} Q_2(\lambda)\, e^{-i\lambda x}\, d\lambda = 0, \qquad x > 0, \tag{62}$$

$$\frac{1}{\sqrt{2\pi}} \int_{-\infty+ic}^{\infty+ic} e^{-i\lambda x}\, d\lambda \left\{ \frac{\lambda}{\gamma_1} Q_1(\lambda) + \frac{\lambda}{\gamma_2} Q_2(\lambda) - \frac{\gamma_3}{\lambda} [Q_1(\lambda) + Q_2(\lambda)] \right\} = 0, \qquad x > 0, \tag{63}$$

$$\frac{1}{\sqrt{2\pi}} \int_{-\infty+ic}^{\infty+ic} e^{-i\lambda x}\, d\lambda \left\{ \frac{a}{\gamma_1} Q_1(\lambda) + \frac{1}{\gamma_2} Q_2(\lambda) \right\} = -2a, \qquad x < 0. \tag{64}$$

We first discuss the solution of the system (57), (58). In equation (57) we transform the x-variable into $x+\xi$ and in (58) into $x-\xi$, with $\xi > 0$. We multiply (57) by a function $N_1(\xi)$ and (58) by $N_2(\xi)$.

We integrate the equations from zero to infinity. We have

$$\frac{1}{\sqrt{2\pi}} \int_{-\infty+ic}^{\infty+ic} \int_0^\infty N_1(\xi)\, e^{-i\lambda\xi}\, d\xi\, P_1(\lambda)\, e^{-i\lambda x}\, d\lambda = 0, \qquad x > 0, \tag{65}$$

$$\frac{1}{\sqrt{2\pi}} \int_{-\infty+ic}^{\infty+ic} \int_0^\infty N_2(\xi)\, e^{-i\lambda\xi}\, d\xi\, P_1(\lambda)\, \gamma_1 K(\lambda)\, e^{-i\lambda x}\, d\lambda = -2ik \int_0^\infty N_2(\xi)\, d\xi, \qquad x > 0. \tag{66}$$

In the equations (65) and (66) the functions $N_1(\xi)$ and $N_2(\xi)$ are arbitrary functions such that the integrals have a meaning.

The function

$$\int_0^\infty N_1(\xi)\, e^{-i\lambda\xi}\, d\xi = N_-(\lambda)$$

is a regular function in a lower half-plane, while the function

$$\int_0^\infty N_2(\xi)\, e^{-i\lambda\xi}\, d\xi = N_+(\lambda)$$

is regular in an upper half-plane. We have

$$\frac{1}{\sqrt{2\pi}} \int_{-\infty+ic}^{\infty+ic} N_-(\lambda)\, P_1(\lambda)\, e^{-i\lambda x}\, d\lambda = 0, \qquad x > 0, \tag{67}$$

$$\frac{1}{\sqrt{2\pi}} \int_{-\infty+ic}^{\infty+ic} N_+(\lambda)\, \gamma_1 K(\lambda)\, P_1(\lambda)\, e^{-i\lambda x}\, d\lambda = -2ikN_+(0), \qquad x > 0. \tag{68}$$

Now we shall determine the functions $N_+(\lambda)$ and $N_-(\lambda)$ so, that we can invert equations (67) and (68). We split

$$\gamma_1 = \sqrt{\lambda - k}\,\sqrt{\lambda + k} \tag{69}$$

and

$$K(\lambda) = K_-(\lambda)\,K_+(\lambda) \tag{70}$$

where the functions $K_+(\lambda)$ and $K_-(\lambda)$ are regular and free from zeros in an upper, and a lower half-plane, respectively.

As $K(\lambda) \to 0$, if $|\lambda| \to \infty$ the possibility of the factorization (70) is not trivial. We can however show, that this factorization is possible. We take

$$N_-(\lambda) = \frac{1}{\sqrt{\lambda - k}}\,\frac{1}{K_+(\lambda)}\,\frac{1}{\lambda - \lambda_1},$$

$$N_+(\lambda) = \sqrt{\lambda - k}\,K_+(\lambda),$$

and the equations (67), (68) become

$$\frac{1}{\sqrt{2\pi}} \int_{-\infty+ic}^{\infty+ic} \sqrt{\lambda - k}\,K_-(\lambda)\,P_1(\lambda)\,\mathrm{e}^{-i\lambda x}\,\mathrm{d}\lambda = 0, \qquad x > 0, \tag{71}$$

$$\frac{1}{\sqrt{2\pi}} \int_{-\infty+ic}^{\infty+ic} \sqrt{\lambda - k}\,K_-(\lambda)\,\frac{P_1(\lambda)}{\lambda + \lambda_1}\,\mathrm{e}^{-i\lambda x}\,\mathrm{d}\lambda = -2ikN_+(0), \qquad x < 0, \tag{72}$$

where λ_1 is an arbitrary complex constant, satisfying

$$\operatorname{Im}\,\lambda_1 > 0,\ |\lambda_1| \text{ sufficiently large.}$$

We multiply (72) by $\mathrm{e}^{-i\lambda_1 x}$ and differentiate with respect to x. We obtain

$$\begin{cases} \dfrac{1}{\sqrt{2\pi}} \displaystyle\int_{-\infty+ic}^{\infty+ic} \sqrt{\lambda - k}\,K_-(\lambda)\,P_1(\lambda)\,\mathrm{e}^{-i\lambda x}\,\mathrm{d}\lambda = -2ikN_+(0)\cdot\lambda_1 \\ \qquad\qquad = -2ik\,\dfrac{1}{\sqrt{k}}\,\dfrac{1}{K_+(0)}, \qquad x < 0. \end{cases} \tag{73}$$

From (71) and (73) we find for $P_1(\lambda)$

$$P_1(\lambda) = -\sqrt{\frac{2}{\pi}}\,\frac{\sqrt{k}}{K_+(0)}\,\frac{1}{\lambda\sqrt{\lambda - k}}\,\frac{1}{K_-(\lambda)}. \tag{74}$$

From (56) we find

$$P_3(\lambda) = a\sqrt{\frac{2}{\pi}}\,\frac{\sqrt{k}}{K_+(0)}\,\frac{1}{\lambda\sqrt{\lambda - k}}\,\frac{1}{K_-(\lambda)}. \tag{75}$$

$$P_6(\lambda) = -i\sqrt{\frac{2}{\pi}}\,\frac{\sqrt{k}}{K_+(0)}\,\frac{(1-a)}{\sqrt{\lambda - k}\,\sqrt{\lambda^2 - l^2}}\,\frac{1}{K_-(\lambda)}. \tag{76}$$

First we see, that we have to take for the constant c a complex number with

$$|\operatorname{Im} c| < \operatorname{Im} k,$$
$$\operatorname{Im} c < 0,$$

if we assume that

$$\operatorname{Im} k \; < (\operatorname{Im} l, \; \operatorname{Im} m).$$

In the second place we remark, that the solutions (74), (75) and (76) satisfy the equations (42), (43), (44), (46) and (47). The integral in (45) diverges. It has to be interpreted as

$$\frac{\mathrm{d}}{\mathrm{d}x} \int_{-\infty+ic}^{\infty+ic} P_6(\lambda) \frac{\gamma_3}{i\lambda} \mathrm{e}^{-i\lambda x} \, \mathrm{d}\lambda = 0, \qquad x > 0.$$

This equation is satisfied.

To solve the system (61), (62), (63) and (64), we introduce the function

$$R(\lambda) = Q_1(\lambda) + Q_2(\lambda)$$

and proceed with the system for $R(\lambda)$ and $Q_1(\lambda)$

$$\frac{1}{\sqrt{2\pi}} \int_{-\infty+ic}^{\infty+ic} Q_1(\lambda) \, \mathrm{e}^{-i\lambda x} \, \mathrm{d}\lambda = 0, \qquad x > 0, \tag{77}$$

$$\frac{1}{\sqrt{2\pi}} \int_{-\infty+ic}^{\infty+ic} R(\lambda) \, \mathrm{e}^{-i\lambda x} \, \mathrm{d}\lambda = 0, \qquad x > 0, \tag{78}$$

$$\begin{cases} \dfrac{1}{\sqrt{2\pi}} \displaystyle\int_{-\infty+ic}^{\infty+ic} Q_1(\lambda) \frac{1}{\gamma_1} L(\lambda) \, \mathrm{e}^{-i\lambda x} \, \mathrm{d}\lambda = \frac{2a}{1-a} + \frac{1}{1-a} \cdot \\ \qquad \cdot \dfrac{1}{\sqrt{2\pi}} \displaystyle\int_{-\infty+ic}^{\infty+ic} \frac{R(\lambda)}{\gamma_2} \mathrm{e}^{-i\lambda x} \, \mathrm{d}\lambda, \qquad x < 0, \end{cases} \tag{79}$$

$$\frac{1}{\sqrt{2\pi}} \int_{-\infty+ic}^{\infty+ic} \gamma_3 R(\lambda) \, \mathrm{e}^{-i\lambda x} \, \mathrm{d}\lambda = \frac{i(1-a)}{\sqrt{2\pi}} \frac{\mathrm{d}}{\mathrm{d}x} \int_{-\infty+ic}^{\infty+ic} \frac{\lambda Q_1(\lambda)}{\gamma_1} \mathrm{e}^{-i\lambda x} \, \mathrm{d}\lambda, \quad x < 0, \tag{80}$$

where the abbrevation

$$L(\lambda) = \frac{(\gamma_1/\gamma_2) - a}{1-a} \tag{81}$$

has been used.

Equations (77), (78), (79) and (80) can be solved (formally) by means of an iteration method. We pose

$$R(\lambda) = 0, \tag{82}$$

and determine $Q_1(\lambda)$ from

$$Q_1(\lambda) = -\frac{ai}{1-a} \sqrt{\frac{2}{\pi}} \frac{\sqrt{k}}{L_+(0)} \frac{\sqrt{\lambda - k}}{\lambda} \frac{1}{L_-(\lambda)}, \tag{83}$$

where $L_+(\lambda)$ and $L_-(\lambda)$ are the factors in the decomposition

$$L(\lambda) = L_-(\lambda) \, L_+(\lambda). \tag{84}$$

A second approximation is found by introducing (83) into (80), solving equations (78) and (80) for $R(\lambda)$ and proceeding with this function in (77),

(79). In this way, we obtain some series in powers of a small parameter for the functions $R(\lambda)$ and $Q_1(\lambda)$. In this paper we restrict to the first approximation. We find from (82), (83)

$$P_2(\lambda) = \frac{-ai}{1-a}\sqrt{\frac{2}{\pi}}\frac{\sqrt{k}}{L_+(0)}\frac{1}{\lambda\sqrt{\lambda+k}}\frac{1}{L_-(\lambda)}, \tag{85}$$

$$P_4(\lambda) = \frac{ai}{1-a}\sqrt{\frac{2}{\pi}}\frac{\sqrt{k}}{L_+(0)}\frac{\sqrt{\lambda-k}}{\lambda\sqrt{\lambda^2-m^2}}\frac{1}{L_-(\lambda)}. \tag{86}$$

$$P_5(\lambda) = 0. \tag{87}$$

4. *The factorization of the kernels*

For the decomposition factors of the kernels $K(\lambda)$ and $L(\lambda)$, we use the well-known formulae

$$\log K_-(\lambda) = -\frac{1}{\sqrt{2\pi i}}\int_{-\infty+ip}^{\infty+ip}\frac{\log K(\xi)}{\xi-\lambda}\,d\xi,$$

$$\log K_-(\lambda) = -\frac{1}{\sqrt{2\pi i}}\int_{-\infty+iq}^{\infty+iq}\frac{\log K(\xi)}{\xi-\lambda}\,d\xi,$$

$$\log L_-(\lambda) = -\frac{1}{\sqrt{2\pi i}}\int_{-\infty+ip}^{\infty+ip}\frac{\log L(\xi)}{\xi-\lambda}\,d\xi,$$

$$\log L_+(\lambda) = +\frac{1}{\sqrt{2\pi i}}\int_{-\infty+iq}^{\infty+iq}\frac{\log L(\xi)}{\xi-\lambda}\,d\xi,$$

where the numbers p and q lie in the strip of regularity and λ satisfies

$$q < \operatorname{Im}\ \lambda < p.$$

If $\operatorname{Im}\lambda<0$, we have

$$K_-(\lambda) = \exp\left[-\frac{\lambda}{\pi i}\int_0^\infty\frac{\log K(\xi)}{\xi^2-\lambda^2}\,d\xi\right], \tag{88}$$

while for $\operatorname{Im}\lambda>0$, we find

$$K_-(\lambda) = \exp\left[\frac{\lambda}{\pi i}\int_0^\infty\frac{\log K(\xi)}{\xi^2-\lambda^2}\,d\xi\right]. \tag{89}$$

From (88) and (89) we derive

$$K_+(\lambda) = K_-(-\lambda), \tag{90}$$

and with the help of this equation we find the value of $K_+(0)$:

$$K_+(0) = K_-(0) = \frac{1}{\sqrt{k}}\sqrt{k-am}. \tag{91}$$

From the asymptotic behaviour of $K(\lambda)$,

$$K(\lambda) \sim -\frac{1}{2}\frac{1}{\lambda^2}(k^2+(1-a)\,l^2-am^2),\quad (|\lambda|\to\infty), \tag{92}$$

we derive

$$K_-(\lambda) \sim \frac{1}{\lambda}\sqrt{\frac{k^2+(1-a)l^2-am^2}{2}}, \quad (|\lambda| \to \infty), \tag{93}$$

$$K_+(\lambda) \sim -\frac{1}{\lambda}\sqrt{\frac{k^2+(1-a)l^2-am^2}{2}}, \quad (|\lambda| \to \infty). \tag{94}$$

The signs in (93), (94) are determined by contour integration (cf. [4]). From the equations for $\log L_+(\lambda)$ and $\log L_-(\lambda)$ we obtain

$$L_+(0) = L_-(0) = \frac{1}{\sqrt{m}}\sqrt{\frac{k-am}{1-a}}. \tag{95}$$

and the asymptotic formulae of the kernels $L_+(\lambda)$, $L_-(\lambda)$ are found from

$$L(\lambda) \sim 1 + \frac{m^2-k^2}{2(1-a)}\frac{1}{\lambda^2}, \quad (|\lambda| \to \infty), \tag{96}$$

to be

$$L_-(\lambda) \sim 1, \quad (|\lambda| \to \infty). \tag{97}$$

$$L_+(\lambda) \sim 1, \quad (|\lambda| \to \infty). \tag{98}$$

5. *The velocity and temperature fields*

From the results we have obtained, we derive expressions for the velocity and temperature fields. We find from (23) to (28), (41), (74) to (76), (85) to (87), (91) and (95) for $y>0$

$$\left\{\begin{aligned} u = {} & \frac{i}{2\pi}\frac{k}{\sqrt{k-am}}\int_{-\infty+ic}^{\infty+ic}\frac{1}{\sqrt{\lambda-k}}\frac{1}{K_+(\lambda)}e^{-i\lambda x}\cdot \\ & \cdot\left\{e^{-\gamma_1 y} - a\frac{\gamma_2}{\gamma_1}e^{-\gamma_2 y} - (1-a)\frac{\lambda^2}{\gamma_1\gamma_3}e^{-\gamma_3 y}\right\}d\lambda \\ & - \frac{1}{2\pi}\frac{a}{\sqrt{1-a}}\frac{\sqrt{km}}{\sqrt{k-am}}\int_{-\infty+ic}^{\infty+ic}\frac{1}{\sqrt{\lambda-k}}\frac{1}{L_+(\lambda)}e^{-i\lambda x}\left\{e^{-\gamma_1 y} - \frac{\gamma_1}{\gamma_2}e^{-\gamma_2 y}\right\}d\lambda, \end{aligned}\right. \tag{99}$$

$$\left\{\begin{aligned} v = {} & -ik\,e^{-iky} + \frac{1}{2\pi}\frac{k}{\sqrt{k-am}}\int_{-\infty+ic}^{\infty+ic}\frac{\sqrt{\lambda-k}}{\lambda}\frac{1}{K_+(\lambda)}e^{-i\lambda x}\cdot \\ & \cdot\left\{e^{-\gamma_1 y} - a\frac{\gamma_2}{\gamma_1}e^{-\gamma_2 y} - (1-a)\frac{\lambda^2}{\gamma_1\gamma_3}e^{-\gamma_3 y}\right\}d\lambda \\ & + \frac{1}{2\pi}\frac{ai}{\sqrt{1-a}}\frac{\sqrt{km}}{\sqrt{k-am}}\int_{-\infty+ic}^{\infty+ic}\frac{\sqrt{\lambda-k}}{\lambda}\frac{1}{L_+(\lambda)}e^{-i\lambda x}\left\{e^{-\gamma_1 y} - e^{-\gamma_2 y}\right\}d\lambda, \end{aligned}\right. \tag{100}$$

$$\left\{\begin{aligned} & -\frac{i\omega R\gamma}{c^2}\frac{A}{k_0^2\gamma A - m^2}T_1 = a\varphi_1 + \varphi_2 = \\ & = a\,e^{-iky} - \frac{a}{2\pi}\frac{k}{\sqrt{k-am}}\int_{-\infty+ic}^{\infty+ic}\frac{1}{\lambda\sqrt{\lambda-k}}\frac{1}{K_-(\lambda)}e^{-i\lambda x}\left\{e^{-\gamma_1 y} - e^{-\gamma_2 y}\right\}d\lambda \\ & \frac{ai}{2\pi}\frac{\sqrt{km}}{\sqrt{k-am}}\sqrt{1-a}\int_{-\infty+ic}^{\infty+ic}\frac{1}{\lambda\sqrt{\lambda-k}}\frac{1}{L_-(\lambda)}e^{-i\lambda x}\left\{\frac{\gamma_1/\gamma_2\,e^{-\gamma_2 y} - a\,e^{-\gamma_1 y}}{1-a}\right\}d\lambda. \end{aligned}\right. \tag{101}$$

For $y<0$ we have

$$(102)\quad \begin{cases} u = -\dfrac{i}{2\pi}\dfrac{k}{\sqrt{k-am}}\displaystyle\int_{-\infty+ic}^{\infty+ic}\dfrac{1}{\sqrt{\lambda-k}}\dfrac{1}{K_-(\lambda)}\,e^{-i\lambda x}\cdot \\ \qquad\qquad \cdot\{e^{\gamma_1 y}-a\,e^{\gamma_2 y}-(1-a)\,e^{\gamma_3 y}\}\,d\lambda \\ -\dfrac{1}{2\pi}\dfrac{a}{\sqrt{1-a}}\dfrac{\sqrt{km}}{\sqrt{k-am}}\displaystyle\int_{-\infty+ic}^{\infty+ic}\dfrac{1}{\sqrt{\lambda+k}}\dfrac{1}{L_-(\lambda)}\,e^{-i\lambda x}\left\{e^{\gamma_1 y}-\dfrac{\gamma_1}{\gamma_2}e^{\gamma_2 y}\right\}d\lambda. \end{cases}$$

$$(103)\quad \begin{cases} v = -ik\,e^{-iky}+\dfrac{1}{2\pi}\dfrac{k}{\sqrt{k-am}}\displaystyle\int_{-\infty+ic}^{\infty+ic}\dfrac{\sqrt{\lambda-k}}{k}\dfrac{1}{K_-(\lambda)}\,e^{-i\lambda x}\cdot \\ \qquad\qquad \cdot\left\{e^{\gamma_1 y}-a\dfrac{\gamma_2}{\gamma_1}e^{\gamma_2 y}-(1-a)\dfrac{\lambda}{\gamma_1\gamma_3}e^{\gamma_3 y}\right\}d\lambda \\ -\dfrac{1}{2\pi}\dfrac{ai}{\sqrt{1-a}}\dfrac{\sqrt{km}}{\sqrt{k-am}}\displaystyle\int_{-\infty+ic}^{\infty+ic}\dfrac{\sqrt{\lambda-k}}{\lambda}\dfrac{1}{L_-(\lambda)}\,e^{-i\lambda x}\{e^{\gamma_1 y}-e^{\gamma_2 y}\}\,d\lambda, \end{cases}$$

$$(104)\quad \begin{cases} a\varphi_1+\varphi_2 = a\,e^{-iky}+\dfrac{a}{2\pi}\dfrac{k}{\sqrt{k-am}}\displaystyle\int_{-\infty+ic}^{\infty+ic}\dfrac{1}{\lambda\sqrt{\lambda-k}}\dfrac{1}{K_-(\lambda)}\,e^{-i\lambda x}\cdot \\ \qquad\qquad \cdot\{e^{\gamma_1 y}-e^{\gamma_2 y}\}\,d\lambda \\ +\dfrac{ai}{2\pi}\dfrac{\sqrt{km}}{\sqrt{k-am}}\sqrt{1-a}\displaystyle\int_{-\infty+ic}^{\infty+ic}\dfrac{1}{\lambda\sqrt{\lambda+k}}\dfrac{1}{L_-(\lambda)}\,e^{-i\lambda x}\left\{\dfrac{\gamma_1/\gamma_2\,e^{\gamma_2 y}-a\,e^{\gamma_1 y}}{1-a}\right\}d\lambda. \end{cases}$$

From the equations (99) to (104) we derive the integral representations, which hold at $y=0$,

$$(105)\quad u = \frac{1}{2\pi}\frac{a}{\sqrt{1-a}}\frac{\sqrt{km}}{\sqrt{k-am}}\int_{-\infty+ic}^{\infty+ic}\frac{1}{\sqrt{\lambda+k}}\left(1-\frac{\sqrt{\lambda^2-k^2}}{\sqrt{\lambda^2-m^2}}\right)\frac{e^{-i\lambda x}}{L_-(\lambda)}\,d\lambda.$$

$$(106)\quad v = -ik+\frac{1}{2\pi}\frac{k}{\sqrt{k-am}}\int_{-\infty+ic}^{\infty+ic}\frac{\sqrt{\lambda+k}}{\lambda}K_+(\lambda)\,e^{-i\lambda x}\,d\lambda.$$

$$(107)\quad a\varphi_1+\varphi_2 = a+\frac{ai}{2\pi}\frac{\sqrt{km}}{\sqrt{k-am}}\sqrt{1-a}\int_{-\infty+ic}^{\infty+ic}\frac{L_+(\lambda)}{\lambda\sqrt{\lambda+k}}\,e^{-i\lambda x}\,d\lambda.$$

At the edge $x=0$, the velocities and temperature remain finite. This follows from the asymptotic expansions (93), (94), (97), (98). More precisely stated, the velocity u tends to zero like $\sqrt{x^3}$, while v and T_1 tend to zero like $\sqrt{x}$.

For the case of small viscosity and small heat-conductivity the contribution to the diffracted field of the exponential terms with $\gamma_2 y$ and $\gamma_3 y$ can be neglected at some distance from the screen. As can be expected, the influence of viscosity and heat-conductivity is restricted to the

boundary-layer regions in first approximation. The kernel function $K_-(\lambda)$ also contains terms with l and m and the form of the far-field will in second approximation depend on these parameters. A complete discussion of the fields will not be given here. We refer to [4] for the case of viscosity only.

For the study of higher approximations, we need the numerical evaluation of the integrals. This can be simplified by taking $|l| \to \infty$, $|m| \to \infty$ in (99) to (104) for $|y| > \delta > 0$, and using the integrals (105) to (107) for $y = 0$.

6. *Verification of the formal solution and uniqueness*

The analysis we have given is a formal one and we have to prove that our solution satisfies the equations (2) with the boundary conditions (a) to (f).

The functions u, v and T_1 are derived from φ_1, φ_2 and ψ, which conform to (17), (18) and (19), as differentiation under the integral sign is permitted, because of the exponential character of the integrands. The functions u, v and T_1 are continuous at $y = 0$, as follows from the integral representations. The derivatives of these functions are also continuous at $y = 0$, for $x > 0$. The functions $\partial v/\partial y$ and $\partial T_1/\partial y$ are not continuous at $y = 0$, $x < 0$.

From (106) and (107) it can easily be seen that the boundary conditions $v = 0$, for $y = 0$, $x < 0$ and $T_1 = 0$ for $y = 0$, $x < 0$ are met with. The boundary condition $u = 0$ is not exactly satisfied, as we have used an approximate solution of the system (77) to (80). The value of u can be expected to be very small everywhere and we can improve the result in the way indicated. However there is no need of such an improvement.

The question of the uniqueness is important. We can add to our solutions other ones, obtained by differentiation with expect to x of the formulae (99) to (104). The new solutions meet all the conditions, with the exception of the edge conditions: the velocity and temperature fields become infinite as $x \to 0$, $y = 0$. The energy integral however remains finite. The stringent condition that in this problem the temperature must be bounded everywhere, leads to the exclusion of the fields with singularities, as the temperature and velocity fields are coupled.

Acknowledgment

The author is indebted to his colleague C. J. Bouwkamp for his helpful comments.

REFERENCES

1. Sommerfeld, A., Math. Ann., **45**, 263 (1894); **47**, 317 (1896); Gött. Nachr. (1894), 338; (1895), 267; Proc. Lond. Math. Soc. (1), **28**, 395 (1897); Math. Phys. **46**, 11 (1901).
2. Bouwkamp, C. J., Physica, **12**, 467 (1946); Philips Res. Rep., **5**, 401 (1950); Rep. Progr. Phys., **17**, 35 (1954).
3. Meixner, J., Ann. Physik, **6**, 1 (1949).
4. Alblas, J. B., Appl. Sci. Res., A, **6**, 237 (1957).

5. Lighthill, M. J., Math. Rev., **18**, 967 (1957).
6. Kirchhoff, G., Poggend. Ann. Phys., **134**, 177 (1868).
7. Carrier, G. F., private communication.
8. Lighthill, M. J., Phil. Mag., **40**, 1179 (1949).
9. Kuo, Y. H., J. Math. Phys., **32**, 83 (1953).
10. Tsien, H. S., Adv. Appl. Mech., **4**, 281 (1956).
11. Noble, B., Methods based on the Wiener-Hopf technique, Pergamon Press, London (1958).

THEORY OF TRANSPORT AND RELAXATION PHENOMENA IN A GAS MIXTURE. I

VELOCITY DISTRIBUTION AND TRANSPORT PROPERTIES

BY

M. J. OFFERHAUS

(Communicated by Prof. J. DE BOER at the meeting of January 28, 1961)

9. *Introduction and Survey* [1])

In a previous article [1] [2]) we have given a theory of relaxation phenomena in a *single* monatomic gas. In the present article, we will give an extension of this theory to the case of an N-component monatomic gas *mixture*. Like in the one-component theory, it will be shown that the kinetic stage, of a duration of a few "times-between-collisions", is characterized by relaxation phenomena leading to the hydrodynamical stage. In describing both stages, stress will be laid on those elements of mixture theory which differ considerably from the treatment of the single gas.

In part I we give a short discussion of the velocity distribution and the transport properties in the *hydrodynamical* (HD) stage (ch. 10), summarizing the treatments first given by CHAPMAN (see [2]), ENSKOG [3] and HELLUND and UEHLING [4] for a binary mixture and the one given by HIRSCHFELDER *e.a.* [5] for a mixture of more than two components. This survey is necessary for the derivation of the basic equations for the velocity distribution in the *kinetic* stage (ch. 11), as well as for the theory presented in chs. 12–17 of this publication.

In part II we discuss the entropy production in a mixture during the kinetic and HD stages (ch. 12). This discussion is followed by some remarks on the use of a variational principle for the approximative determination of the transport coefficients (ch. 13).

Finally, part III gives an account of the properties of a multicomponent Maxwellian gas mixture (characterized by a r^{-4}-repulsive potential between all pairs of molecules). This account begins with the

[1]) *Some abbreviations used thoughout parts I–III*:
BE Boltzmann equation; HDE hydrodynamical equations; HD hydrodynamical; MB Maxwell–Boltzmann; ChE Chapman–Enskog; LHS left hand side; RHS right hand side; $\approx$ of the order-of-magnitude of, or: approximately equal to.

[2]) We will occasionally refer to the chapters of [1], numbered 1–8, and to the equations of [1], numbered (1.1)–(8.17).

eigenvalue theory of the linearized collision operator Ω_{ij} (ch. 14). An outline of the transport properties of the Maxwellian mixture is given; the diffusion in a binary mixture is fully described (ch. 15). After this treatment of the HD stage, the kinetic stage is discussed (ch. 16). The relaxation of the velocity distribution and the quasi-relaxation of the transport currents are characterized by a time scale, in which the "diffusional relaxation time" τ_D is of special importance; this depends on the relative concentration of the mixture components (chs. 16, 17).

10. *Velocity distribution and transport currents in the hydrodynamical stage*

In the following, the subscript i (or j, h, k) will denote a property p_i of the i-th component of a mixture; all equations for p_i will hold for $i=1, \ldots, N$ and all summations $\sum_i$ will extend over $i=1, \ldots, N$, unless otherwise stated.

We start from N Boltzmann equations (BE), one for each component i:

$$\partial_t f_i = -\mathbf{c}\cdot\frac{\partial f_i}{\partial \mathbf{r}} - \mathbf{F}\cdot\frac{\partial f_i}{\partial \mathbf{c}} + \sum_i J(f_i f_{j1}) \equiv \partial_S f_i + \partial_C f_i, \tag{10.1}$$

indicating that the velocity distribution $f_i(\mathbf{c}; \mathbf{r}, t)$ changes due to streaming and to acceleration by external forces, $\mathbf{F}_i$, which may vary with i and depend on $\mathbf{c}$:

$$\partial_S f_i \overset{\text{def}}{=} -\mathbf{c}\cdot\frac{\partial f_i}{\partial \mathbf{r}} - \mathbf{F}\cdot\frac{\partial f_i}{\partial \mathbf{c}}, \tag{10.2}$$

as well as due to collisions:

$$\left.\begin{aligned}\partial_C f_i \overset{\text{def}}{=} \sum_j J(f_i f_{j1}) \equiv \int d\varepsilon \int d\chi \sin\chi \int d\mathbf{c}_1\, \alpha_{ij}(g,\chi)\,\{f_i(\mathbf{c}')\, f_j(\mathbf{c}_1') - \\ - f_i(\mathbf{c})\, f_j(\mathbf{c}_1)\}.\end{aligned}\right\} \tag{10.3}$$

$\mathbf{c}'$ and $\mathbf{c}_1'$ denote velocities-after-collision of particles i and j with initial velocities $\mathbf{c}, \mathbf{c}_1$ ($|\mathbf{c}-\mathbf{c}_1|=g$). All interactions V_{ij} are supposed to have spherical symmetry: $V_{ij}=V_{ij}(r)$.

It is sometimes convenient to consider a function p_i of $\mathbf{c}$, which has a different character depending on the value of i – *e.g.* a function which is connected to the molecular mass m_i – as a function $p_i(\mathbf{c})$ of the continuous variable $\mathbf{c}$ and the discrete variable $i(=1, \ldots, N)$. In this sense, one can state that there are $N+4$ independent collision-invariant functions $\chi^{[0\lambda]}$ of i and $\mathbf{c}$, with the property

$$\chi_i(\mathbf{c}) + \chi_j(\mathbf{c}_1) = \chi_i(\mathbf{c}') + \chi_j(\mathbf{c}_1'), \tag{10.4}$$

viz.

$$\chi_i^{[01,k]} = \delta_{ik} m_k;\quad \boldsymbol{\chi}_i^{[02]} = m_i \mathbf{c};\quad \chi_i^{[03]} = \tfrac{1}{2} m_i c^2. \tag{10.5 a, b, c}$$

(10.5a) implies that a particle of species i, when colliding, retains the amount of mass of species k it carries – *i.e.*, m_i if $k=i$ and zero otherwise.

The integral properties analogous to (2:9,51) include a summation over i and j:

$$\sum_i \sum_j \int d\mathbf{c}\, \chi_i^{[0\lambda]}(\mathbf{c})\, J(f_i f_{j1}) \equiv \sum_i \int d\mathbf{c}\, \chi_i^{[0\lambda]} \partial_{\mathbf{c}} f_i = 0 : \tag{10.6}$$

$$\sum_i \sum_j \int d\mathbf{c}\, \chi_i^{[0\lambda]}(\mathbf{c})\, \{J(f_i g_{j1}) + J(g_i f_{j1})\} = 0. \tag{10.7}$$

The average value of a function $G_i(\mathbf{c})$ for the molecules of component i and that of a function $G_i(\mathbf{c})$ for the mixture as a whole are defined as follows:

$$\langle G \rangle_i \overset{\text{def}}{=} \frac{\int d\mathbf{c} f_i G_i}{\int d\mathbf{c} f_i = n_i} ; \quad \overline{G} \overset{\text{def}}{=} \frac{\sum_i n_i \langle G \rangle_i}{\sum_i n_i = n} = \sum_i x_i \langle G \rangle_i \tag{10.8a, b}$$

(n_i is the number density of component i; $x_i = n_i/n$ is its relative concentration). In particular, we consider the moments of the collisional invariants $\chi^{[0\lambda]}$:

$$\psi_i^{[\lambda]} \overset{\text{def}}{=} n_i \langle \chi^{[0\lambda]} \rangle_i ; \quad \psi^{[\lambda]} \overset{\text{def}}{=} n \overline{\chi^{[0\lambda]}}. \tag{10.9}$$

The $N+4$ values of $\psi^{[\lambda]}(\lambda = 1.1, \ldots, 1.N, \mathbf{2}, 3)$ are of course connected to the $N+4$ basic moments:

$$\varrho_i = n_i m_i ; \quad \mathbf{c}_0 = \overline{m\mathbf{c}}/\overline{m} ; \quad T = (3k)^{-1} \overline{mC^2}, \tag{10.10}$$

and inversely; here, the thermal or peculiar velocity is defined with reference to the "mass-averaged" velocity $\mathbf{c}_0$:

$$\mathbf{C} = \mathbf{c} - \mathbf{c}_0, \text{ so } \overline{m\mathbf{C}} = 0. \tag{10.11}$$

Equations for the t-derivatives of the $\psi^{[\lambda]}$ are found by multiplying the BE (10.1) by $\chi_i^{[0\lambda]}$ and taking $\sum_i d\mathbf{c}$:

$$\partial_t \psi^{[\lambda]} = -\nabla \cdot \boldsymbol{\Psi}^{[\lambda]+} + \sum_i \mathbf{F}_i \cdot \boldsymbol{\psi}_i^{[\lambda]-}, \tag{10.12}$$

in which the "step-up" and "step-down" moments $\boldsymbol{\Psi}^{[\lambda]\pm}$ are defined in analogy to eqs. (2.10a, b). Remodelling these equations, we get the usual hydrodynamical equations (HDE) for a mixture:

$$\begin{cases} \text{(a)} & \partial_t \varrho_i = -\nabla \cdot (\varrho_i \mathbf{c}_0) - \nabla \cdot (\varrho_i \langle \mathbf{C} \rangle_i) \\ \text{(aa)} & \partial_t \varrho = -\nabla \cdot (\varrho \mathbf{c}_0) \qquad (\varrho \equiv \sum_i \varrho_i) \\ \text{(b)} & \partial_t \mathbf{c}_0 = -(\mathbf{c}_0 \cdot \nabla)\mathbf{c}_0 - \varrho^{-1} \nabla \cdot \mathsf{P} + \varrho^{-1} \sum_i \varrho_i \mathbf{F}_i \\ \text{(c)} & \partial_t T = -\mathbf{c}_0 \cdot \nabla T - (2/3kn)(\mathsf{P} : \nabla \mathbf{c}_0 + \nabla \cdot \mathbf{q} - \sum_i \varrho_i \mathbf{F}_i \cdot \langle \mathbf{C} \rangle_i) + \\ & \qquad + (T/n) \nabla \cdot \sum_i n_i \langle \mathbf{C} \rangle_i. \end{cases} \tag{10.13}$$

The RHS contain ϱ_i, $\mathbf{c}_0$, T and $\mathbf{F}_i$, as well as the transport currents: $\langle \mathbf{C} \rangle_i$ and

$$\mathsf{P} = n \overline{m\mathbf{C}\mathbf{C}} ; \quad \mathbf{q} = n \overline{\tfrac{1}{2} m C^2 \mathbf{C}}. \tag{10.14a, b}$$

In the case of a *spatially uniform* mixture, the basic idea of the ChE method – that of a distribution depending on $\mathbf{r}$ and t through the $N+4$ moments $\psi^{[\lambda]}$ – of course leads to a t-independent MB distribution $f_i^{(0)}(\mathbf{c})$, and we shall not repeat the argument given in ch. 2.

The description of the HD stage in a *non-uniform* gas mixture is rather different from the single-component theory. Some important features of this mixture theory shall be given now, because we need them for reference in the chapters on entropy production and on the properties of the Maxwellian mixture. The following treatment is similar to that given in [2], [5] and [6], but our notation shows some differences.

Once more, the ChE solution of the BE is based on the concepts of

1) a distribution depending on $\mathbf{r}$ and t through the $N+4$ moments $\psi^{[\lambda]}$ and their $\mathbf{r}$-derivatives of various order:

$$f_i(\mathbf{c};\mathbf{r},t)=f_i(\mathbf{c}|\psi^{[\lambda]}(\mathbf{r},t)); \tag{10.15}$$

2) series development of f_i, with the local MB distribution $f_i^{(0)}(\mathbf{c})$ as the first term:

$$f_i=\sum_{r=0}^{\infty} f_i^{(r)}=f_i^{(0)}(1+\sum_{r=1}^{\infty}\phi_i^{(r)})=f_i^{(0)}(1+\phi_i); \tag{10.16}$$

3) normalization of these terms, such that the first of them leads to the correct moments $\psi^{[\lambda]}$ and all higher ones have zero moments:

$$\psi^{[\lambda](0)}=\psi^{[\lambda]}\ ;\quad \psi^{[\lambda](1)}=\ldots=0 \qquad (\psi^{[\lambda](r)}\overset{\text{def}}{=}\sum_i\int d\mathbf{c}\, f_i^{(r)}\chi_i^{[0\lambda]}); \tag{10.17}$$

4) separation of groups of terms in the BE with the use of a parameter θ.

Application of these principles leads to a series of equations closely resembling (2.31), the difference being that

a) $J(f^{(r)}f_1^{(s)})$ is replaced by $\sum_j J(f_i^{(r)}f_{j1}^{(s)})$;

b) all other f (or ϕ) receive the subscript i.

Now we introduce, instead of Ω, operators Y and Z, such that

$$Y_{ij}\phi_i\overset{\text{def}}{=}\int d\varepsilon\int d\chi\,\sin\chi\int d\mathbf{c}_1\, f_j^{(0)}(\mathbf{c}_1)\,\alpha_{ij}(g,\chi)\,\{\phi_i(\mathbf{c})-\phi_i(\mathbf{c}')\}; \tag{10.18a}$$

$$Z_{ij}\phi_j\overset{\text{def}}{=}\int d\varepsilon\int d\chi\,\sin\chi\int d\mathbf{c}_1\, f_j^{(0)}(\mathbf{c}_1)\,\alpha_{ij}(g,\chi)\,\{\phi_j(\mathbf{c}_1)-\phi_j(\mathbf{c}_1')\}. \tag{10.18b}$$

Clearly, their sum:

$$\Omega_{ij}\phi\overset{\text{def}}{=}Y_{ij}\phi_i+Z_{ij}\phi_j \tag{10.19a}$$

and, in particular, the sum-over-j:

$$\Omega_i\phi\overset{\text{def}}{=}\sum_j\Omega_{ij}\phi \tag{10.19b}$$

are found in the following approximation of the collision term for small ϕ_i:

$$\sum_j J(f_if_{j1})\approx -f_i^{(0)}\Omega_i\phi, \tag{10.20}$$

as well as in the (exact) equations for successive terms of the $\sum_i f_i^{(r)}$ series, which we can write in the form:

$$\sum_j J(f_i^{(0)} f_{j1}^{(0)}) = 0; \tag{10.21a}$$

$$\boxed{F_i^{(r)} = \Omega_i \phi^{(r)}} \quad (r \geqslant 1). \tag{10.21b}$$

Here, the LHS $F_i^{(r)}$ depends on all $f_j^{(\varrho)}$ with $j = 1, \ldots, N$; $\varrho = 0, \ldots, r-1$, as follows:

$$F_i^{(r)} \equiv (1/f_i^{(0)}) \{\partial_S f_i^{(r-1)} - \sum_{\varrho=0}^{r-1} \partial_t^{(r-1-\varrho)} f_i^{(\varrho)} + \sum_j \sum_{\varrho=1}^{r-1} J(f_i^{(\varrho)} f_{j1}^{(r-\varrho)})\}. \tag{10.22}$$

The "partial t-derivatives" are of course defined by:

$$\partial_t^{(s)} u_i(\mathbf{c}|\psi) \stackrel{\text{def}}{=} \sum_\lambda \frac{\delta u_i}{\delta \psi^{[\lambda]}} \partial_t^{(s)} \psi^{[\lambda]}, \tag{10.23}$$

in which $\partial_t^{(s)} \psi^{[\lambda]}$ is the extra contribution to the RHS of the HDE (10.13) caused by calculating the currents $\mathsf{P}, \boldsymbol{q}, \langle \mathbf{C} \rangle_i$ with the use of $\sum_{r=0}^{s} f_i^{(r)}$ instead of $\sum_{r=0}^{s-1} f_i^{(r)}$.

Apart from Ω_{ij} and Ω_i, we introduce the operators

$$W_{ij}\phi \stackrel{\text{def}}{=} Z_{ij}\phi_j + \delta_{ij} \sum_k Y_{ik}\phi_i \tag{10.24a}$$

and

$$W_i \phi \stackrel{\text{def}}{=} \sum_j W_{ij}\phi = \Omega_i \phi; \tag{10.24b}$$

apparently, in the basic integral equations (10.21b), Ω_i can also be written as W_i. The use of W lies in the property:

$$W_{ij}(a\phi) = a_j W_{ij}\phi\ ; \quad W_i(a\phi) = \sum_j a_j W_{ij}\phi, \tag{10.25a}$$

as compared to the "linearity behaviour" of Y_{ij}, Z_{ij} and Ω_{ij}, which reads:

$$Y_{ij}(a_i\phi_i) = a_i Y_{ij}\phi_i;\ Z_{ij}(a_j\phi_j) = a_j Z_{ij}\phi_j;\ \Omega_{ij}(a\phi) = a_i Y_{ij}\phi_i + a_j Z_{ij}\phi_j. \tag{10.25b}$$

Next we define scalar products:

$$(F_i, G_i)_i \stackrel{\text{def}}{=} \int d\mathbf{c}\, f_i^{(0)} F_i G_i;\ (F, G) \stackrel{\text{def}}{=} \sum_i (F_i, G_i)_i, \tag{10.26a, b}$$

and matrix elements:

$$\left\{ \begin{aligned} [F, G] \stackrel{\text{def}}{=} (F, \Omega G) &= \sum_i (F_i, \Omega_i G)_i = \sum_i \sum_j (F_i, \Omega_{ij} G)_i \\ &= (F, WG) = \sum_i (F_i, W_i G)_i = \sum_i \sum_j (F_i, W_{ij} G)_i \\ &= \sum_i \sum_j \{(F_i, Y_{ij} G_i)_i + (F_i, Z_{ij} G_j)_i\}. \end{aligned} \right. \tag{10.27}$$

The scalar product is, of course, symmetrical in F and G:

$$(F_i, G_i)_i = (G_i, F_i)_i;\ (F, G) = (G, F); \tag{10.28}$$

the symmetry relation for $[F, G]$ is derived from those holding for the Y and Z matrix elements:

$$\left.\begin{aligned} &(F_i, Y_{ij} G_i)_i = (G_i, Y_{ij} F_i)_i: \\ &(F_i, Z_{ij} G_j)_i = (G_j, Z_{ji} F_i)_i;\ [F, G] = [G, F]. \end{aligned}\right\} \tag{10.29a, b, c}$$

The diagonal matrix element of Ω is non-negative:

$$[F, F] \geqslant 0, \tag{10.30}$$

$=$ holding only if F is one of the $N+4$ collisional invariants $\chi^{[0\lambda]}$, or if $F = 0$.

For the system of N coupled integral equations (10.21b), at a fixed value of the index r in the Hilbert series $\sum_r f_i^{(r)}$, there are $N+4$ integrability conditions:

$$(F^{(r)}, \chi^{[0\lambda]}) = 0. \tag{10.31}$$

To the solutions $\phi_i^{(r)} (i = 1, \ldots, N)$ one may add a linear combination of the $N+4$ solutions to the corresponding homogeneous equation $\Omega_i \phi^{(r)} = 0$, *i.e.*, a combination of the $N+4$ collisional invariants $\chi_i^{[0\lambda]}$. We have already used up this freedom by applying the normalizing conditions (10.17):

$$(\phi^{(r)}, \chi^{[0\lambda]}) = 0. \tag{10.32}$$

Again, in proving that the conditions (10.31), at a certain r, are fulfilled, one makes use of the normalization (10.32) of all ϕ up to $r-1$.

We quote the explicit form of the first equation (10.21b), $r = 1$; cf. eq. (10.22):

$$F_i^{(1)} \equiv -2 \mathsf{C}_i^* \overset{\circ}{\mathsf{C}}_i^* : \overset{(\circ)}{\nabla \mathsf{c}_0} + (\tfrac{5}{2} - C_i^{*2}) \mathsf{C} \cdot \nabla \ln T - \mathsf{C} \cdot (\mathsf{d}_i / x_i) = \Omega_i \phi^{(1)}, \tag{10.33}$$

in which

$$\mathsf{d}_i \overset{\text{def}}{=} \nabla x_i - x_i \{(m_i / \overline{m}) - 1\} \nabla \ln (nkT) - (\varrho_i / nkT) \{\mathsf{F}_i - (\overline{m\mathsf{F}} / \overline{m})\}, \tag{10.34}$$

so that

$$\sum_i \mathsf{d}_i = 0. \tag{10.35}$$

Thus, the expression (10.33) for $F_i^{(1)}$ contains N gradients $\mathsf{d}_1, \ldots, \mathsf{d}_N$, which are related by (10.35). As a consequence, the solution to (10.33), which reads:

$$\phi_i^{(1)} = \mathsf{A}_i^{(\lambda)} \cdot \nabla \ln T + \mathsf{A}_i^{(\mu)} : \overset{\circ}{\overline{\nabla \mathsf{c}_0}} + \sum_j \mathsf{A}_i^{(j)} \cdot \mathsf{d}_j, \tag{10.36}$$

contains N vector coefficients $\mathsf{A}_i^{(j)} (j = 1, \ldots, N)$ which are dependent (one

could always add a constant vector to all of them). In order to fully determine these coefficients $\mathbf{A}$, we arbitrarily require that

$$\sum_j x_j \mathbf{A}_i^{(j)} = 0 \tag{10.37}$$

for each i.

For later use, we mention that the coefficients A must have the following vector or tensor shape:

$$\begin{cases} \mathbf{A}_i^{(\lambda)} = A_i^{(\lambda)}(C_i^{*2})\,\mathbf{C}; \quad \mathsf{A}_i^{(\mu)} = A_i^{(\mu)}(C_i^{*2})\,\mathbf{C}_i^{*}\mathring{\mathbf{C}}_i^{*}; \\ \qquad\qquad\qquad\qquad\qquad\qquad \mathbf{A}_i^{(j)} = A_i^{(j)}(C_i^{*2})\,\mathbf{C}. \qquad (j=1,\ldots,N) \end{cases} \tag{10.38}$$

Now from (10.36) we eliminate one gradient, say $\mathbf{d}_h$, using (10.35). By substituting (10.36) into (10.33) and equalizing coefficients of the independent gradients: $\overset{\circ}{\overline{\nabla \mathbf{c}_0}}$, $\nabla \ln T$, $\mathbf{d}_i$ $(i \neq h)$, we obtain separate integral equations for A:

$$\mathbf{G}_i^{(\lambda)} \equiv (\tfrac{5}{2} - C_i^{*2})\,\mathbf{C} = \Omega_i \mathbf{A}^{(\lambda)}; \tag{10.39a}$$

$$\mathsf{G}_i^{(\mu)} \equiv -2\mathbf{C}_i^{*}\mathring{\mathbf{C}}_i^{*} = \Omega_i \mathsf{A}^{(\mu)}; \tag{10.39b}$$

$$(\mathbf{C}/x_i)(\delta_{ih} - \delta_{ij}) = \Omega_i(\mathbf{A}^{(j)} - \mathbf{A}^{(h)}), \tag{10.40}$$

of which we simplify the last one by taking $\sum_j x_j$ over both sides and applying (10.37):

$$\mathbf{G}_i^{(j)} \equiv \mathbf{C}\{1 - (\delta_{ij}/x_j)\} = \Omega_i \mathbf{A}^{(j)} \qquad (j \neq h). \tag{10.39c}$$

Of course, from $\mathbf{A}^{(j)}$ with $j \neq h$, the coefficient $\mathbf{A}^{(h)}$ is found by using (10.37).

Eqs. (10.39a, c) are supplemented by the normalization (10.32), which leads to:

$$(\mathbf{A}^{(\lambda)}, m\mathbf{C}) = 0; \quad (\mathbf{A}^{(j)}, m\mathbf{C}) = 0. \qquad (j=1,\ldots,N) \tag{10.41a, b}$$

If we introduce "transport forces" as follows:

$$\mathbf{X}^{(\lambda)} = -\nabla \ln T; \quad \mathsf{X}^{(\mu)} = -\overset{\circ}{\overline{\nabla \mathbf{c}_0}}; \quad \mathbf{X}^{(j)} = -\mathbf{d}_j, \tag{10.42}$$

we can write:

$$F_i^{(1)} = -\sum_{\varkappa} G_i^{(\varkappa)} X^{(\varkappa)}; \quad \phi_i^{(1)} = -\sum_{\varkappa} A_i^{(\varkappa)} X^{(\varkappa)}. \tag{10.43a, b}$$

In this notation, the integral equations (10.39) and the normalizing conditions (10.41) are summarized as:

$$G_i^{(\varkappa)} = \Omega_i A^{(\varkappa)}; \tag{10.44}$$

$$(A^{(\varkappa)}, m\mathbf{C}) = 0. \tag{10.45}$$

In all this, $\varkappa = \lambda, \mu, 1, \ldots, N$.

For the most useful definition of "transport currents" in a mixture, we introduce the unweighed average velocity of all particles:

$$\boldsymbol{u} = \overline{\mathbf{c}}, \tag{10.46}$$

and the peculiar velocity of a particle referred to $\boldsymbol{u}$:

$$\boldsymbol{\gamma} = \boldsymbol{c} - \boldsymbol{u}. \tag{10.47}$$

Apparently there is the following difference between $\boldsymbol{u}$ and $\boldsymbol{c}_0$, and between $\boldsymbol{C}$ and $\boldsymbol{\gamma}$:

$$\boldsymbol{C} - \boldsymbol{\gamma} = \boldsymbol{u} - \boldsymbol{c}_0 = \overline{\boldsymbol{c}} - \boldsymbol{c}_0 = \overline{\boldsymbol{C}}. \tag{10.48}$$

In the following, we do not consider the heat current $\boldsymbol{q}$ (eq. 10.14b) but the enthalpy current $\boldsymbol{\Gamma}$ which, providing that the distribution f_i does not depart too much from $f_i^{(0)}$, coincides with the heat current defined with the use of $\boldsymbol{\gamma}$ instead of $\boldsymbol{C}$:

$$\boldsymbol{\Gamma} \equiv \boldsymbol{q} - \tfrac{5}{2} nk\boldsymbol{u} \approx n\, \overline{\tfrac{1}{2} m \gamma^2 \boldsymbol{\gamma}}. \tag{10.49}$$

The three "transport currents" are now given by definitions which ensure that each product $J^{(\varkappa)} X^{(\varkappa)}$ has the dimension of an energy density:

$$\boldsymbol{J}^{(\lambda)} = \boldsymbol{\Gamma}; \quad \mathsf{J}^{(\mu)} = \overset{\circ}{\mathsf{P}}; \quad \boldsymbol{J}^{(j)} = nkT \langle \boldsymbol{\gamma} \rangle_j. \tag{10.50}$$

It is easily seen that, in the approximation $f_i \approx f_i^{(0)}(1 + \phi_i^{(1)})$,

$$\boldsymbol{J}^{(\lambda)} = -kT(\boldsymbol{G}^{(\lambda)}, \phi^{(1)}); \quad \mathsf{J}^{(\mu)} = -kT(\mathsf{G}^{(\mu)}, \phi^{(1)}); \quad \boldsymbol{J}^{(j)} = -kT(\boldsymbol{G}^{(j)}, \phi^{(1)}), \tag{10.51a}$$

or, in short,

$$J^{(\varkappa)} = -kT(G^{(\varkappa)}, \phi^{(1)}) \qquad (\varkappa = \lambda, \mu, 1, \ldots, N). \tag{10.51b}$$

Substituting (10.43b), we get the phenomenological equations connecting the currents J to the forces X by means of coefficients L:

$$J^{(\varkappa)} = kT(G^{(\varkappa)}, \sum_{\varkappa'} A^{(\varkappa')} X^{(\varkappa')}) = \sum_{\varkappa'} L^{(\varkappa\varkappa')} X^{(\varkappa')}, \tag{10.52}$$

in which, using (10.44),

$$\begin{cases} L^{(\varkappa\varkappa')} = kT\alpha_{\varkappa'}(G^{(\varkappa)}, A^{(\varkappa')}) = kT\alpha_{\varkappa'}[A^{(\varkappa)}, A^{(\varkappa')}] \\ \qquad\qquad (\alpha_\lambda = \alpha_1 = \ldots = \alpha_N = \tfrac{1}{3};\ \alpha_\mu = \tfrac{1}{5}), \end{cases} \tag{10.53}$$

because, on taking a vector $\boldsymbol{X}$ out of the scalar product (*e.g.*, $\boldsymbol{X}^{(\lambda)}$ out of $(\boldsymbol{G}^{(\lambda)}, \boldsymbol{A}^{(\lambda)} \cdot \boldsymbol{X}^{(\lambda)})$), one has to put in a factor $\frac{1}{3}$, and likewise one includes $\frac{1}{5}$ for a tensor X.

On the other hand, the transport coefficients are usually introduced by writing down the phenomenological equations in the form:

$$\overset{\circ}{\mathsf{P}} = -2\mu\, \overline{\overline{\nabla \boldsymbol{c}_0}}; \tag{10.54a}$$

$$\boldsymbol{\Gamma} = -\lambda' \nabla T - nkT \sum_i D'_{Ti} \boldsymbol{d}_i; \tag{10.54b}$$

$$\langle \boldsymbol{\gamma} \rangle_j = -D_{Tj} \nabla \ln T - \sum_i D_{ji} \boldsymbol{d}_i. \tag{10.54c}$$

Comparing (10.53) and (10.54), we can express the $L^{(\varkappa\varkappa')}$ in terms of the usual transport coefficients:

$$(10.55)\quad L^{(\varkappa\varkappa')} = \begin{array}{c} \\ \varkappa=\mu \\ \lambda \\ 1 \\ \vdots \\ N \end{array} \begin{array}{c} \begin{array}{ccccc} \varkappa'=\mu & \lambda & 1 & \dots & N \end{array} \\ \begin{pmatrix} 2\mu & 0 & 0 & \dots & 0 \\ 0 & \lambda' T & nkTD'_{T1} & \dots & nkTD'_{TN} \\ 0 & nkTD_{T1} & nkTD_{11} & \dots & nkTD_{1N} \\ \vdots & \vdots & \vdots & & \vdots \\ 0 & nkTD_{TN} & nkTD_{N1} & \dots & nkTD_{NN} \end{pmatrix} \end{array}.$$

Inversely, using (10.53), one can put down expressions for the transport coefficients linear or quadratic in the A:

viscosity coefficient:

$$(10.56a)\qquad \mu = \tfrac{1}{10}kT\ \ (\mathsf{G}^{(\mu)}, \mathsf{A}^{(\mu)}) = \tfrac{1}{10}kT\ \ [\mathsf{A}^{(\mu)}, \mathsf{A}^{(\mu)}]$$

heat conductivity coefficient:

$$(10.56b)\qquad \lambda' = \tfrac{1}{3}k\ \ (\mathbf{G}^{(\lambda)}, \mathbf{A}^{(\lambda)}) = \tfrac{1}{3}k\ \ [\mathbf{A}^{(\lambda)}, \mathbf{A}^{(\lambda)}]$$

diffusion thermo-effect coefficient:

$$(10.56c)\qquad D'_{Ti} = (1/3n)(\mathbf{G}^{(\lambda)}, \mathbf{A}^{(i)}) = (1/3n)[\mathbf{A}^{(\lambda)}, \mathbf{A}^{(i)}]$$

thermal diffusion coefficient:

$$(10.56d)\qquad D_{Tj} = (1/3n)(\mathbf{G}^{(j)}, \mathbf{A}^{(\lambda)}) = (1/3n)[\mathbf{A}^{(j)}, \mathbf{A}^{(\lambda)}]$$

multi-component diffusion coefficient:

$$(10.56e)\qquad D_{ji} = (1/3n)(\mathbf{G}^{(j)}, \mathbf{A}^{(i)}) = (1/3n)[\mathbf{A}^{(j)}, \mathbf{A}^{(i)}].$$

These results imply a number of relations between the transport coefficients, which follow from (10:29, 37):

$$(10.57)\qquad D'_{Ti} = D_{Ti}\ ;\quad D_{ij} = D_{ji};$$

$$(10.58)\qquad \sum_i x_i D_{Ti} = 0\ ;\quad \sum_i x_i D_{ij} = \sum_j x_j D_{ij} = 0.$$

Eqs. (10.57) bear out the symmetry of the L matrix (Onsager relations). In (10.56b), λ' is not the coefficients of heat conductivity as it is usually defined. To bring the heat current equation (10.54b) in a form containing the usual λ, we introduce multi-component thermal diffusion ratios k_{Ti} according to:

$$(10.59a)\qquad D_{Tj} = \sum_i D_{ji} k_{Ti};$$

$$(10.59b)\qquad 0 = \sum_i k_{Ti},$$

(here (10.59b) has been added because the N eqs. (10.59a) are dependent)

and we replace $\boldsymbol{d}_i$ in the RHS of (10.54b) by its value as following from (10.54c); this leads to the hybrid expression:

$$\boldsymbol{\Gamma} = -\lambda \nabla T + nkT \sum_i k_{Ti} \langle \boldsymbol{\gamma} \rangle_i, \tag{10.60}$$

in which

$$\lambda = \lambda' - nk \sum_i k_{Ti} D_{Ti} \tag{10.61}$$

is the heat conductivity in the usual sense. An elegant expression for λ in terms of the coefficients A is found by introducing

$$\boldsymbol{\alpha}^{(\lambda)} \stackrel{\text{def}}{=} \boldsymbol{A}^{(\lambda)} - \sum_i k_{Ti} \boldsymbol{A}^{(i)}. \tag{10.62}$$

Using this definition and substituting (10.56b, d) into (10.61), we find:

$$\lambda = \tfrac{1}{3} k [\boldsymbol{A}^{(\lambda)}, \boldsymbol{\alpha}^{(\lambda)}] \tag{10.63}$$

and by substituting (10.56d, e) into (10.59a),

$$[\boldsymbol{A}^{(j)}, \boldsymbol{\alpha}^{(\lambda)}] = 0. \tag{10.64}$$

Combining (10:62, 63, 64), we obtain

$$\lambda = \tfrac{1}{3} k [\boldsymbol{\alpha}^{(\lambda)}, \boldsymbol{\alpha}^{(\lambda)}] = \lambda' - \tfrac{1}{3} k [\sum_i k_{Ti} \boldsymbol{A}^{(i)}, \sum_i k_{Ti} \boldsymbol{A}^{(i)}] \equiv \lambda' - \lambda''. \tag{10.65}$$

λ, λ' and λ'' are all >0 on account of (10.30); $\lambda' > \lambda$ implies that, for a given ∇T, the heat current in the absence of concentration gradients is greater than the one holding in the absence of diffusion currents. In fact, the former situation will develop into the latter if a fixed ∇T is maintained: gradients ∇x_i will establish tending to reduce $\boldsymbol{\Gamma}$ by means of the diffusion thermo-effect (Dufour effect).

Introduction of k_{Ti} in the diffusion equations (10.54c) gives:

$$\langle \boldsymbol{\gamma} \rangle_j = -\sum_i D_{ji} (k_{Ti} \nabla \ln T + \boldsymbol{d}_i). \tag{10.66}$$

For use in the expressions giving the irreversible entropy production (ch. 12), we now give a formulation of the phenomenological relations in terms of independent forces $\hat{X}$, currents $\hat{J}$ and coefficients $\hat{L}$, instead of the present X, J and L which are subject to

$$\sum_i x_i \boldsymbol{J}^{(i)} = 0\,; \quad \sum_i \boldsymbol{X}^{(i)} = 0\,; \quad \det L = 0. \tag{10.67}$$

For this purpose we define $N-1$ forces $\hat{\boldsymbol{X}}^{(i)}$ and $N-1$ currents $\hat{\boldsymbol{J}}^{(i)}$ by

$$\hat{\boldsymbol{X}}^{(i)} = -\boldsymbol{d}_i\,; \quad \hat{\boldsymbol{J}}^{(i)} = nkT \langle \hat{\boldsymbol{\gamma}} \rangle_i \equiv nkT (\langle \boldsymbol{\gamma} \rangle_i - \langle \boldsymbol{\gamma} \rangle_N) \quad (i = 1, \ldots, N-1) \tag{10.68a, b}$$

and $N-1$ thermal diffusion coefficients $\hat{D}_{Ti}$ as well as $(N-1)^2$ concentration diffusion coefficients $\hat{D}_{ij}$ by:

$$\left.\begin{aligned} \hat{D}_{Ti} &= D_{Ti} - D_{TN} && (10.69a) \\ \hat{D}_{ij} &= D_{ij} - D_{iN} - D_{Nj} + D_{NN} && (10.69b) \end{aligned}\right\} \; i, j = 1, \ldots, N-1.$$

Instead of (10.59a, b), $N-1$ independent thermal diffusion ratios k_{Ti} (which coincide with the old k_{Ti} for $i=1, \ldots, N-1$) follow from

$$\hat{D}_{Tj} = \hat{\sum_i} \hat{D}_{ji} k_{Ti}; \tag{10.70}$$

$\hat{\sum}_i$ indicates a summation over $i=1, \ldots, N-1$.

Now both forms of the heat transport equation (10:54b, 60) remain formally unchanged:

$$\left\{ \begin{aligned} \mathbf{\Gamma} &= -\lambda' \nabla T - nkT \hat{\sum_j} \hat{D}_{Tj} \mathbf{d}_j \\ &= -\lambda \nabla T + nkT \hat{\sum_j} k_{Tj} \langle \hat{\boldsymbol{\gamma}}_{/j} \end{aligned} \right. \tag{10.71a, b}$$

the same holds for the equivalent forms of the diffusion equation (10:54c, 66):

$$\left\{ \begin{aligned} \langle \hat{\boldsymbol{\gamma}} \rangle_j &= -\hat{D}_{Tj} \nabla \ln T - \hat{\sum_i} \hat{D}_{ji} \mathbf{d}_i \\ &= -\hat{\sum_i} \hat{D}_{ji} (k_{Ti} \nabla \ln T + \mathbf{d}_i) \end{aligned} \right. \quad \left\{ \; j = 1, \ldots, N-1. \right. \tag{10:72a, b}$$

In particular, for a binary mixture, i and j take the value 1 only; eqs. (10:70, 71, 72) now read:

$$\hat{D}_{T1} = \hat{D}_{11} k_{T1}; \tag{10.73}$$

$$\left\{ \begin{aligned} \mathbf{\Gamma} &= -\lambda' \nabla T - nkT \hat{D}_{T1} \mathbf{d}_1 \\ &= -\lambda \nabla T + nkT k_{T1} \langle \hat{\boldsymbol{\gamma}} \rangle_1 ; \end{aligned} \right. \tag{10.74a, b}$$

$$\left\{ \begin{aligned} \langle \hat{\boldsymbol{\gamma}} \rangle_1 &= -\hat{D}_{T1} \nabla \ln T - \hat{D}_{11} \mathbf{d}_1 \\ &= -\hat{D}_{11} (k_{T1} \nabla \ln T + \mathbf{d}_1). \end{aligned} \right. \tag{10.75a, b}$$

Of course, $\langle \hat{\boldsymbol{\gamma}} \rangle_1$ is the usual diffusion velocity; $\hat{D}_{T1}$ and k_{T1} are the usual coefficient and ratio of binary thermal diffusion; $\hat{D}_{11}$ differs from the binary diffusion coefficient D by a factor $x_1 x_2$:

$$\langle \hat{\boldsymbol{\gamma}} \rangle_1 = \langle \mathbf{C} \rangle_1 - \langle \mathbf{C} \rangle_2 \; ; \quad \hat{D}_{T1} = D_T \; ; \quad k_{T1} = k_T \; ; \quad \hat{D}_{11} = D / x_1 x_2. \tag{10.76a, b, c, d}$$

Finally, we should mention that a formal solution of the integral equations (10.21b) with the use of eigenvalues and eigenfunctions of the collision operators shall be discussed in connection with the Maxwellian gas mixture (chs. 14, 15).

11. *Velocity distribution in the kinetic stage*

We shall now tackle the set of BE (10.1) for an N-component mixture from an starting point more general than that of the ChE theory, like we did for a single gas in chs. 3 and 4. First we shall discuss the case of a *spatially uniform* gas, without external forces; there are N coupled BE reading

$$\partial_t f_i = \sum_j J(f_i f_{j1}) \tag{11.1}$$

and the $N+4$ moments $\psi^{[\lambda]}$ are not only uniform in space, but also constant in time, on account of the integral property (10.6).

In ch. 10 we have already stated that the ChE supposition of a distribution depending on $\mathbf{r}$ and t through $\psi^{[\lambda]}$ leads to the equilibrium solution $f_i^{(0)}(\mathbf{c})$; this MB distribution contains the given values of $\psi^{[\lambda]}$ (or ϱ_i, $\mathbf{c}_0$ and T) as parameters. In the more general method of solving (11.1), there is room for an initial condition:

$$f_i(0) \stackrel{\text{def}}{=} f_i(\mathbf{c}; t=0). \tag{11.2}$$

We write both the solution and its initial value as $f_i^{(0)}$ + a correction term:

$$f_i(\mathbf{c}; t) = f_i^{(0)}(\mathbf{c}; \psi^{[\lambda]}) + \tilde{f}_i(\mathbf{c}; t) = f_i^{(0)}(1 + \tilde{\phi}_i(\mathbf{c}; t)); \tag{11.3}$$

$$f_i(0) = f_i^{(0)}(1 + \tilde{\phi}_i(0)) \tag{11.4}$$

so that both $\tilde{\phi}_i$, for which we are looking, and its initial value $\tilde{\phi}_i(0)$ have the normalization conditions:

$$(\tilde{\phi}, \chi^{[0\lambda]}) = 0; \tag{11.5}$$

$$(\tilde{\phi}(0), \chi^{[0\lambda]}) = 0. \tag{11.6}$$

As we intend to give here a combined discussion of the uniform and the non-uniform case, we immediately write down the general form and the initial value of the general, *non-uniform* solution to (10.1):

$$f_i(\mathbf{c}; \mathbf{r}, t) = f_i^{\mathrm{Ch}}(\mathbf{c}|\psi^{[\lambda]}) + \tilde{f}_i(\mathbf{c}; \mathbf{r}, t) = f_i^{(0)}\{1 + \phi_i + \tilde{\phi}_i(\mathbf{c}; \mathbf{r}, t)\}; \tag{11.7}$$

$$f_i(0) \stackrel{\text{def}}{=} f_i(\mathbf{c}; \mathbf{r}; t=0) = f_i^{\mathrm{Ch}} + f_i^{(0)} \tilde{\phi}_i(0). \tag{11.8}$$

Once more, both the given function $\tilde{\phi}_i(0)$ and the function which we are going to determine, $\tilde{\phi}_i$, have the normalization (11:5, 6).

For both the uniform and the non-uniform case, we now follow chs. 3 and 4: the functions f_i (11:3, 7) are put in the BE (11.1, 10.1); the BE for the ChE parts of f_i are subtracted; a series development of $\tilde{\phi}_i$ is carried out and a parameter θ is duly inserted for separating groups of terms. This leads to a number of integro-differential equations:

$$\boxed{\begin{aligned} &\partial_t \tilde{\phi}_i^{(1)} = -\Omega_i \tilde{\phi}^{(1)}; \qquad (11.9a) \\ &\partial_t \tilde{\phi}_i^{(r)} = \tilde{F}_i^{(r)} - \Omega_i \tilde{\phi}^{(r)} \qquad (11.9b) \end{aligned}} \quad (r \geq 2).$$

Here $\tilde{F}_i^{(r)}$ has different meanings, depending on whether the uniform or the non-uniform mixture is considered; we need not put down the complete expressions, for they can be derived from (3.14) and (4.18) in the same way as $F_i^{(r)}$ (10.22) was derived from $F^{(r)}$ (2.34b), *i.e.*, by

a) replacing $J(f^{(r)} f_1^{(s)})$ by $\sum_j J(f_i^{(r)} f_{j1}^{(s)})$;

b) adding the subscript i to all other f and ϕ.

We assign the whole initial value $\tilde{\phi}_i(0)$ to the first term $\tilde{\phi}_i^{(1)}$:

$$\tilde{\phi}_i^{(1)}(t=0)=\tilde{\phi}_i(0)\ ;\quad \tilde{\phi}_i^{(2)}(t=0)=\ldots=0. \tag{11.10}$$

Again, we normalize the N functions $\tilde{\phi}_i^{(r)}(i=1, \ldots, N)$ by $N+4$ conditions

$$(\tilde{\phi}^{(r)}, \chi^{[0\lambda]})=0; \tag{11.11}$$

between these equations and the $N+4$ solubility conditions for (11.9b):

$$(\tilde{F}^{(r)}, \chi^{[0\lambda]})=0 \tag{11.12}$$

there is the usual relation: (11.11) for $1, \ldots, r-1$ is used in the proof of (11.12), during which, of course, use is made of the properties (10:6, 7).

As we did in the preceding chapter, we postpone a solution of the basic equations which we have formulated (11.9), until the eigenvalue theory of the Maxwellian mixture has been given in ch. 14.

(To be continued)

THEORY OF TRANSPORT AND RELAXATION PHENOMENA IN A GAS MIXTURE. II

ENTROPY PRODUCTION AND THE VARIATIONAL PRINCIPLE

BY

M. J. OFFERHAUS

(Communicated by Prof. J. DE BOER at the meeting of January 28, 1961)

12. *Entropy production*

We start from a definition of the entropy density in a gas mixture in terms of the distribution, analogous to eq. (5.5):

$$s(\boldsymbol{r}) = k \sum_i \int d\boldsymbol{c}\, f_i\{1 + 3 \ln (m_i/h) - \ln f_i\}. \tag{12.1}$$

Like in the single-component case, $\partial_t s$ can be divided in two ways:

$$\text{a)} \qquad \partial_t s = \partial_t (s^{(0)} + s^{(2)} + s^{(3)} + \ldots), \tag{12.2}$$

in which $s^{(0)}$ is based on $f_i^{(0)}$; $s^{(2)}$ contains, in its integrand, the square of the deviation

$$\phi_i = (f_i/f_i^{(0)}) - 1, \tag{12.3}$$

and so on;

$$\text{b)} \qquad \partial_t s = \partial_S s + \partial_C s, \tag{12.4}$$

i.e. s changes due to streaming and to collisions. A comparison between the terms of (12.2) and those of (12.4), for the kinetic and HD stages leads to results completely analogous to those of ch. 5 (see eqs. 5: 29, 34, 37). In particular, the irreversible production of entropy is given by an expression similar to eq. (5.29):

$$\partial_C s \approx k \sum_i (\phi_i, \Omega_i \phi) \equiv k[\phi, \phi]. \tag{12.5}$$

We will now make one remark about the "streaming" term $\partial_S s$, which equally applies to the $N = 1$ case. This term contains contributions of streaming proper and of external forces:

$$\partial_S s = k \sum_i \int d\boldsymbol{c} \left(-\boldsymbol{c} \cdot \frac{\partial f_i}{\partial \boldsymbol{r}} - \boldsymbol{F}_i \cdot \frac{\partial f_i}{\partial \boldsymbol{c}} \right) \{3 \ln (m_i/h) - \ln f_i\}. \tag{12.6}$$

If we take $f_i \approx f_i^{(0)}$ and if $\boldsymbol{F}_i$ is independent of $\boldsymbol{c}$, the $\boldsymbol{F}_i$ contribution vanishes, leaving

$$\partial_S s \approx -\nabla \cdot \boldsymbol{s}, \tag{12.7}$$

in which the entropy current $\boldsymbol{s}$ is logically defined as

$$\boldsymbol{s} = k \sum_i \int d\boldsymbol{c}\, f_i \{1 + 3 \ln (m_i/h) - \ln f_i\}\, \boldsymbol{c}. \tag{12.8}$$

This gives, as the s-balance,

$$\partial_t s + \nabla \cdot \boldsymbol{s} \approx k[\phi, \phi]. \tag{12.9}$$

Comparing this to the HDE for the t-derivatives of ϱ_i, $\boldsymbol{c}_0$ and T (10.12), which read (providing we leave out the $\boldsymbol{F}_i$-term on similar grounds):

$$\partial_t \psi^{[\lambda]} + \nabla \cdot \boldsymbol{\psi}^{[\lambda]+} = 0, \tag{12.10}$$

we see that in both cases the streaming terms are comparable ($\boldsymbol{\psi}^{[\lambda]+}$ is a "ψ-current" defined in a way analogous to (12.8)), but in the s-case there is a "source of entropy" to the amount $k[\phi, \phi]$, whereas the HDE are conservation laws, which express the fact that there are no "ψ-sources".

The result (12.9) holds both in the kinetic and in the HD stage (in the kinetic stage, ϕ_i is the complete deviation (12.3), *i.e.* $\phi_i + \tilde{\phi}_i$ in the notation of ch. 11). In particular, the irreversible entropy production during the *HD stage* can once more be translated in terms of the forces X and currents J. We shall indicate two equivalent methods to obtain this result:

a) starting from the RHS of (12.9), taking $\phi \approx \phi^{(1)}$ and successively applying (10: 21b, 43a, 51b), we find:

$$\left.\begin{aligned} & k[\phi^{(1)}, \phi^{(1)}] = k(\phi^{(1)}, F^{(1)}) = k(\phi^{(1)}, -\sum_\varkappa G^{(\varkappa)} X^{(\varkappa)}) = \\ & \qquad = -k \sum_\varkappa X^{(\varkappa)}(\phi^{(1)}, G^{(\varkappa)}) = T^{-1} \sum_\varkappa J^{(\varkappa)} X^{(\varkappa)}. \end{aligned}\right\} \tag{12.11}$$

This result provides a justification for the choice of forces X and currents J made in (10: 42, 50). (For the relation of the entropy production to X and J in the thermodynamics of irreversible processes, see also De Groot [7]. This reference gives $\partial_C s = \sum JX$, which is obtained by a slightly different definition of X or J).

b) One can also take the LHS of (12.9) and consider this from the thermodynamical viewpoint, following Prigogine [8]. The computation is much longer and we give only the essential points of the reasoning.

According to (12.2), $s \approx s^{(0)}$ (up to terms with $\phi_i{}^2$ and higher); this implies that s can be expressed in terms of $f_i{}^{(0)}$, *i.e.* in terms of n_i, $\boldsymbol{c}_0$ and T, but $\boldsymbol{c}_0$ drops out. In fact,

$$s^{(0)} = T^{-1}(e + p - \sum_i \mu_i n_i), \tag{12.12}$$

in which

$$e = \tfrac{3}{2} nkT \quad \text{and} \quad \mu_i = kT \ln \{n_i (h^2/2\pi m_i kT)^{3/2}\} \tag{12.13a, b}$$

are the internal (kinetic) energy in unit volume and the thermodynamic potential of component i, respectively. The differential relation corre-

sponding to (12.12), if we use n_i and T as independent variables, reads

$$ds^{(0)} = \tfrac{3}{2}\frac{nk}{T}\,dT + \sum_i \left(\tfrac{3}{2}k - \frac{\mu_i}{T}\right) dn_i \tag{12.14}$$

or, with n_i and e as variables,

$$ds^{(0)} = \frac{1}{T}\,de - \sum_i \frac{\mu_i}{T}\,dn_i, \tag{12.15}$$

which is the usual thermodynamical expression (Gibbs' relation per unit volume). Now (12.14) or (12.15) can be used to determine the derivatives of $s(\boldsymbol{r}, t)$ with respect to both $\boldsymbol{r}$ and t; *e.g.*,

$$\partial_t s^{(0)} = \tfrac{3}{2}\frac{nk}{T}\,\partial_t T + \sum_i \left(\tfrac{3}{2}k - \frac{\mu_i}{T}\right) \partial_t n_i. \tag{12.16}$$

Next, (12.3) is put in the definition (12.8) of $\boldsymbol{s}$ and the first two terms are retained, of which the second contains one power ϕ_i in the integrand. This gives

$$\boldsymbol{s} \approx \boldsymbol{s}^{(0)} + \boldsymbol{s}^{(1)} = T^{-1}\{(e+p)\,\boldsymbol{c}_0 - \boldsymbol{q} - \sum_i \mu_i n_i \langle \boldsymbol{c} \rangle_i\}. \tag{12.17}$$

Now we substitute the HDE for $\partial_t n_i$ and $\partial_t T$ (10.13) into (12.16). This leads, together with (12.17), to the following t-derivative of s, corrected for the outflow of entropy:

$$\left.\begin{aligned} \partial_t s + \nabla\cdot\boldsymbol{s} \approx{}& \partial_t s^{(0)} + \nabla\cdot(\boldsymbol{s}^{(0)} + \boldsymbol{s}^{(1)}) = \\ ={}& -\frac{1}{T}\,\mathring{\mathsf{P}}:\nabla\boldsymbol{c}_0 - \frac{1}{T}\,\boldsymbol{q}\cdot\nabla \ln T + \tfrac{3}{2}kn\,\overline{\boldsymbol{C}}\cdot\nabla \ln T - \\ & - k\sum_i \langle \boldsymbol{C}\rangle_i\cdot\nabla n_i + \frac{1}{T}\sum_i \varrho_i \boldsymbol{F}_i\cdot\langle \boldsymbol{C}\rangle_i \\ ={}& -\frac{1}{T}\,\mathring{\mathsf{P}}:\nabla\boldsymbol{c}_0 - \frac{1}{T}\,\boldsymbol{\Gamma}\cdot\nabla \ln T - nk\sum_i \langle \boldsymbol{\gamma}\rangle\cdot\boldsymbol{d}_i - \frac{1}{T}\sum_\varkappa J^{(\varkappa)} X^{(\varkappa)}. \end{aligned}\right\} \tag{12.18}$$

Eqs. (12.11) and (12.18) show that both sides of (12.9) yield approximately $T^{-1}\sum JX$. Apparently, the ChE character of ϕ_i, which was essential for the derivation of (12.11), has also been used in deriving (12.18): only for a ϕ_i of the ChE type, $\partial_t s^{(2)}$, $\nabla\cdot\boldsymbol{s}^{(2)}$ and higher terms may be neglected.

In order to translate $\partial_C s$ into a quadratic form in the forces X or in the currents J, we make use of the alternative forms of the equations of heat conduction and of diffusion (10: 60, 66). We abbreviate these equations by introducing a heat current $\boldsymbol{\Gamma}'$ instead of $\boldsymbol{\Gamma}$ and a diffusion force $\boldsymbol{d}_i'$ instead of d_i as follows:

$$\boldsymbol{\Gamma}' \overset{\text{def}}{=} \boldsymbol{\Gamma} - nkT\sum_i k_{Ti}\langle \boldsymbol{\gamma}\rangle_i; \tag{12.19a}$$

$$\boldsymbol{d}_i' \overset{\text{def}}{=} \boldsymbol{d}_i + k_{Ti}\nabla \ln T. \tag{12.19b}$$

Now eqs. (10: 60, 66), together with (10.54a), form a set of diagonalized phenomenological equations:

$$\mathring{\mathsf{P}} = -2\mu\,\overset{\circ}{\overline{\nabla\boldsymbol{c}_0}}; \tag{12.20a}$$

$$\boldsymbol{\Gamma}' = -\lambda\nabla T; \tag{12.20b}$$

$$\langle \boldsymbol{\gamma}\rangle_j = -\sum_i D_{ji}\boldsymbol{d}_i'. \tag{12.20c}$$

The choice (12.19) has the merit that $T^{-1}\sum JX$ does not change when we replace $\mathbf{\Gamma}$ by $\mathbf{\Gamma}'$ and $\boldsymbol{d}_i$ by $\boldsymbol{d}_i'$; instead of (12.18), we get

$$\frac{1}{T}\sum JX = -\frac{1}{T}\overset{\circ}{\mathsf{P}}{:}\nabla\boldsymbol{c}_0 - \frac{1}{T}\mathbf{\Gamma}'\cdot\nabla\ln T - nk\sum_i \langle\boldsymbol{\gamma}\rangle_i\cdot\boldsymbol{d}_i'. \tag{12.21}$$

Now we can substitute either (10.54) into (12.18) or (12.20) into (12.21):

$$\left.\begin{aligned}\frac{1}{T}\sum JX &= \frac{1}{T}\sum_{\varkappa}\sum_{\varkappa'} L^{(\varkappa\varkappa')}X^{(\varkappa)}X^{(\varkappa')}\\ &= \frac{2\mu}{T}(\dot{\overline{\nabla\boldsymbol{c}_0}})^2 + \lambda'(\nabla\ln T)^2 + 2nk\sum_i D_{Ti}(\nabla\ln T\cdot\boldsymbol{d}_i) + nk\sum_i\sum_j D_{ij}\boldsymbol{d}_i\cdot\boldsymbol{d}_j \qquad (12.22a)\\ &= \frac{2\mu}{T}(\dot{\overline{\nabla\boldsymbol{c}_0}})^2 + \lambda(\nabla\ln T)^2 + nk\sum_i\sum_j D_{ij}\boldsymbol{d}_i'\cdot\boldsymbol{d}_j'. \qquad (12.22b)\end{aligned}\right\}$$

The RHS equals $k[\phi^{(1)},\phi^{(1)}]$ and it is therefore $\geqslant 0$ even if $\dot{\overline{\nabla\boldsymbol{c}_0}}$ and $\nabla T = 0$; apparently the D-matrix must be positive semi-definite.

In fact, $\det D = 0$ and we must recur to a system of independent forces and currents with a positive definite L-matrix, like we did ad the end of ch. 10, in order to invert the eqs. (12.20c). So we introduce $\langle\hat{\boldsymbol{\gamma}}\rangle_i$ and $\hat{D}_{ij}$ by (10: 68b, 69b); we retain the first $N-1$ diffusion forces $\boldsymbol{d}_i'$ as in (12.19b) and also the heat current $\mathbf{\Gamma}'$ as given by (12.19a), which is unchanged, because

$$\mathbf{\Gamma} - nkT\sum_i k_{Ti}\langle\boldsymbol{\gamma}\rangle_i = \mathbf{\Gamma} - nkT\sum_i \hat{k}_{Ti}\langle\hat{\boldsymbol{\gamma}}\rangle_i. \tag{12.23}$$

Eqs. (12.20a, b) do not change, but (12.20c) is replaced by

$$\langle\hat{\boldsymbol{\gamma}}\rangle_j = -\sum_i \hat{D}_{ji}\boldsymbol{d}_i'; \tag{12.24a}$$

this $\hat{D}_{ji}$ is positive definite and we can use the inversion:

$$\boldsymbol{d}_i' = -\sum_j (\hat{D}^{-1})_{ij}\langle\hat{\boldsymbol{\gamma}}\rangle_j. \tag{12.24b}$$

Now we substitute (12: 20a, b; 24b) into (12.21) to obtain:

$$\left.\begin{aligned}\frac{1}{T}\sum JX &= \frac{1}{T}\sum_{\varkappa}\sum_{\varkappa'}(L^{-1})^{(\varkappa\varkappa')}J^{(\varkappa)}J^{(\varkappa')}\\ &= \frac{1}{2\mu T}\overset{\circ}{\mathsf{P}}^2 + \frac{1}{\lambda T^2}\mathbf{\Gamma}'^2 - nk\sum_i\sum_j(\hat{D}^{-1})_{ij}\langle\hat{\boldsymbol{\gamma}}\rangle_i\cdot\langle\hat{\boldsymbol{\gamma}}\rangle_j.\end{aligned}\right\} \tag{12.25}$$

Finally, we give the forms of eqs. (12: 22, 25) for a binary mixture, using (10.76a, c, d):

$$\left.\begin{aligned}\vartheta_{\mathrm{C}}s &\approx \frac{2\mu}{T}(\dot{\overline{\nabla\boldsymbol{c}_0}})^2 + \lambda(\nabla\ln T)^2 + \frac{nkD}{x_1x_2}(\boldsymbol{d}_1 + k_T\nabla\ln T)^2\\ &= \frac{1}{2\mu T}\overset{\circ}{\mathsf{P}}^2 + \frac{1}{\lambda T^2}\{\mathbf{\Gamma} - nkTk_T(\langle\boldsymbol{C}\rangle_1 - \langle\boldsymbol{C}\rangle_2)\}^2 + \frac{nkx_1x_2}{D}(\langle\boldsymbol{C}\rangle_1 - \langle\boldsymbol{C}\rangle_2)^2.\end{aligned}\right\} \tag{12.26}$$

13. *Hydrodynamical solutions by the variational principle*

We would like to give an analysis of the use of the variational principle for obtaining approximative solutions to the integral equations (10.44) for the coefficients A in the HD distribution function $f_i^{(0)}(1-\sum_\varkappa A_i^{(\varkappa)} X^{(\varkappa)})$. By introducing the obvious notation:

$$\hat{\boldsymbol{G}}_i^{(j)} \equiv \boldsymbol{G}_i^{(j)} - \boldsymbol{G}_i^{(N)} \; ; \quad \hat{\boldsymbol{A}}_i^{(j)} \equiv \boldsymbol{A}_i^{(j)} - \boldsymbol{A}_i^{(N)} \tag{13.1}$$

we can write the eqs. (10.44) in the form:

$$\boldsymbol{G}_i^{(\lambda)} = \Omega_i \boldsymbol{A}^{(\lambda)} \; ; \quad \mathsf{G}_i^{(\mu)} = \Omega_i \mathsf{A}^{(\mu)} \; ; \quad \hat{\boldsymbol{G}}_i^{(j)} = \Omega_i \hat{\boldsymbol{A}}^{(j)}, \tag{13.2}$$

or, together,

$$G_i^{(\varkappa)} = \Omega_i A^{(\varkappa)} \qquad (\varkappa = \lambda, \mu, 1, \ldots, N-1). \tag{13.3}$$

Two methods are found in literature for obtaining approximative solutions to the eqs. (13.3): series development of A (Chapman) and the variational method of Enskog. Later in this chapter we will compare these methods and discuss the literature on this subject; it is convenient to postpone this discussion until we have given a survey of the variational treatment.

By the variation method, coefficients A are determined which correspond to maximal values of the *transport coefficients* μ, λ' and $\hat{D}_{jj}$ under certain auxiliary conditions. The physical implications of this maximum requirement are seen by successively taking three situations, in each of which only one type of gradient is present:

a) $\nabla \boldsymbol{c}_0$ only;

b) ∇T only (all $\boldsymbol{d}_i = 0$, cf. (10.34); *e.g.*, $\nabla x_i = 0$; $\boldsymbol{F}_i = 0$; $\nabla \ln n = -\nabla \ln T$, so that the hydrostatic pressure is uniform);

c) ∇x_j only (components other than j and N have uniform concentrations).

For each case, we write down the irreversible entropy production (12.22a):

$$\begin{cases} \text{(a)} \quad \partial_C s \approx (2\mu/T)\,(\overset{\circ}{\overline{\overline{\nabla \boldsymbol{c}_0}}})^2; \\ \text{(b)} \quad \partial_C s \approx \lambda'(\nabla \ln T)^2; \\ \text{(c)} \quad \partial_C s \approx \hat{D}_{jj}(\nabla x_j)^2, \end{cases} \tag{13.4}$$

as well as the "transport current":

$$\begin{cases} \text{(a)} \quad \overset{\circ}{\mathsf{P}} = -2\mu\, \overset{\circ}{\overline{\overline{\nabla \boldsymbol{c}_0}}}; \\ \text{(b)} \quad \boldsymbol{\Gamma} = -\lambda' \nabla T; \\ \text{(c)} \quad \langle \boldsymbol{C} \rangle_j - \langle \boldsymbol{C} \rangle_N \equiv \langle \hat{\boldsymbol{\gamma}} \rangle_j \\ \qquad\qquad = -\hat{D}_{jj} \nabla x_j \equiv -(D_{jj} - D_{jN} - D_{Nj} + D_{NN}) \nabla x_j \; (10.72). \end{cases} \tag{13.5}$$

Clearly, the requirement that μ, λ' and $\hat{D}_{jj}$ shall be maximized, implies that, for given values of the "transport forces" $\nabla \boldsymbol{c}_0$, ∇T and ∇x_j, one obtains:

1) the greatest possible dissipative entropy production, and
2) the greatest possible yield of the transport process.

Now μ, λ' and $\hat{D}_{jj}$ are connected to the coefficients A by means of the eqs. (10.56a, b, e):

$$\left.\begin{array}{ll} \text{(a)} & 10\mu/kT = (\mathsf{G}^{(\mu)}, \mathsf{A}^{(\mu)}) = [\mathsf{A}^{(\mu)}, \mathsf{A}^{(\mu)}]; \\ \text{(b)} & 3\lambda'/k = (\mathsf{G}^{(\lambda)}, \mathsf{A}^{(\lambda)}) = [\mathsf{A}^{(\lambda)}, \mathsf{A}^{(\lambda)}]; \\ \text{(c)} & 3n\,\hat{D}_{jj} = (\hat{\mathsf{G}}^{(j)}, \hat{\mathsf{A}}^{(j)}) = [\hat{\mathsf{A}}^{(j)}, \hat{\mathsf{A}}^{(j)}], \end{array}\right\} \tag{13.6}$$

or, comprehensively,

$$\tau^{(\varkappa)} = (G^{(\varkappa)}, A^{(\varkappa)}) = [A^{(\varkappa)}, A^{(\varkappa)}]. \tag{13.7}$$

This transport coefficient $\tau^{(\varkappa)}$, then, we are going to maximize. If we denote the approximative value of A by $\bar{A}$ and leave out the $\varkappa$ index, we have the requirements that $\bar{A}$ shall be an approximate solution to (13.3):

$$G \approx \Omega\bar{A}, \tag{13.8}$$

and that the approximative value of $\tau^{(\varkappa)}$ obtained by taking, in (13.7), $\bar{A}$ instead of A, shall be an extreme:

$$\delta(G, \bar{A}) = 0 \quad \text{or} \quad \delta[\bar{A}, \bar{A}] = 0. \tag{13.9}$$

Now, instead of (13.8), we introduce the following assumptions, the second of which serves as an auxiliary condition for the extremal value problem:

a) the solution A shall have the form of a finite development in a series of ξ known functions of i and C:

$$A_i(\mathsf{C}) = \sum_{\varrho=0}^{\xi-1} \lambda^{(\varrho)} \sigma_i^{(\varrho)}(\mathsf{C}), \tag{13.10}$$

in which the coefficients λ, which we are going to determine by applying the variational principle, do not depend on i;

b) A shall be orthogonal to the difference between the sides of eq. (13.8):

$$(\bar{A}, G - \Omega\bar{A}) = [\bar{A}, A - \bar{A}] = 0. \tag{13.11}$$

The last three equations: (13: 9, 10, 11) are placed at the base of the approximation method.

As a first consequence of eq. (13.11), we see that one approximative value $\bar{\tau}$ of the transport coefficient τ follows from both expressions (13.7), with $\bar{A}$ instead of A, one linear and one quadratic in $\bar{A}$:

$$\bar{\tau} = (G, \bar{A}) = [\bar{A}, \bar{A}]. \tag{13.12}$$

Secondly, it follows from (13.11) that

$$[A, \bar{A}] = [\bar{A}, A] = [\bar{A}, \bar{A}]. \tag{13.13}$$

This implies that the approximation $\bar{\tau}$ is smaller than the exact τ:

$$\tau - \bar{\tau} = [A, A] - [\bar{A}, \bar{A}] = [A - \bar{A}, A - \bar{A}] > 0 \tag{13.14}$$

because, for any F, $[F, F] \geqslant 0$ (10.30), but the equality sign in (13.14) would only apply if $A - \bar{A}$ were a linear combination of collisional invariants, but these are absent from both A and $\bar{A}$ on account of the usual normalizing conditions, or if $\bar{A} = A$, and this is, of course, excluded.

If we first look for a solution (13.10) consisting of one term only: $\bar{A}_i = \alpha^{(0)} \sigma_i^{(0)}(\mathbf{C})$, the orthogonality condition (13.11) alone is sufficient to fix the one coefficient $\alpha^{(0)}$:

$$\alpha^{(0)} = (\sigma^{(0)}, G)/(\sigma^{(0)}, \Omega\sigma^{(0)}) = G^{(0)}/\Omega^{(00)}, \tag{13.15}$$

in which we have introduced the notation:

$$G^{(\varrho)} \equiv (\sigma^{(\varrho)}, G); \quad \Omega^{(\varrho\varrho')} \equiv (\sigma^{(\varrho)}, \Omega\sigma^{(\varrho')}). \tag{13.16}$$

When the trial function $\bar{A}$ is to consist of two or more terms, its coefficients $\alpha^{(\varrho)}$ are determined by the maximum requirement (13.9) together with the condition (13.11). According to the Lagrange theory, this is equivalent to determining the following *free* extreme:

$$\delta\{(G, \bar{A}) + \lambda(\bar{A}, G - \Omega\bar{A})\} = 0. \tag{13.17}$$

Now the coefficients $\alpha^{(\varrho)} (\varrho = 0, \ldots, \xi - 1)$ and the Lagrange multiplier λ follow from (13: 11, 17). We write these equations using the notation of (13.16):

$$\sum_{\varrho} \alpha^{(\varrho)} G^{(\varrho)} - \sum_{\varrho} \sum_{\varrho'} \alpha^{(\varrho)} \alpha^{(\varrho')} \Omega^{(\varrho\varrho')} = 0; \tag{13.18}$$

$$\delta\{(1 + \lambda) \sum_{\varrho} \alpha^{(\varrho)} G^{(\varrho)} - \lambda \sum_{\varrho} \sum_{\varrho'} \alpha^{(\varrho)} \alpha^{(\varrho')} \Omega^{(\varrho\varrho')}\} = 0, \tag{13.19}$$

i.e.,

$$\frac{\partial}{\partial \alpha^{(\varrho)}} \{ \} = (1 + \lambda) G^{(\varrho)} - 2\lambda \sum_{\varrho'} \alpha^{(\varrho')} \Omega^{(\varrho\varrho')} = 0 \qquad (\varrho = 0, \ldots, \xi - 1). \tag{13.20}$$

If we multiply each equation (13.20) by the corresponding $\alpha^{(\varrho)}$ and sum over ϱ, we get (13.18), provided we take $\lambda = 1$. This determines the value of the multiplier, and now we rewrite (13.20) as ξ equations for the coefficients $\alpha^{(\varrho)}$:

$$G^{(\varrho)} = \sum_{\varrho'} \alpha^{(\varrho')} \Omega^{(\varrho\varrho')} \tag{13.21a}$$

or

$$(\sigma^{(\varrho)}, G - \Omega\bar{A}) = 0. \tag{13.21b}$$

Thus, for $\xi > 1$, the extremal condition (13.9) narrows down the orthogo-

nality condition (13.11), to the effect that $G-\Omega\bar{A}$ is now perpendicular not only to $\bar{A}$, but to each separate function $\sigma^{(\varrho)}$ in the series (13.10) for $\bar{A}$.

We will next discuss the choice of the functions $\sigma_i^{(\varrho)}(\boldsymbol{C})$ to be used in the development (13.10). Of course, if the exact A is required to have the vector or tensor form given in (10.38), we choose all σ to have this same character. The further dependence of σ on $\boldsymbol{C}$ will now be discussed for a *simple gas*. It is by no means necessary to use an orthogonal or complete set of functions σ for the development of $\bar{A}$; one does not generally go further than 1 or 2 terms and if these are suitably chosen, $\bar{\tau}$ will approach τ fairly well. For the coefficient connected with heat conductivity, one usually takes a series:

$$\text{(13.22a)} \qquad \boldsymbol{A}^{(\lambda)} = \sum_{\varrho=0}^{\xi-1} \alpha^{(\lambda)}\, m\boldsymbol{C} S_{3/2}^{(\varrho+1)}(C^{*2}) = m\boldsymbol{C}\{\alpha^{(0)}(\tfrac{5}{2}-C^{*2})+\ldots\}$$

and for the coefficient connected to the viscosity:

$$\text{(13.22b)} \qquad \mathsf{A}^{(\mu)} = \sum_{\varrho=0}^{\xi-1} \alpha^{(\varrho)}\, \overset{\circ}{\boldsymbol{C}}{}^{*}\overset{\circ}{\boldsymbol{C}}{}^{*} S_{3/2}^{(\varrho)}(C^{*2}) = \tfrac{1}{2}\frac{m\overset{\circ}{\boldsymbol{C}}\overset{\circ}{\boldsymbol{C}}}{kT}\{\alpha^{(0)}+\ldots\}.$$

These are developments in eigenfunctions of the operator Ω_{M} for a Maxwellian potential, arranged in order of increasing eigenvalues ω_{M}; in both cases, the first term is proportional to G, the corresponding LHS of the integral equation (13.5), so that, of course, one term only would give an exact solution if we have a *Maxwellian* intermolecular potential. In order to see which choice of $\sigma^{(0)}$ must be made if we treat the *non-Maxwellian* case with a development (13.10) consisting of one term, we write down the transport coefficient $\bar{\tau}$, which follows from (13: 12, 10, 15) if we use $\sigma^{(0)}$ only:

$$\text{(13.23)} \qquad \bar{\tau} = \frac{(\sigma^{(0)},G)^2}{(\sigma^{(0)},\Omega\sigma^{(0)})} = \frac{(\sigma^{(0)},G)^2}{[\sigma^{(0)},\sigma^{(0)}]}.$$

We now compare the $\bar{\tau}$ values as found by successively using, as a one-term trial function $\sigma^{(0)}$, the function G occurring in the LHS of (13.8) and a different function F:

$$\text{(13.24)} \quad \Delta\bar{\tau} = \bar{\tau}_G - \bar{\tau}_F = \frac{(G,G)^2}{[G,G]} - \frac{(F,G)^2}{[F,F]} = \frac{(G,G)^2[F,F]-(F,G)^2[G,G]}{[F,F][G,G]}.$$

G constitutes the best trial function, when this expression is positive for all $F \neq G$. Sufficient for $\Delta\bar{\tau}$ to be >0 is, that Schwarz's inequality:

$$\text{(13.25)} \qquad (F,F)(G,G) > (F,G)^2$$

is supplemented by

$$\text{(13.26)} \qquad \frac{(F,\Omega F)}{(F,F)} > \frac{(G,\Omega G)}{(G,G)}.$$

This last condition is clearly fulfilled, for both the λ- and μ-equations, in the Maxwellian case, if only because $\bar{\tau}_G$ now equals the exact τ and $\bar{\tau}_F$

does not, so that (13.14) applies. For other potentials we have argued in ch. 7 that $(G, \Omega G)/(G, G)$ can be used as an approximation to the lowest positive eigenvalue of Ω corresponding to any eigenfunction of the required vector or tensor character, and therefore, for any F of this same character but different from G, (13.26) will continue to hold.

In the case of the *N-component mixture*, the functions σ used in (13.10) also depend on i, and, instead of (13.22), one might try to use:

$$\text{(13.27a, b)} \quad \bar{\mathbf{A}}_i^{(\lambda;j)} = \sum_{\varrho} \alpha^{(\varrho)} m_i \mathbf{C} S_{ij}^{(\varrho)}(C_i{}^{*2}); \quad \bar{\mathsf{A}}_i^{(\mu)} = \sum_{\varrho} \alpha^{(\varrho)} \mathbf{C}_i{}^{*} \overset{\circ}{\mathbf{C}}_i{}^{*} S_{ij}^{(\varrho)}(C_i{}^{*2}).$$

These developments are satisfying as the $\mathbf{C}$-dependence goes, but they are not subtle enough to render the i-dependence of A. In fact, the use of (13.27b), for $N=2$, leads to an expression for the viscosity of a binary mixture:

$$\text{(13.28)} \qquad \frac{1}{\mu} = \frac{x_1{}^2}{\mu_1} + 2\frac{x_1 x_2}{\mu_{12}} + \frac{x_2{}^2}{\mu_2},$$

which amounts to combining the cross-sections for the three types of collisions in this mixture according to the relative frequency of each collision; this could only serve as a very first approximation.

For the description of binary diffusion, a choice of $\bar{\mathbf{A}}^{(j)}$ as in (13.27a) cannot even roughly serve, because here it is essential that $\mathbf{A}^{(1)}$ and $\mathbf{A}^{(2)}$ should, for each $\mathbf{C}$ value, have opposite signs. That is why we improve (13.27) by taking a development in ξN functions:

$$\text{(13.29)} \quad \sigma_i^{(\varrho)} \equiv \sigma_i^{(r,j)} = \delta_{ij} s_i^{(r)}(\mathbf{C}) \qquad (r=0, \ldots, \xi-1; j=1, \ldots, N),$$

which gives:

$$\text{(13.30a)} \qquad \bar{A}_i(\mathbf{C}) = \sum_r \sum_j \alpha^{(r,j)} \sigma_i^{(r,j)}(\mathbf{C})$$

$$\text{(13.30b)} \qquad = \sum_r a_i^{(r)} s_i^{(r)}(\mathbf{C}) \qquad (\alpha^{(r,i)} \equiv a_i^{(r)}).$$

Using functions σ which contain Kronecker δ's is clearly equivalent to allowing the coefficients α in (13.10) to depend on i.

The scalar product of $\sigma_i^{(r,j)}(\mathbf{C})$, with another function F of i and $\mathbf{C}$, is of course defined according to (10.26):

$$\text{(13.31)} \qquad (\sigma^{(r,j)}, F) = \sum_i \delta_{ij} (s_i^{(r)}, F_i)_i = (s_j^{(r)}, F_j)_j;$$

therefore (13.21b) can be further narrowed down to read:

$$\text{(13.32)} \qquad \boxed{(s_i^{(r)}, G_i \quad \Omega_i \bar{A})_i = 0}$$

for each separate i.

This final result could also have been reached by applying the conditions (13: 9, 11) in order to determine the ξN coefficients $a_i^{(r)}$ in (13.30b), instead of the ξ coefficients $\alpha^{(\varrho)}$ in (13.10). Such a treatment is found in the original formulation of the variational method by Enskog [3],

as well in the accounts of this method given by HELLUND and UEHLING [4] and by HIRSCHFELDER *e.a.* [5]. However, the discussions in references [3] and [4] are limited to single gases and binary mixtures, whereas in the treatment of [5], which holds for an arbitrary number of components, the variational problem (13.9) for $\bar{\tau}$ is unnecessarily subjected to N subsidiary conditions

$$(\bar{A}_i, G_i - \Omega_i \bar{A})_i = 0 \tag{13.33}$$

instead of the one condition (13.11); hence one multiplier λ_i has to be introduced for each i, and, of course, they all prove to be $= 1$. The present treatment shows that one condition (13.11) is sufficient; from the result (13.32) it follows that the N conditions (13.33) are automatically satisfied, and it is not necessary to introduce them *a priori*.

On the other hand, the approximation method for $\bar{A}$, valid for $N = 1$ and 2, as given by CHAPMAN and COWLING [2] does not explicitly introduce the variational principle, but it leads to identical results by way of cutting off determinants of infinite size. Perhaps these authors lay too much stress on the possibility of reaching accurate results by using series developments of the type (13.30b), for the rate of convergence of such a series will markedly depend on the potential field $V(r)$; it is very cumbersome to compute coefficients $a_i^{(r)}$ with $r > 1$, and, when the number of them, ξ, is increased, they all have to be calculated over again. Moreover these higher terms are not even of great interest, because the $\bar{\tau}$ calculated at $\xi = 1$ or 2 are optimal and, in general, they compare favourably to experimental data.

We shall finally give the explicit form of the result (13.32). To this end, (13.30b) is substituted into (13.32). As we also did in (10.24b), we replace the operator Ω_i by W_i, which has a more simple linearity property (see 10.25). (We would like to point out that the rather special "linearity character" of the Ω_i operator has not played a role whatever in the variational treatment). This leads to:

$$(s_i^{(r)}, G_i)_i = \sum_{r'} \sum_j a_j^{(r')} (s_i^{(r)}, W_{ij} s^{(r')}) \tag{13.34a}$$

or

$$G_i^{(r)} = \sum_{r'} \sum_j a_j^{(r')} W_{ij}^{(rr')}, \tag{13.34b}$$

if we use an obvious notation analogous to (13.16). This provides us with ξN equations which determine the coefficients $a_j^{(r')}$. Of course, G_i has a different meaning, depending on whether we consider the μ-, λ- or j-equations (see 10.39), and so have $s_i^{(r)}$. In fact, the coefficients $a_i^{(r)}$ should bear an additional index μ, λ or j, which we have omitted for convenience (moreover, the a vary with the degree of approximation ξ).

We mention for completeness that, in the λ- and j-cases, the system (13.34) contains N dependent equations, viz. those with $r = 0$; one of

them is superfluous and must be replaced by the normalizing condition (10.45):

$$(m\mathbf{C}, \mathbf{A}) = 0 \quad \text{or} \quad \sum_j a_j^{(0)} x_j m_j = 0. \tag{13.35}$$

The transport coefficients are expressed in terms of the a by substituting (13.30b) into (13.12):

$$\bar{\tau} = (G, \bar{A}) = \sum_r \sum_i (G_i, a_i^{(r)} s_i^{(r)})_i = \sum_r \sum_i a_i^{(r)} G_i^{(r)}. \tag{13.36}$$

Eqs. (13: 34, 35, 36) summarize the results of the variational treatment. The choice of an orthogonal set of functions $s^{(r)}$, which includes G, is mainly useful because all but one of the coefficients $G_i^{(r)} \equiv (s_i^{(r)}, G_i)_i$, occurring in both (13.34) and (13.36), are zero.

(To be continued)

THEORY OF TRANSPORT AND RELAXATION PHENOMENA IN A GAS MIXTURE. III

THE MAXWELLIAN MIXTURE

BY

M. J. OFFERHAUS

(Communicated by Prof. J. DE BOER at the meeting of January 28, 1961)

14. *Eigenvalue theory*

In ch. 7 it was shown that the theory of transport and relaxation in a simple gas is considerably simplified in the case of the Maxwellian intermolecular potential. The fact that the differential cross-section $\alpha(g, \chi)$ does not depend on the relative velocity $g = |\mathbf{c} - \mathbf{c}_1|$ of the colliding particles, makes it possible to find the eigenvalues and eigenfunctions of the Ω operator.

In a mixture, a similar simplification takes place if one supposes that the interaction between all pairs of molecules (i, j) is of the Maxwell form:

$$V_{ij}(r) = \varkappa_{ij}/r^4. \tag{14.1}$$

As in the single-component theory, the exact results for this Maxwellian mixture will be closely analogous to those holding for the general potential field in first approximation. Therefore we shall, in chs. 14–17, consider the Maxwellian mixture only; the symbols will not carry the subscript M.

In this chapter we shall discuss the eigenvalue problem of the operator:

$$\left\{ \begin{aligned} \Omega_{ij}\,\phi(\mathbf{c}) \equiv \int d\varepsilon \int d\chi \sin\chi \int d\mathbf{c}_1 f_j^{(0)}(\mathbf{c}_1)\, \varkappa_{ij}(g,\chi) \cdot \\ \cdot \{\phi_i(\mathbf{c}) + \phi_j(\mathbf{c}_1) - \phi_i(\mathbf{c}') - \phi_j(\mathbf{c}_1')\} \\ = \omega_{ij}\,\phi_i(\mathbf{c}). \end{aligned} \right. \tag{14.2}$$

The only property of the Maxwell interaction (14.1) of which we shall make use, is the fact that α_{ij} does not depend on g. This property is characteristic of a wider class of interaction potentials, and the present discussion applies to all these.

As to the Maxwell case, α_{ij} has the form:

$$\alpha_{ij}(\chi) = (\varkappa_{ij}/\mu_{ij})^{\frac{1}{4}} \alpha^*(\chi), \tag{14.3}$$

in which μ_{ij} is the reduced mass of the i-j pair:

$$\mu_{ij} = m_i\, m_j/(m_i + m_j) \tag{14.4}$$

and $\alpha^*(\chi)$ is a dimensionless function of χ common to all pairs i-j, which was already determined by J. C. MAXWELL himself; for its explicit form, we refer to [9].

We shall now solve the eigenvalue problem (14.2) by the method of generating functions, which has been applied by WALDMANN [6] to the case of a single Maxwell gas. It is clear that the solutions will contain the parameters n_j, $\mathbf{c}_0$ and T occurring in the MB distribution:

$$f_j^{(0)}(\mathbf{c}_1) = n_j (m_j/2\pi kT)^{3/2} \exp\{-(m_j/2kT)(\mathbf{c}_1 - \mathbf{c}_0)^2\}. \tag{14.5}$$

Of these, n_j will only enter as a factor in the eigenvalue ω_{ij}. As for $\mathbf{c}_0$, we shall first suppose it to be $=0$; it is easy to see that, once the eigenvalue problem for this special case:

$$\Omega_{ij}^{(0)}\,\phi(\mathbf{c}) \overset{\text{def}}{=} \Omega_{ij}^{(\mathbf{c}_0=0)}\,\phi(\mathbf{c}) = \omega_{ij}\,\phi_i(\mathbf{c}) \tag{14.6}$$

has been solved, we can use these eigenvalues ω_{ij}, along with the ϕ_i at the value $\mathbf{c} - \mathbf{c}_0$ of the argument, as solutions for the case $\mathbf{c}_0 \neq 0$:

$$\Omega_{ij}\,\phi(\mathbf{c} - \mathbf{c}_0) = \omega_{ij}\,\phi_i(\mathbf{c} - \mathbf{c}_0). \tag{14.7}$$

The temperature T will occur in the eigenfunctions ϕ_i; it disappears when we introduce dimensionless reduced velocities as follows:

$$\mathbf{c}^*/c = \mathbf{c}'^*/c' = (m_i/2kT)^{\frac{1}{2}}; \quad \mathbf{c}_1^*/c_1 = \mathbf{c}_1'^*/c_1' = (m_j/2kT)^{\frac{1}{2}}. \tag{14.8a, b}$$

In this notation, the Ω_{ij} operator for $\mathbf{c}_0 = 0$ reads:

$$\left.\begin{aligned} \Omega_{ij}^{(0)}\,\phi(\mathbf{c}) = \pi^{-3/2} n_j \int d\varepsilon \int d\chi \sin\chi\, \alpha_{ij}(\chi) \int d\mathbf{c}_1 \exp(-\mathbf{c}_1^2) \cdot \\ \cdot \{\phi_i(\mathbf{c}) + \phi_j(\mathbf{c}_1) - \phi_i(\mathbf{c}') - \phi_j(\mathbf{c}_1')\}. \end{aligned}\right\} \tag{14.9}^*$$ [1]

The motion of particles i and j with velocities $\mathbf{c}, \mathbf{c}_1$ before collision can be separated into:

a) motion of centre of gravity: mass $m_i + m_j$, velocity

$$\mathbf{g}_0 = \beta^2 \mathbf{c} + \beta_1^2 \mathbf{c}_1; \tag{14.10a}$$

b) relative motion: mass μ_{ij} (14.4), velocity

$$\mathbf{g} = -\mathbf{c} + \mathbf{c}_1. \tag{14.10b}$$

Here we have introduced:

$$\beta = \{m_i/(m_i + m_j)\}^{\frac{1}{2}}; \quad \beta_1 = \{m_j/(m_i + m_j)\}^{\frac{1}{2}} \qquad (\beta^2 + \beta_1^2 = 1). \tag{14.11}$$

After collision, i and j have velocities $\mathbf{c}', \mathbf{c}_1'$; $\mathbf{g}_0$ has not changed, but

$$\mathbf{g}' = -\mathbf{c}' + \mathbf{c}_1' \text{ with } g' = g. \tag{14.10c}$$

In the course of the following derivation, we shall temporarily introduce

---

[1] * after the *equation* number indicates that all occurring velocities are reduced ones.

a fixed velocity vector $\mathbf{v}$; velocities from which $\mathbf{v}$ has been subtracted are indicated by corresponding capital letters:

$$\mathbf{C} = \mathbf{c} - \mathbf{v}, \text{ etc. } ; \quad \mathbf{G}_0 = \mathbf{g}_0 - \mathbf{v}. \tag{14.12}$$

Earlier we used this notation to denote peculiar velocities, but there is no danger of confusion because $\mathbf{v}$ will disappear from eq. (14.42) onwards and the peculiar velocities will not return until eq. (14.46b).

$\mathbf{C}$ and $\mathbf{C}'$ are reduced as in (14.8a), $\mathbf{C}_1$ and $\mathbf{C}_1'$ as in (14.8b), whereas:

$$\mathbf{g}_0^*/g_0 - \mathbf{G}_0^*/G_0 = \mathbf{v}^*/v = \{(m_i + m_j)/2kT\}^{\frac{1}{2}}; \tag{14.13a}$$

$$\mathbf{g}^*/g - \mathbf{g}'^*/g' = (\mu_{ij}/2kT)^{\frac{1}{2}}. \tag{14.13b}$$

The following relations hold between the reduced velocities, instead of (14: 10, 12):

$$\mathbf{g}_0 = \beta\mathbf{c} + \beta_1\mathbf{c}_1 \; ; \quad \mathbf{g} = -\beta_1\mathbf{c} + \beta\mathbf{c}_1 \; ; \quad \mathbf{g}' = -\beta_1\mathbf{c}' + \beta\mathbf{c}_1' \; ; \quad g' = g; \tag{14.14}*$$

$$\mathbf{C}^{(\prime)} = \mathbf{c}^{(\prime)} - \beta\mathbf{v} \; ; \quad \mathbf{C}_1^{(\prime)} = \mathbf{c}_1^{(\prime)} - \beta_1\mathbf{v} \; ; \quad \mathbf{G}_0 = \mathbf{g}_0 - \mathbf{v}. \tag{14.15}*$$

The rotation of the $\mathbf{g}$ vector [1]), which takes place in the course of a collision, is described by

$$\mathbf{g}' = \mathbf{g}\cos\chi + \mathbf{h}\sin\chi\cos\varepsilon + \mathbf{k}\sin\chi\sin\varepsilon, \tag{14.16}*$$

in which $\mathbf{g}$, $\mathbf{h}$ and $\mathbf{k}$ are three mutually orthogonal vectors of equal length. The direction for which the azimuth $\varepsilon = 0$ can be chosen arbitrarily in the plane $\perp \mathbf{g}$; a choice on the intersection of this plane with the plane of $\mathbf{g}$ and $\mathbf{G}_0$ is convenient, because now

$$\mathbf{G}_0 \cdot \mathbf{k} = 0 \; ; \quad \mathbf{G}_0 \cdot \mathbf{h} = \pm|\mathbf{G}_0 \wedge \mathbf{g}| = \pm|\mathbf{C} \wedge \mathbf{C}_1|. \tag{14.17}*$$

We use these relations to derive expressions for C'^2 and $C_1'^2$ in terms of $\mathbf{C}$ and $\mathbf{C}_1$. First, C'^2 is expressed in $\mathbf{G}_0$ and $\mathbf{g}'$ (see 14: 14, 15), then $\mathbf{g}'$ is expressed in $\mathbf{g}$, $\mathbf{h}$ and $\mathbf{k}$ (14.16):

$$\left\{ \begin{aligned} C'^2 = (\beta\mathbf{G}_0 - \beta_1\mathbf{g}')^2 = \beta^2 G_0^2 - 2\beta\beta_1 \mathbf{G}_0 \cdot (\mathbf{g}\cos\chi + \mathbf{h}\sin\chi\cos\varepsilon + \\ + \mathbf{k}\sin\chi\sin\varepsilon) + \beta_1^2 g^2. \end{aligned} \right. \tag{14.18}*$$

Now we return to $\mathbf{C}$ and $\mathbf{C}_1$ by means of (14.17) and

$$\left\{ \begin{aligned} G_0^2 &= \beta^2 C^2 + 2\beta\beta_1 \mathbf{C}\cdot\mathbf{C}_1 + \beta_1^2 C_1^2; \\ g^2 &= \beta_1^2 C^2 - 2\beta\beta_1 \mathbf{C}\cdot\mathbf{C}_1 + \beta^2 C_1^2; \\ \mathbf{G}_0 \cdot \mathbf{g} &= -\beta\beta_1 C^2 + (\beta^2 - \beta_1^2)\mathbf{C}\cdot\mathbf{C}_1 + \beta\beta_1 C_1^2. \end{aligned} \right. \tag{14.19}*$$

This leads to:

$$C'^2 = PC^2 + P_1 C_1^2 + 2Q\,\mathbf{C}\cdot\mathbf{C}_1 \pm 2R|\mathbf{C} \wedge \mathbf{C}_1|\cos\varepsilon; \tag{14.20a}*$$

$$C_1'^2 = P_1 C^2 + P C_1^2 - 2Q\,\mathbf{C}\cdot\mathbf{C}_1 \pm 2R|\mathbf{C} \wedge \mathbf{C}_1|\cos\varepsilon, \tag{14.20b}*$$

[1]) From now on up to eq. (14.45), all symbols in the *text* are also supposed to be reduced.

in which we have used the abbreviations:

$$(14.21)\qquad \begin{cases} P=1-4\beta^2\beta_1{}^2\cos^2\psi\,; & P_1=4\beta^2\beta_1{}^2\cos^2\psi; \\ Q=2\beta\beta_1(\beta^2-\beta_1{}^2)\cos^2\psi\,; & R=2\beta\beta_1\sin\psi\cos\psi. \end{cases}$$

Here ψ is used instead of χ:

$$(14.22)\qquad \chi+2\psi=\pi.$$

Evidently,

$$(14.23)\qquad P+P_1=1\,;\quad PP_1=Q^2+R^2.$$

We quote the following integrals for future reference:

$$(14.24a)\qquad \int d\boldsymbol{x}\exp\left(-Ax^2\pm 2\boldsymbol{B}\cdot\boldsymbol{x}\right)=\pi^{3/2}A^{-3/2}\exp\left(B^2/A\right);$$

$$(14.24b)\qquad \begin{cases} \int d\varepsilon\int d\boldsymbol{x}\exp\left(-Ax^2\pm 2\boldsymbol{B}\cdot\boldsymbol{x}\pm 2|\boldsymbol{D}\wedge\boldsymbol{x}|\cos\varepsilon\right)= \\ \qquad =2\pi^{5/2}A^{-3/2}\exp\left\{(B^2+D^2)/A\right\}\cdot I_0(2|\boldsymbol{B}\wedge\boldsymbol{D}|/A). \end{cases}$$

Here $I_0(z)$ is the zero-order Bessel function of the imaginary argument iz.

Now we are ready for the determination of the eigenvalues and eigenfunctions of Ω_{ij} as given by (14.9). To this end, $\Omega_{ij}{}^{(0)}$ is applied to the generating function of the Sonine polynomials with argument C^2, which reads:

$$(14.25)^*\qquad \mathcal{S}_{l+\frac{1}{2}}(C^2;s)\equiv(1-s)^{-l-3/2}\exp\left(-\sigma C^2\right),$$

in which

$$(14.26)\qquad \sigma\overset{\text{def}}{=}s/(1-s).$$

Omitting the numerical factor $(1-s)^{-l-3/2}$ for the time being, we obtain:

$$(14.27)^*\qquad \Omega_{ij}{}^{(0)}\exp\left(-\sigma C^2\right)\equiv\pi^{-3/2}n_j\int d\chi\sin\chi\,\alpha_{ij}(\chi)(J+J_1-J'-J_1');$$

of the four integrals J, the last three can be handled by using (14.24a, b):

$$(14.27a)^*\qquad J=\int d\varepsilon\int d\boldsymbol{c}_1\exp\left(-c_1{}^2-\sigma C^2\right)=2\pi^{5/2}\exp\left(-\sigma C^2\right);$$

$$(14.27b)^*\qquad \begin{cases} J_1=\int d\varepsilon\int d\boldsymbol{c}_1\exp\left(-c_1{}^2\quad\sigma C_1{}^2\right)\cdot \\ \quad=2\pi\int d\boldsymbol{c}_1\exp\left\{-(1+\sigma)c_1{}^2+2\sigma\beta_1\,\boldsymbol{v}\cdot\boldsymbol{c}_1-\sigma\beta_1{}^2v^2\right\}= \\ \quad=2\pi^{5/2}(1-s)^{3/2}\exp\left(-s\beta_1{}^2v^2\right); \end{cases}$$

$$(14.27c)^*\qquad \begin{cases} J'=\int d\varepsilon\int d\boldsymbol{C}_1\exp\left(-c_1{}^2-\sigma C'^2\right)= \\ \quad=\int d\varepsilon\int d\boldsymbol{C}_1\exp\left\{-(\boldsymbol{C}_1+\beta_1\boldsymbol{v})^2\right. \cdot \\ \qquad\qquad\left.-\sigma(PC^2+P_1C_1{}^2+2Q\boldsymbol{C}\cdot\boldsymbol{C}_1\pm 2R|\boldsymbol{C}\wedge\boldsymbol{C}_1|\cos\varepsilon)\right\}= \\ \quad=2\pi^{5/2}\{(1-s)/(1-sP)\}^{3/2}\exp\left\{s(1-sP)^{-1}\cdot\right. \\ \qquad\qquad\left.\cdot(PC^2+P_1\beta_1{}^2v^2+2Q\beta_1\boldsymbol{C}\cdot\boldsymbol{v})\right\}\cdot \\ \qquad\qquad\cdot I_0\{s(1-sP)^{-1}\cdot 2R\beta_1|\boldsymbol{C}\wedge\boldsymbol{v}|\}; \end{cases}$$

$$(14.27d)^*\quad \begin{cases} J_1' = \int d\varepsilon \int d\mathbf{C}_1 \exp\,(-c_1^2 - \sigma C_1'^2) = \\ \quad = 2\pi^{5/2}\{(1-s)/(1-sP_1)\}^{3/2} \exp\,\{s(1-sP_1)^{-1}\cdot \\ \qquad\qquad \cdot (P_1 C^2 + P\beta_1^2 v^2 - 2Q\beta_1\, \mathbf{C}\cdot\mathbf{v})\}\cdot \\ \qquad\qquad\qquad \cdot I_0\{s(1-sP_1)^{-1}\cdot 2R\beta_1 |\mathbf{C}\wedge\mathbf{v}|\}. \end{cases}$$

Now we return from $\mathbf{C}$ to $\mathbf{c}$ by means of (14.15); if $\varkappa$ denotes the angle between $\mathbf{c}$ and $\mathbf{v}$,

$$(14.28)^*\qquad \mathbf{c}\cdot\mathbf{v} = cv\cos\varkappa;\ |\mathbf{C}\wedge\mathbf{v}| = |\mathbf{c}\wedge\mathbf{v}| = cv\sin\varkappa.$$

This gives:

$$(14.29)^*\quad \begin{cases} \Omega_{ij}^{(0)} \exp\,\{-\sigma(c^2 - 2\beta cv\,\cos\varkappa + \beta^2 v^2)\} = \\ = 2\pi n_j \int d\chi \sin\chi\ \alpha_{ij}(\chi)\cdot \\ \qquad \cdot [\exp\{-\sigma(c^2 - 2\beta cv\cos\varkappa + \beta^2 v^2)\} + (1-s)^{3/2}\exp(-s\beta_1^2 v^2) - \\ \quad - \{(1-s)/(1-sP\ )\}^{3/2}\cdot \\ \qquad \cdot \exp\{-sP\ (1-sP\ )^{-1}c^2 + 2s(1-sP\ )^{-1}\cdot \\ \qquad\qquad\qquad \cdot (1-2\beta_1^2\cos^2\psi)\,\beta cv\cos\varkappa - V\ v^2\}\cdot \\ \qquad\quad \cdot I_0\{\ \ 4s\ \ (1-sP\ )^{-1}\beta\beta_1^2\sin\psi\cos\psi\ cv\sin\varkappa\} - \\ \quad \{(1\ \ s)\ (1\ \ sP_1)\}^{3/2}\cdot \\ \qquad \cdot \exp\{-sP_1(1-sP_1)^{-1}c^2 + 4s(1-sP_1)^{-1}\cdot \\ \qquad\qquad\qquad \cdot \beta\beta_1^2\cos^2\psi\cdot cv\cos\varkappa\ \ \ -\ \ \ V_1 v^2\}\cdot \\ \qquad\quad \cdot I_0\{\ \ 4s\ \ \ (1-sP_1)^{-1}\beta\beta_1^2\sin\psi\cos\psi\ cv\sin\varkappa\}], \end{cases}$$

in which V and V_1 are coefficients which we do not write down explicitly, because they will not be needed. We write the $\varkappa$-dependent factors in the terms of the expression between square brackets [ ] as follows:

$$(14.30)\quad \begin{cases} K(\varkappa) \overset{\text{def}}{=} \exp\,(\Theta\cos\varkappa); \\ K'(\varkappa) \overset{\text{def}}{=} \exp\,(\Theta'\sin\theta\cos\varkappa)\cdot I_0(\Theta'\cos\theta\sin\varkappa); \\ K_1'(\varkappa) \overset{\text{def}}{=} \exp\,(\Theta_1'\cos\psi\cos\varkappa)\cdot I_0(\Theta_1'\sin\psi\sin\varkappa), \end{cases}$$

in which

$$(14.31)\qquad \operatorname{tg}\theta = (1-2\beta_1^2\cos^2\psi)/(2\beta_1^2\sin\psi\cos\psi);$$

$$(14.32)^*\quad \begin{cases} \Theta &= 2\sigma\beta cv; \\ \Theta' &= 2s(1-sP)^{-1}\beta cvP^{\frac{1}{2}}; \\ \Theta_1' &= 2s(1-sP_1)^{-1}\beta_1 cvP_1^{\frac{1}{2}}. \end{cases}$$

The three functions $K(\varkappa)$ shall now be developed in Legendre polynoms $P_l(\cos\varkappa)$. As for the first one,

$$(14.33)\qquad K(\varkappa) = \exp\,(\Theta\cos\varkappa) = \sum_{l=0}^{\infty} P_l(\cos\varkappa)(2l+1)\,i^l j_l(-i\Theta),$$

in which j_l is a Bessel function of half-odd order:

$$j_l(z) \stackrel{\text{def}}{=} (\pi/2z)^{\frac{1}{2}} J_{l+\frac{1}{2}}(z). \tag{14.34}$$

As for K' and K_1', I_0 came in during the integration (14.24b). We go back one step and put

$$I_0(z) = (2\pi)^{-1} \int_0^{2\pi} d\lambda \exp(z \cos\lambda); \tag{14.35}$$

this gives

$$K_1'(\varkappa) = (2\pi)^{-1} \int_0^{2\pi} d\lambda \exp(\Theta_1' \cos\xi), \tag{14.36}$$

in which ξ is the angle between two vectors with polar coordinates $(\theta, 0)$ and $(\varkappa, \lambda)$. Now we develop $\exp(\Theta_1' \cos\xi)$ in $P_l(\cos\xi)$ as in (14.33), then develop $P_l(\cos\xi)$ in sperical harmonics of $(\theta, 0)$ and $(\varkappa, \lambda)$, and finally integrate over λ:

$$K_1'(\varkappa) = \sum_{l=0}^{\infty} P_l(\cos\varkappa)\, P_l(\cos\psi)(2l+1)\, i^l j_l(-i\Theta_1'); \tag{14.37b}$$

$$K'(\varkappa) = \sum_{l=0}^{\infty} P_l(\cos\varkappa)\, P_l(\sin\theta)(2l+1)\, i^l j_l(-i\Theta'). \tag{14.37a}$$

Substitution of (14: 30, 33, 37) into (14.29) gives:

$$\sum_{l=0}^{\infty} L_l (2l+1)\, P_l(\cos\varkappa) = 0, \tag{14.38a}*$$

in which L_l is the following operator:

$$\left.\begin{aligned} L_l \equiv\ & \Omega_{ij}^{(0)}\, [\exp\{-\sigma(c^2+\beta^2 v^2)\, k_l(\Theta)\}] - \\ & - 2\pi n_j \int d\chi \sin\chi\, \alpha_{ij}(\chi) \cdot [\exp\{-\sigma(c^2+\beta^2 v^2)\, k_l(\Theta)\} + \\ & + (1-s)^{3/2} \exp(-s\beta_1{}^2 v^2)\, \delta_{l0} - \\ & - \{(1-s)/(1-sP)\}^{3/2} \exp\{-sP\,(1-sP)^{-1} c^2 - V\, v^2\} \cdot \\ & \cdot P_l(\sin\theta)\, k_l(\Theta') - \\ & - \{(1-s)/(1-sP_1)\}^{3/2} \exp\{-sP_1(1-sP_1)^{-1} c^2 - V_1 v^2\} \cdot \\ & \cdot P_l(\cos\psi)\, k_l(\Theta_1')]. \end{aligned}\right\} \tag{14.38b}*$$

Here it is understood that $\Omega_{ij}^{(0)}$ acts on $[\ ]\,(2l+1)\, P_l(\cos\varkappa)$; k_l is an abbreviation of:

$$k_l(z) \stackrel{\text{def}}{=} i^l j_l(-iz). \tag{14.39}$$

Now we develop $P_l(\cos\varkappa)$ in spherical harmonics $Y_{lm}^{(*)}$ of the directions of **c** and **v**, which we call $(\vartheta\varphi)$ and $(\vartheta'\varphi')$; next we multiply by $Y_{l'm'}(\vartheta'\varphi')$, and then integrate over all directions $(\vartheta'\varphi')$. It appears that (14.38a) is narrowed down to read:

$$L_l Y_{lm}(\vartheta\varphi) = 0 \tag{14.40}*$$

for each separate l, m. Each term of L_l contains a factor $k_l(\text{const.}\, v)$;

$k_l(z)$ shares with $j_l(z)$ the property that a series development in powers of z starts with z^l:

$$k_l(z) = 2^l\, l!\, \{(2l+1)!\}^{-1} z^l + \mathcal{O}(z^{l+1}). \tag{14.41}$$

Using this property, we divide (14.40) by $l!\, 2^l v^l/(2l+1)!$ and then take the limit $v \to 0$:

$$\begin{aligned} &\Omega_{ij}^{(0)}\,\{\exp(-\sigma c^2)\cdot(2\sigma\beta c)^l\, Y_{lm}(\vartheta\varphi)\} = \\ &= 2\pi n_j \int d\chi \sin\chi\, \alpha_{ij}(\chi)\, Y_{lm}(\vartheta\varphi)\cdot\{\exp(-\sigma c^2)\cdot(2\sigma\beta c)^l\,(1-s)^{s}\delta_{l0} \\ &\quad -\{(1-s)/(1-sP)\}^{s/2}\exp\{-sP(1-sP)^{-1}c^2\}\cdot \\ &\qquad\cdot P_l(\sin\theta)\{2s(1-sP)^{-1}\beta c P^{\frac{1}{2}} \quad\} - \\ &\quad -\{(1-s)/(1-sP_1)\}^{s/2}\exp\{-sP_1(1-sP_1)^{-1}c^2\}\cdot \\ &\qquad\cdot P_l(\cos\psi)\{2s(1-sP_1)^{-1}\beta_1 c P_1^{\frac{1}{2}}\}]. \end{aligned} \tag{14.42}^*$$

Divide by $(2s)^l(1-s)^{s/2}$ and introduce the generating function $\mathscr{S}$ according to (14.25):

$$\begin{aligned} &\Omega_{ij}^{(0)}\,\{(\beta c)^l\, \mathscr{S}_{l+\frac{1}{2}}(c^2; s)\, Y_{lm}(\vartheta\varphi)\} = \\ &\qquad = 2\pi n_j \int d\chi \sin\chi\, \alpha_{ij}(\chi)\,(\beta c)^l\, Y_{lm}(\vartheta\varphi)\cdot \\ &\cdot\{\mathscr{S}_{l+\frac{1}{2}}(c^2; s) + \delta_{l0} - \mathscr{S}_{l+\frac{1}{2}}(c^2; sP)\, P^{\frac{1}{2}l} P_l(\sin\theta) - \\ &\qquad - \mathscr{S}_{l+\frac{1}{2}}(c^2; sP_1)\, P_1^{\frac{1}{2}l}(\beta_1/\beta)^l P_l(\cos\psi)\}. \end{aligned} \tag{14.43}^*$$

Differentiate r times with respect to s and let $s \to 0$: the $\mathscr{S}$-functions render Sonine polynomials according to

$$S_{l+\frac{1}{2}}^{(r)}(x) = \lim_{s\to 0}\left(\frac{\partial}{\partial s}\right)^r \mathscr{S}_{l+\frac{1}{2}}(x; s), \tag{14.44}$$

and we get the eigenvalue equation for $\mathbf{c}_0 = 0$:

$$\begin{aligned} &\Omega_{ij}^{(0)}\,\{(\beta c)^l\, S_{l+\frac{1}{2}}^{(r)}(c^2)\, Y_{lm}(\vartheta\varphi)\} = 2\pi n_j \int d\chi \sin\chi\, \alpha_{ij}(\chi)\cdot \\ &\qquad\cdot\{1 + \delta_{l0}\,\delta_{r0} - P^{r+\frac{1}{2}l} P_l(\sin\theta) - P_1^{r+\frac{1}{2}l}(\beta_1/\beta)^l P_l(\cos\psi)\}\cdot \\ &\qquad\qquad\cdot\{(\beta c)^l\, S_{l+\frac{1}{2}}^{(r)}(c^2)\, Y_{lm}(\vartheta\varphi)\}. \end{aligned} \tag{14.45}^*$$

Now we give the results of the following four steps:

(a) return to natural values of $\mathbf{c}$ instead of reduced ones;

(b) derive the result for the general Ω_{ij} (for $\mathbf{c}_0 \neq 0$) from $\Omega_{ij}^{(0)}$ (for $\mathbf{c}_0 = 0$), in the way indicated in (14.7);

(c) introduce the symbol $\mathbf{C}$ in the original meaning of $\mathbf{c} - \mathbf{c}_0$;

(d) multiply both sides by $\{2kT(m_i + m_j)\}^{\frac{1}{2}l}$.

This gives the general eigenvalue equations:

$$\Omega_{ij}\,\chi_i^{(lmr)} = \omega_{ij}^{(lr)}\,\chi_i^{(lmr)}; \tag{14.46}$$

$$\omega_{ij}^{(lr)} = 2\pi n_j \int d\chi \sin\chi\, \alpha_{ij}(\chi)\cdot \cdot\{1 + \delta_{l0}\delta_{r0} - P^{r+\frac{1}{2}l} P_l(\sin\theta) - P_1^{r+\frac{1}{2}l}(\beta_1/\beta)^l P_l(\cos\psi)\}; \tag{14.46a}$$

$$\chi_i^{(lmr)}(C, \vartheta, \varphi) = (m_i C)^l\, S_{l+\frac{1}{2}}^{(r)}(m_i C^2/2kT)\, Y_{lm}(\vartheta\varphi). \tag{14.46b}$$

We have not changed the notation $(\vartheta\varphi)$, which was used in (14: 40–45) to denote the polar angles of c; in (14.46b), of course, polar angles of C are meant.

As far as the C-dependence of the eigenfunctions $\chi_i^{(lmr)}$ goes, they are identical to the $\chi^{(lmr)}$ for the single gas case (eqs. 7: 3, 5). Of course, the difference lies in the fact that, in the eigenfunctions for $N>1$, m_i occurs and the operator Ω_{ij} works on both the C- and the i-dependence of χ.

In the derivation of (14.46), all RHS contain four terms corresponding to the four terms: $\phi_i, \phi_{j1}, -\phi_i', -\phi_{j1}'$ in the definition (14.2) of Ω_{ij}. If we had accordingly split up Ω_{ij} into four parts from the beginning:

$$(14.47)\qquad \begin{cases} \Omega_{\mathrm{I}}\phi &= \int d\varepsilon \int d\chi \sin\chi \int d\mathsf{c}_1 f_j^{(0)}(\mathsf{c}_1)\,\alpha_{ij}(\chi)\,\phi_i(\mathsf{c}) \\ \Omega_{\mathrm{II}}\phi &= \phi_j(\mathsf{c}_1) \\ \Omega_{\mathrm{III}}\phi &= \phi_i(\mathsf{c}_1') \\ \Omega_{\mathrm{IV}}\phi &= \phi_j(\mathsf{c}_1'), \end{cases}$$

we would have found four separate eigenvalue equations:

$$(14.48\text{a, b, c, d})\qquad \Omega_{\mathrm{I,II,III,IV}}\,\chi(\mathsf{c}) = \omega_{\mathrm{I,II,III,IV}}\,\chi_i(\mathsf{c}),$$

in which $\omega_{\mathrm{I},\ldots,\mathrm{IV}}$, in the given order, are the four terms of the eigenvalue $\omega_{ij}^{(lr)}$ (14.46a) and χ_i is the eigenfunction given in (14.46b). The first two equations (14.48a, b) are trivial (at least in the case of a Maxwellian mixture, in which α does not depend on g), for Ω_{I} is a mere multiplication and Ω_{II} applied to any of the functions (14.46b), apart from $\chi_i^{(000)}=1$, yields zero on account of the orthogonality properties of the Sonine polynomials and those of the spherical harmonics.

This also means that we have solved the eigenvalue problems of the operators

$$(14.49)\qquad Y_{ij} \equiv \Omega_{\mathrm{I}} + \Omega_{\mathrm{III}}\,; \quad Z_{ij} \equiv \Omega_{\mathrm{II}} + \Omega_{\mathrm{IV}}.$$

The solutions read:

$$(14.50)\qquad Y_{ij}\,\chi_i^{(lmr)} = y_{ij}^{(lr)}\,\chi_i^{(lmr)}\,; \quad Z_{ij}\,\chi_j^{(lmr)} = z_{ij}^{(lr)}\,\chi_i^{(lmr)}.$$

Here, $\chi_i^{(lmr)}$ are the functions given in (14.46b); the eigenvalues y_{ij} and z_{ij} together yield ω_{ij} as of (14.46a):

$$(14.50\text{a})\qquad \begin{cases} y_{ij}^{(lr)} = 2\pi n_j \int d\chi \sin\chi\,\alpha_{ij}(\chi)\cdot \\ \cdot\{1-(1-4\beta^2\beta_1^2\cos^2\psi)^{r+\frac{1}{2}l} P_l([1-2\beta_1^2\cos^2\psi][1-4\beta^2\beta_1^2\cos^2\psi]^{-\frac{1}{2}})\}\,; \end{cases}$$

$$(14.50\text{b})\qquad z_{ij}^{(lr)} = -2\pi n_j \int d\chi \sin\chi\,\alpha_{ij}(\chi)\,(2\beta\beta_1\cos\psi)^{2r+l} P_l(\cos\psi);$$

$$(14.51)\qquad y_{ij}^{(lr)} + z_{ij}^{(lr)} = \omega_{ij}^{(lr)}.$$

Moreover, the χ_i are also eigenfunctions of the W_{ij} operator defined in (10.24):

$$(14.52\text{a, b})\qquad W_{ij}\,\chi^{(lmr)} = w_{ij}^{(lr)}\,\chi_i^{(lmr)}\,; \quad w_{ij}^{(lr)} = z_{ij}^{(lr)} + \delta_{ij}\sum_k y_{ik}^{(lr)}.$$

In the multi-component case considered, simple recursion formulae between the eigenvalues, like those holding for the single Maxwell gas, are not obvious. Here we shall mention only those eigenvalues y, z and eigenfunctions χ, which correspond to an eigenvalue $\omega_{ij}=0$:

$$
\left\{\begin{array}{ll}
\text{(a)} & l=0,\ r=0\colon\ \chi_i^{(000)} = 1; \qquad\qquad y_{ij}^{(00)} = -z_{ij}^{(00)} = 0. \\
\text{(b)} & l=1,\ r=0\colon\ \chi_i^{(1m0)} = m_i C Y_{1m}(\vartheta\varphi);\ y_{ij}^{(10)} = -z_{ij}^{(10)} = \\
 & \qquad\qquad = 2\pi n_j\ \beta_1{}^2 \int d\chi \sin\chi\ \alpha_{ij}(\chi)(1-\cos\chi). \\
\text{(c)} & l=0,\ r=1\colon\ \chi_i^{(001)} = \tfrac{3}{2} - \dfrac{m_i C^2}{2kT};\qquad y_{ij}^{(01)} = -z_{ij}^{(01)} = \\
 & \qquad\qquad = 4\pi n_j \beta^2 \beta_1{}^2 \int d\chi \sin\chi\ \alpha_{ij}(\chi)(1-\cos\chi).
\end{array}\right. \tag{14.53}
$$

We have found only five eigenfunctions χ_i with $\omega_{ij}=0$, whereas we stated in (10.5) that there are $N+4$ collional invariants χ_i. This is because the method used above generates functions χ of C which only depend parametrically on i. On the other hand, for the derivation of the N conservation laws for the mass densities ϱ_i (10.13a), we have, instead of the one function $\chi_i^{(000)}=1$ of (14.53a), used the N collisional invariants $\chi_i^{[01.k]}=\delta_{ik}m_k$ (10.5a), which are all eigenfunctions of both Y_{ij} and Z_{ij} at the eigenvalue $y_{ij}=z_{ij}=0$. This last property is shared by each function $\chi_i(m_1, \ldots, m_N)$ of all N masses, and conservation laws could be formulated for the moments of all these functions, but the conservation laws (10.13a) for the moments of the $\chi_i^{[01.k]}$ are of special importance.

We may remark that, for the l-r-combinations (00), (10) and (01), corresponding to $\omega_{ij}^{(lr)}=0$, the eigenvalues of W_{ij} take an especially simple form:

$$
\left\{\begin{array}{ll}
i=j\colon & w_{ii} = \sum_{k\neq i}{}' y_{ik} = -\sum_{k\neq i}{}' z_{ik}; \\
i\neq j\colon & w_{ij} = z_{ij} = -y_{ij}.
\end{array}\right. \tag{14.54}
$$

The $\chi_i^{(lmr)}$ as defined in (14.46b) are mutually orthogonal but not normalized. Normalization is of course possible, but it should be noticed that, if we use normalized eigenfunctions:

$$
\bar{\chi}_i^{(lmr)} = \alpha_i^{(lr)}\, \chi_i^{(lmr)}, \tag{14.55}
$$

in which

$$
\{\alpha_i^{(lr)}\}^{-2} = (ii)^{(lr)} \overset{\text{def}}{=} (\chi_i^{(lmr)*}, \chi_i^{(lmr)})_i, \tag{14.56}
$$

some of the corresponding eigenvalues are different from those given in (14: 46a, 50a, 50b, 52b). This is seen by looking at the linearity properties (10.25):

$$
\left\{\begin{array}{l}
Y_{ij}\chi_i = y_{ij}\chi_i \to Y_{ij}(\alpha_i\chi_i) = y_{ij}\alpha_i\chi_i; \\
Z_{ij}\chi_j = z_{ij}\chi_i \to Z_{ij}(\alpha_j\chi_j) = (\alpha_j/\alpha_i)\cdot z_{ij}\alpha_i\chi_i.
\end{array}\right. \tag{14.57a}
$$

Evidently, when we replace the eigenfunction $\chi_i^{(lmr)}$, with eigenvalues $(y, z, w, \omega)_{ij}^{(r)}$, by the normalized eigenfunction (14.55), we get eigen-

values, some of which are now different:

$$(14.58)\quad \begin{cases} \bar{y}_{ij}^{(lr)} = y_{ij}^{(lr)} \ ; \quad \bar{z}_{ij}^{(lr)} = (\alpha_j^{(lr)}/\alpha_i^{(lr)})\, z_{ij}^{(lr)} ; \\ \bar{\omega}_{ij}^{(lr)} = \bar{y}_{ij} + \bar{z}_{ij}^{(lr)} \ ; \quad \bar{w}_{ij}^{(lr)} = \bar{z}_{ij}^{(lr)} + \delta_{ij} \sum_k \bar{y}_{ik}^{(lr)}. \end{cases}$$

In ch. 16, where the normalization of the χ plays a role, we do not use these $\bar{\chi}$ and $\bar{w}$, etc.; the old values will be used and $(ii)^{(lr)}$ is introduced when necessary.

15. *Transport properties*

We shall now indicate how the eigenvalue theory given in ch. 14 is put to use for determining the transport properties of the Maxwellian mixture by the procedure outlined in ch. 10.

We recall that the relative deviation of f_i^{Ch} from a local MB distribution $f_i^{(0)}$ is given by $\phi_i^{(1)}$ as of (10.36); the coefficients A occurring in this ϕ follow from the integral equations (10.39a, b, c) supplemented by the normalizing conditions (10.41a, b). The special advantage of considering a Maxwellian mixture lies in the fact that the functions G, which are the LHS of the eqs. (10.39), are found among the χ_i, the eigenfunctions of the operators Ω_{ij}, Y_{ij}, Z_{ij} and W_{ij} of the Maxwellian gas mixture:

$$(15.1)\qquad \mathbf{G}_i^{(\lambda)} \to \chi_i^{(1m1)} \ ; \quad \mathsf{G}_i^{(\mu)} \to \chi_i^{(2m0)} \ ; \quad \mathbf{G}_i^{(j)} \to \chi_i^{(1m0)}.$$

In each case $\varkappa$, the $\to$ sign indicates that the independent components of $G_i^{(\varkappa)}$ are linear combinations of the $2l+1$ degenerate $\chi_i^{(lmr)}$ (l and r fixed). Therefore the exact solutions to each eq. (10.39) will be given by its LHS, G, times an i-dependent coefficient:

$$(15.2\mathrm{a,b,c})\quad \mathbf{A}_i^{(\lambda)} = a_i^{(\lambda)} (\tfrac{5}{2} - C_i^{*2})\, m_i \mathbf{C} ; \ \mathsf{A}_i^{(\mu)} = a_i^{(\mu)}\, \mathbf{C}_i^* \overset{\circ}{\mathbf{C}}_i^* ; \ \mathbf{A}_i^{(j)} = a_i^{(j)}\, m_i \mathbf{C},$$

in which the coefficients a are found by substituting (15.2) back into (10.39) and (10.41). The resulting equations are brought in the nicest form by using W_i instead of Ω_i, so that the linearity property (10.25a) of the W operator can be used:

$$(15.3\mathrm{a})\qquad (\tfrac{5}{2} - C_i^{*2})\, \mathbf{C} = W_i \{ a^{(\lambda)} (\tfrac{5}{2} - C_i^{*2})\, \mathbf{C} \} = (\tfrac{5}{2} - C_i^{*2})\, m_i \mathbf{C} \sum_j w_{ij}^{(11)}\, a_j^{(\lambda)},$$

$$\text{or} \qquad 1/m_i = \sum_j w_{ij}^{(11)}\, a_j^{(\lambda)} ;$$

$$(15.3\mathrm{b})\qquad -2\mathbf{C}_i^* \overset{\circ}{\mathbf{C}}_i^* = W_i (a^{(\mu)}\, \mathbf{C}_i^* \overset{\circ}{\mathbf{C}}_i^*) \quad = \mathbf{C}_i^* \overset{\circ}{\mathbf{C}}_i^* \sum_j w_{ij}^{(20)}\, a_j^{(\mu)},$$

$$\text{or} \qquad -2 = \sum_j w_{ij}^{(20)}\, a_j^{(\mu)} ;$$

$$(15.3\mathrm{c})\qquad \{1 - (\delta_{ik}/x_i)\}\, \mathbf{C} = W_i (a^{(k)} m \mathbf{C}) \quad = m_i \mathbf{C} \sum_j w_{ij}^{(10)}\, a_j^{(k)},$$

$$\text{or} \quad (1/m_i)\{1 - (\delta_{ik}/x_i)\} = \sum_j w_{ij}^{(10)}\, a_j^{(k)} ;$$

$$(15.3\mathrm{d})\qquad 0 = (a^{(k)} m \mathbf{C}, m \mathbf{C}),$$

$$\text{or} \qquad 0 = \sum_j x_j m_j a_j^{(k)}.$$

The normalization of $\mathbf{A}^{(\lambda)}$ (10.41a) does not give rise to a separate equation, because $\mathbf{A}^{(\lambda)}$ as given by (15.2a) is already orthogonal to $m\mathbf{C}$. The normalization of $\mathbf{A}^{(k)}$ (10.41b) is expressed by (15.3d); this is a useful supplement to the eqs. (15.3c), because the matrix $w_{ij}^{(10)}$ is of rank $N-1$ (cf. eq. 14.54).

The transport coefficients are expressed by eqs. (10.56) in terms of G and A; substitute G and A from (10.39; 15.2):

$$(15.4)\quad \begin{cases} \text{(a)} & \mu = \frac{1}{10}kT \sum_j (-2\mathbf{C}_j{}^{\circ}\mathbf{C}_j{}^{*}, a_j^{(\mu)}\mathbf{C}_j{}^{*}\mathbf{C}_j{}^{\circ}\mathbf{C}_j{}^{*})_j = -\tfrac{1}{2}nkT\sum_j x_j a_j^{(\mu)}; \\ \text{(b)} & \lambda' = \lambda = \tfrac{1}{3}k \sum_j ([\tfrac{5}{2} \quad C_j{}^{*2}]\mathbf{C}, a_j^{(\lambda)}[\tfrac{5}{2} - C_j{}^{*2}]m_j\mathbf{C})_j = \tfrac{5}{2}nk^2T\sum_j x_j a_j^{(\lambda)}; \\ \text{(c)} & D_{Tl} = (1/3n)\sum_j ([1-(\delta_{ij}/x_i)]\mathbf{C}, a_j^{(\lambda)}[\tfrac{5}{2} - C_j{}^{*2}]m_j\mathbf{C})_j = 0; \\ \text{(d)} & D_{ik} = (1/3n)\sum_j ([1-(\delta_{ij}/x_i)]\mathbf{C}, a_j^{(k)}m_j\mathbf{C}) = kT(\sum_j x_j a_j^{(k)} - a_i^{(k)}). \end{cases}$$

The thermal diffusion coefficients are all zero; according to (10.61), λ and λ' coincide.

Eqs. (15: 3, 4) give the framework for an exact calculation of the transport coefficients of a Maxwellian mixture. They are analogous to the approximate expressions (13: 34, 35, 36) for the general potential field. The eqs. of ch. 13 contained matrix elements of the W_{ij} operator between eigenfunctions of the Maxwellian Ω_{ij} and W_{ij}; instead of these, the eqs. of this chapter, of course, contain the eigenvalues w_{ij}. In both chapters, the coefficients a and the transport coefficients (τ, or μ, λ, D) have similar meanings.

To get explicit values of the transport coefficients, the w_{ij} values given by (14: 50, 52b) should be inserted in (15.3). We shall illustrate this on the simple case of *binary diffusion*. First we introduce

$$(15.5)\quad M_1 = m_1/(m_1+m_2)\,; \quad M_2 = m_2/(m_1+m_2)\,; \quad \mu_{12} = m_1m_2/(m_1+m_2);$$

$$(15.6)\quad r = \varrho/\{n(m_1+m_2)\} = x_1M_1 + x_2M_2.$$

From (14: 54, 53b) we see that the elements of the w_{ij} matrix for $N=2, l=1, r=0$ can all be expressed in one quantity containing the 1-2 differential cross-section only:

$$(15.7)\quad w \overset{\text{def}}{=} 2\pi n\mu_{12}\int d\chi \sin\chi\, \varkappa_{12}(\chi)\,(1-\cos\chi),$$

as follows:

$$(15.8)\quad \begin{cases} w_{11} = \quad y_{12} = \quad wx_2/m_1 & w_{12} = -y_{12} = -wx_2/m_1 \\ w_{21} = -y_{21} = -wx_1/m_2 & w_{22} = \quad y_{21} = \quad wx_1/m_2. \end{cases}$$

For $k=1$, the two equations (15.3c), which are identical and (15.3d) can be written as follows:

$$(15.9a)\quad \begin{cases} 1/x_1w = \quad -a_1^{(1)} \quad +a_2^{(1)} \\ \qquad 0 = x_1M_1a_1^{(1)} + x_2M_2a_2^{(1)}, \end{cases}$$

with the solution:

(15.10a) $$a_1^{(1)} = -x_2 M_2/x_1 rw;\ a_1^{(2)} = M_1/rw.$$

Similarly, for $k=2$,

(15.9b) $$\begin{cases} 1/x_2 w = a_1^{(2)} - a_2^{(2)} \\ 0 = x_1 M_1 a_1^{(2)} + x_2 M_2 a_2^{(2)}; \end{cases}$$

(15.10b) $$a_1^{(2)} = M_2/rw;\ a_2^{(2)} = -x_1 M_1/x_2 rw.$$

Substituting (15.10a, b) into (15.2c) and thence into (10.36), we conclude that, for a binary Maxwellian mixture with a concentration gradient $\nabla x = \nabla x_1 = -\nabla x_2$ only, the *distribution* ϕ_i reads:

(15.11) $$\phi_1 = -\frac{\mu_{12}}{rw}\mathbf{C}\cdot\frac{\nabla x}{x_1};\quad \phi_2 = \frac{\mu_{12}}{rw}\mathbf{C}\cdot\frac{\nabla x}{x_2}.$$

According to (10.76d), the binary *diffusion coefficient* reads:

(15.12) $$D = x_1 x_2\,\hat{D}_{11} = x_1 x_2\,(D_{11} - D_{12} - D_{21} + D_{22}).$$

Substitute the D_{ik} as given by (15.4d):

(15.13a) $$D = kT x_1 x_2(-a_1^{(1)} + a_1^{(2)} + a_2^{(1)} - a_2^{(2)}),$$

or, inserting the a-coefficients from (15.10a, b) and using (15.6),

(15.13b) $$\boxed{D = kT/w \equiv kT/\{2\pi\mu_{12}\textstyle\int d\chi \sin\chi\,\alpha_{12}(\chi)(1-\cos\chi)\}.}$$

We compare this result to the usual ChE formulae for the first approximation to D:

(15.14) $$[D]_1 = 3kT/(16\, n\mu_{12}\Omega_{12}^{(1,1)})$$

with

(15.15) $$\Omega_{12}^{(1,1)} = \pi^{\frac{1}{2}}\int_0^\infty e^{-g^{*2}} g^{*4}\,dg^* \int_0^\pi d\chi \sin\chi\,\alpha_{12}(g^*,\chi)(1-\cos\chi)$$

($\mathbf{g}^*$ as defined in (14.13b)). Introducing the property of the Maxwell interaction: α_{12} independent of g^*, we get:

(15.16) $$\Omega_{12}^{(1,1)} = \pi^{\frac{1}{2}}\cdot\tfrac{3}{8}\pi^{\frac{1}{2}}\cdot(w/2\pi n\mu_{12})$$

and (15:14, 15, 16) together yield (15.13b): the ChE first approximation leads, for a binary Maxwellian mixture, to the exact value of the diffusion coefficient, as it should.

If we substitute the A coefficients of (15.2) back into (10.36), the resulting $\phi_i^{(1)}$ is an exact solution of the integral equation $F_i^{(1)} = \Omega_i\phi^{(1)}$ (10.21b, $r=1$). Thus, for a Maxwellian mixture, the formal developments of $F_i^{(1)}$ and $\phi_i^{(1)}$ in eigenfunctions of Ω (cf. the developments (2: 46, 47) for the $N=1$ case) break off very soon.

16. *Relaxation of the velocity distribution*

In the preceding chapter it was shown that, for a Maxwellian mixture, the development of the first non-MB term in the ChE velocity distribution, $\phi_1^{(1)}$, in eigenfunctions of Ω_{ij} consists of a few terms only. We now turn to the equations derived in ch. 11 for the *non-ChE* or *kinetic* terms of f_i: $\tilde{\phi}_i^{(r)}(r = 1, 2, \ldots)$:

a) integral equations (11.9);
b) initial conditions (11.10);
c) normalizing conditions (11.11);
d) normalization of the initial condition (11.6).

The formal solution is again based on development of the $\tilde{\phi}_i^{(r)}$ in eigenfunctions, $\chi_i^{(lmr)}$, of Ω_{ij}. As has been mentioned at the end of ch. 14, we shall use χ which are mutually orthogonal but not normalized:

$$(\chi_i^{(lmr)*}, \chi_i^{(l'm'r')})_i = \delta_{lmr,l'm'r'}(ii)^{(lr)} \tag{16.1}$$

(cf. eq. 14.56). In the following, we shall suppose that all χ_i are real (to this end, spherical harmonics with real φ-dependent parts are used); now the complex-conjugate sign * can be omitted from all scalar products.

We start with the first equation, (11.9a); develop $\tilde{\phi}_i^{(1)}$ in χ_i:

$$\tilde{\phi}_i^{(1)} = \sum_{lmr} \chi_i^{(lmr)} \tilde{\varphi}_i^{(lmr)} \tag{16.2}$$

and

$$\tilde{\phi}_i^{(1)}(t=0) = \tilde{\phi}_i(0) = \sum_{lmr} \chi_i^{(lmr)} \varphi_i^{(lmr)}(0), \tag{16.3}$$

in which the coefficients

$$\tilde{\varphi}_i^{(lmr)}(0) = (\tilde{\phi}_i(0), \chi_i^{(lmr)})_i / (ii)^{(lr)} \tag{16.4}$$

are known. Substituting (16.2) into the equations (11.9a), we find, for each lmr, N coupled first-order differential equations for $\tilde{\varphi}_i^{(lmr)}$:

$$\partial_t \tilde{\varphi}_i^{(lmr)} = -\sum_j w_{ij}^{(lr)} \tilde{\varphi}_j^{(lmr)}. \tag{16.5}$$

The solutions read, of course:

$$\tilde{\varphi}_i^{(lmr)} = \sum_k \tilde{\varphi}_{ik}^{(lmr)} \exp(-w_k^{(lr)} t); \tag{16.6}$$

putting this back in (16.5) and equalizing coefficients of each $\exp(-w_k t)$, we find:

$$\tilde{\varphi}_{ik}^{(lmr)} w_k^{(lr)} = \sum w_{ij}^{(lr)} \tilde{\varphi}_{jk}^{(lmr)} \tag{16.7a}$$

or

$$\sum_j (w_{ij}^{(lr)} - \delta_{ij} w_k^{(lr)}) \tilde{\varphi}_{jk}^{(lmr)} = 0; \tag{16.7b}$$

for fixed lr, each w_k occurring in the exponents of (16.6) is an eigenvalue of the $w_{ij}^{(lr)}$-matrix, and the eqs. (16.7) determine the components

$\tilde{\varphi}_{ik}(i=1, \ldots, N)$ of the corresponding eigenvector, together with the N initial conditions:

$$\tilde{\varphi}_i^{(lmr)}(0) = \sum_k \tilde{\varphi}_{ik}^{(lmr)}, \tag{16.8}$$

where the LHS are given by (16.4).

The key role of inverse relaxation times is played by the eigenvalues, $w_k^{(lr)}$, of the $w_{ij}^{(lr)}$ matrix. There are $\nu(\leqslant N)$ of these; we number them by $k(=0, \ldots, \nu-1)$. If w_k has a multiplicity $m_k(\sum_k m_k = N)$, the N equations (16.7b) for fixed $lmrk$ at $i=1, \ldots, N$ have a coefficient matrix of rank $N-m_k$. So the number of independent equations supplied by eqs. (16: 7, 8) amounts to

$$\sum_{k=0}^{\nu-1} (N-m_k) + N = N\nu - \sum_{k=0}^{\nu-1} m_k + N = N\nu, \tag{16.9}$$

which equals the number of coefficients $\tilde{\varphi}_{ik}$ to be determined.

We now recall that the matrix element $[F, F] \equiv (F, WF)$ is positive unless F is a collisional invariant, when it is 0 (eq. 10.30); if we put $F_i = \chi_i^{(lmr)}$, we find:

$$\sum_i \sum_j (ii)^{(lr)} w_{ij}^{(lr)} \geqslant 0. \tag{16.10}$$

It follows that, for general χ, the $w_{ij}^{(lr)}$-matrix is positive definite and all its eigenvalues $w_k > 0$. An exception is formed by the collisional invariants. For $\chi_i^{(000)} = 1$, all $w_{ij}^{(00)} = 0$; for $\chi_i^{(1m0)}$ and $\chi_i^{(001)}$, the w_{ij}-matrix is given by eq. (14.54):

$$(w_{ij}) = \begin{pmatrix} z_{11} - \sum_j z_{1j} & z_{12} & \cdots & z_{1N} \\ z_{21} & z_{22} - \sum_j z_{2j} & & \cdot \\ \vdots & \vdots & & \cdot \\ z_{N1} & z_{N2} & \cdots & z_{NN} - \sum_j z_{Nj} \end{pmatrix} \tag{16.11}$$

Clearly $\det w = 0$, as is seen by adding all columns. The matrix for N components, to be indicated by the symbol $w(N)$, is positive semi-definite and of rank $N-1$. This is proved by induction as follows: for $N=1$, $w(1)$ consists of one element 0. Suppose $w(2)$ to be positive semi-definite of rank 1; ...; $w(N-1)$ to be positive semi-definite of rank $N-2$. For each of these matrices, this implies that all principal submatrices are positive definite and the corresponding determinants (principal minors) are >0.

Now consider the $N-1$ principal submatrices of $w(N)$ found by taking only the elements with $i, j \leqslant n (n=1, \ldots, N-1)$ and call them $p(n)$. Such a $p(n)$ differs from $w(n)$ in that its diagonal elements are greater by an amount

$$p_{ii}(n) - w_{ii}(n) = -\sum_{j=n+1}^{N} z_{ij} = q_{ii}(n), \tag{16.12}$$

which is >0 because all α_{ij} are >0 and $1-\cos\chi\geqslant 0$ (see 14.53b, c). If one adds one positive term $q_{ii}(n)$ to the ii-element of $w(n)$, det $w(n)$ is increased by an amount $q_{ii}(n)m_{ii}(n)$, where $m_{ii}(n)$ is the minor of the ii-element in $w(n)$. Both q and m are >0, so the replacement of one diagonal element in the positive semi-definite matrix $w(n)$ by the corresponding element of $p(n)$ already yields a positive definite matrix, and continuing in this way we find a complete $p(n)$ which is certainly positive definite.

Evidently, det $w(N)=0$ and all its principal minors of increasing size: det $p(n)$ with $n=1, \ldots, N-1$ are >0. This proves that $w(N)$ is a positive semi-definite matrix of rank $N-1$, Q.E.D.

We conclude that the inverse relaxation times of (16.6) have the following signs:

$$\begin{cases} lr=10,01: w_0^{(lr)}=0;\ w_1^{(lr)}, \ldots, w_{\nu-1}^{(lr)}>0; \\ l+r>1 \quad : w_0^{(lr)}, \ldots, w_{\nu-1}^{(lr)}>0. \end{cases} \tag{16.13}$$

The only terms in (16.6) which do not die out in time are the constant ones at $lr=10, 01$; $k=0$. These, however, are ruled out by the normalization of $\tilde{\phi}_t$, as can be shown in the following way.

Apply (11.11) to the solution $\tilde{\phi}^{(1)}$ given by (16: 2, 6):

$$(\tilde{\phi}^{(1)}, \chi^{(lmr)}) = \sum_i (ii)^{(lr)} \sum_k \tilde{\varphi}_{ik}^{(lmr)} \exp(-w_k^{(lr)} t) = 0, \quad (lmr = 1m0, 001) \tag{16.14}$$

which for each separate k value yields:

$$\sum_i (ii)^{(lr)} \tilde{\varphi}_{ik}^{(lmr)} = 0 \qquad (lmr = 1m0, 001). \tag{16.15}$$

For each of the four lmr values concerned, this gives ν additional conditions on the $\tilde{\varphi}_{ik}$, but we have already argued (see 16.9) that these $N\nu$ coefficients are fully determined by the eqs. (16: 7, 8). Now it can be shown, to begin with, that the eqs. (16.15) for $k=1, \ldots, \nu-1$ are dependent on the set (16.7). To this end, we multiply each eq. (16.7a) by $(ii)^{(lr)}$ and take $\sum_i$:

$$\begin{cases} w_k^{(lr)} \sum_i (ii)^{(lr)} \tilde{\varphi}_{ik}^{(lmr)} = \sum_j \tilde{\varphi}_{jk}^{(lmr)} \sum_i w_{ij}^{(lr)} (ii)^{(lr)} = \\ \qquad\qquad = \sum \tilde{\varphi}_{jk}^{(lmr)} \sum_i W_{ij}^{(lr)} = 0, \end{cases} \tag{16.16}$$

in which

$$W_{ij}^{(lr)} \equiv (\chi i^{(lmr)}, W_{ij} \chi^{(lmr)})_t = w_{ij}^{(lr)} (ii)^{(lr)}. \tag{16.17}$$

These $W_{ij}^{(lr)}$ can be expressed in terms of $Z_{ij}^{(lr)}$ in the same way as we wrote $w_{ij}^{(lr)}$ in terms of $z_{ij}^{(lr)}$ (16.11), viz.

$$W_{ij}^{(lr)} = Z_{ij}^{(lr)} - \delta_{ij} \sum_k Z_{ik}^{(lr)}. \qquad (lr = 10, 01) \tag{16.18}$$

It follows that

$$\sum_i W_{ij}^{(lr)} = \sum_i Z_{ij}^{(lr)} - \sum_i Z_{ji}^{(lr)} = 0, \tag{16.19}$$

which vanishes on account of the symmetry of the Z matrix element (see 10.29b). Consequently, (16.16) gives:

$$w_k^{(lr)} \sum_i (ii)^{(lr)} \tilde{\varphi}_{ik}^{(lmr)} = 0 : \qquad (lmr = 1m0,\ 001) \tag{16.20}$$

the $\tilde{\varphi}_{ik}^{(lmr)}$ with $lmr = 1m0,\ 001$ and $w_k > 0$ (*i.e.*, $k \geqslant 1$) as determined by (16: 7, 8) do satisfy the normalizing condition (16.15).

In order to prove (16.15) also for $k = 0$, $w_k = 0$, we make use of the normalization (11.6) of the initial values $\tilde{\phi}_i(0)$, which yields the equivalent of (16.14) at $t = 0$:

$$\sum_i (ii)^{(lr)} \tilde{\varphi}_i^{(lmr)}(0) = \sum_k \sum_i (ii)^{(lr)} \tilde{\varphi}_{ik}^{(lmr)} = 0. \qquad (lmr = 1m0,\ 001). \tag{16.21}$$

Comparing this result with (16.15), which, as we have seen, is satisfied for $k = 1, \ldots, \nu - 1$, we find that (16.15) does hold for $k = 0$:

$$\sum_i (ii)^{(lr)} \tilde{\varphi}_{i0}^{(lmr)} = 0. \qquad (lmr = 1m0,\ 001). \tag{16.15a}$$

This equation is *not* dependent upon the N equations (16.7) with $k = 0$, $w_k = 0$, which read:

$$0 = \sum_j w_{ij}^{(lr)} \tilde{\varphi}_{j0}^{(lmr)}. \qquad (lmr = 1m0,\ 001). \tag{16.7c}$$

The matrix of these equations is of rank $N - 1$, so (16.15a) and (16.7c) form N independent homogeneous eqs. which have the zero solution only:

$$\tilde{\varphi}_{i0}^{(lmr)} = 0. \qquad (lmr = 1m0,\ 001). \tag{16.22}$$

This implies that e-powers with exponent zero, corresponding to infinite relaxation times ($lr = 10,\ 01$; $k = 0$; $w_k^{(lr)} = 0$) do not occur in (16.6).

We sum up the preceding argument: the requirements (a, b, d) mentioned at the beginning of this chapter lead to eqs. (16: 7, 8, 21), from which the $\tilde{\varphi}_{ik}$ can be determined. These $\tilde{\varphi}_{ik}$ automatically satisfy the conditions (16.15) derived from requirement (c). In particular, coefficients corresponding to non-negative exponents vanish, which enables us to write, combining eqs. (16: 2, 6):

$$\tilde{\phi}_i^{(1)} = \sum_{lmr} \chi_i^{(lmr)} \sum_k \tilde{\varphi}_{ik} \exp(-w_k^{(lr)} t) \qquad (w > 0). \tag{16.23}$$

It is possible to extend this treatment to higher approximations: $\tilde{\phi}_i^{(2)}$, etc., like we did for a single gas in ch. 3. The occurring relaxation times will of course be sums of the positive w_k, the eigenvalues of the w_{ij} matrices. We will not do this explicitly.

To conclude this chapter, we shall now illustrate the $r = 1$ theory by the following simple example: in a binary mixture, an initial deviation of the ChE distribution is given which, at $t = 0$, consists of a term proportional to $\chi_i^{(1m0)} = m_i \mathbf{C}$ only, and which satisfies the normalization (16.21):

$$\tilde{\phi}_1^{(1)}(0) = (\boldsymbol{\varphi}/x_1) \cdot \mathbf{C}\ ; \quad \tilde{\phi}_2^{(1)}(0) = -(\boldsymbol{\varphi}/x_2) \cdot \mathbf{C} \tag{16.24}$$

($\boldsymbol{\varphi}$ is a constant vector). The w_{ij}-matrix for the $N=2$ case is quoted in (15.8); its eigenvalues follow from

$$\begin{vmatrix} (wx_2/m_1)-w_k & -wx_2/m_1 \\ -wx_1/m_2 & (wx_1/m_2)-w_k \end{vmatrix} = 0, \tag{16.25}$$

which gives:

$$w_0=0\,;\ w_1=rw/\mu_{12}=w(x_1m_1+x_2m_2)/m_1m_2. \tag{16.25a}$$

(Definitions of r and w as given in (15: 6, 7)).

It is now easy to find the solution $\tilde{\boldsymbol{\phi}}^{(1)}$, of the form (16.23):

$$\tilde{\boldsymbol{\phi}}_1{}^{(1)}=(\boldsymbol{\varphi}/x_1)\cdot\boldsymbol{C}e^{-w_1t}\,;\quad \tilde{\boldsymbol{\phi}}_2{}^{(1)}=-(\boldsymbol{\varphi}/x_2)\cdot\boldsymbol{C}e^{-w_1t}. \tag{16.26}$$

One can show that this $\tilde{\boldsymbol{\phi}}^{(1)}$ does in fact satisfy the equations (11.9a).

17. *Quasi-relaxation and the kinetic time scale*

We shall now discuss the "quasi-relaxation" of the diffusion current, as we did for the transport of heat and momentum in ch. 6. The discussion will concern a binary mixture in both the kinetic and HD stages. In either case, ϕ will be used as a symbol for the relative deviation from a local MB distribution, like in the entropy treatment (12.3).

From eqs. (10: 50, 51), we see that the average velocities $\langle\boldsymbol{\gamma}\rangle_{1,2}$ of components 1 and 2 relative to the mean particle velocity $\boldsymbol{u}$ are given by

$$nkT\,\langle\boldsymbol{\gamma}\rangle_j=(\boldsymbol{H}^{(j)},\phi), \tag{17.1}$$

in which we have replaced $\boldsymbol{G}_i{}^{(j)}$ by

$$\boldsymbol{H}_i{}^{(j)}=-kT\boldsymbol{G}_i{}^{(j)}=kT\{(\delta_{ij}/x_i)-1\}\,\boldsymbol{C}, \tag{17.2}$$

like in (6.2). Subtracting the two eqs. (17.1), we get the following expression for nkT times the diffusion current:

$$\boldsymbol{J}_D=nkT(\langle\boldsymbol{C}\rangle_1-\langle\boldsymbol{C}\rangle_2)=(\boldsymbol{H}^{(1)}-\boldsymbol{H}^{(2)},\phi)\equiv(\boldsymbol{H},\phi), \tag{17.3}$$

in which

$$\boldsymbol{H}\overset{\text{def}}{=}\boldsymbol{H}^{(1)}-\boldsymbol{H}^{(2)},\ \textit{i.e.}\ \boldsymbol{H}_1=kT\boldsymbol{C}/x_1\,;\quad \boldsymbol{H}_2=-kT\boldsymbol{C}/x_2. \tag{17.4}$$

Now we calculate the collisional part of $\partial_t\boldsymbol{J}_D$, introducing the approximation $\phi\ll 1$:

$$\begin{cases} \partial_C\boldsymbol{J}_D=\sum_i\int d\boldsymbol{c}\,\boldsymbol{H}\,\partial_C f_i=\sum_i\sum_j\int d\boldsymbol{c}\,\boldsymbol{H}_iJ(f_if_{j1}) \\ \qquad\approx-\sum_i\sum_j\int d\boldsymbol{c}\,f_i{}^{(0)}\boldsymbol{H}_i\Omega_{ij}\phi=-[\boldsymbol{H},\phi]. \end{cases} \tag{17.5}$$

Comparison of (17: 3, 5) gives a result equivalent to (6.12b):

$$\boxed{\partial_C(\boldsymbol{H},\phi)=-[\boldsymbol{H},\phi].} \tag{17.6}$$

Like in ch. 6, we can develop $\boldsymbol{H}$ and $\boldsymbol{J}$ in eigenfunctions χ_l of Ω_{ij}, and equations analogous to (6.15) will show that each lmr-mode of $\boldsymbol{J}_D$ decays

with relaxation times which are the inverse of the eigenvalues of the $w_{ij}^{(lr)}$-matrix. We shall demonstrate this for the HD distribution ϕ in a binary mixture with a concentration gradient ∇x only; this ϕ is given by eq. (15.11). We use it to calculate $\boldsymbol{J}_D$ and $\partial_C \boldsymbol{J}_D$ from (17: 3, 5):

$$\frac{\boldsymbol{J}_D}{nkT} = -\frac{\nabla x}{x_1 x_2}\frac{kT}{w}, \tag{17.7a}$$

in agreement with $D = kT/w$, (15.13), and

$$\frac{\partial_C \boldsymbol{J}_D}{nkT} = \frac{\nabla x}{x_1 x_2} kT \frac{r}{\mu_{12}}; \tag{17.7b}$$

so

$$\partial_C \boldsymbol{J}_D / \boldsymbol{J}_D = -rw/\mu_{12} = -w_1 \tag{17.8}$$

as defined in (16.25a). Like the corresponding equations for μ and λ (7.32), this implies that collisions try to break down the transport (in this case, the transport of particles), a process with a characteristic time $1/w_1$. In the HD stage, of course, this tendency is exactly compensated by the streaming terms, $(\partial_S + \partial_H)\boldsymbol{J}_D$.

We now compare the following expressions, which we have derived for a binary Maxwellian mixture:

a) distribution for the HD stage in the case of a gradient ∇x: (15.11);

b) distribution for the kinetic stage in the case of an initial $\tilde{\phi}_i$ proportional to $m_i \boldsymbol{C}$: (16.26);

c) quasi-relaxation of the particle current: (17.8).

In all three equations, we encounter the following characteristic time:

$$\tau_D = \frac{1}{w_1} = \frac{\mu_{12}}{rw} = \frac{m_1 + m_2}{\varrho} \cdot \frac{1}{2\pi \int d\chi \sin\chi \alpha_{12}(\chi)(1 - \cos\chi)}. \tag{17.9}$$

Introducing this τ_D, we write the expressions (15.11; 16.26; 17.8) as follows:

$$\phi_1 = -\tau_D \boldsymbol{C} \cdot \nabla x / x_1 \; ; \quad \phi_2 = \tau_D \boldsymbol{C} \cdot \nabla x / x_2; \tag{17.10a}$$

$$\tilde{\phi}_1 = \boldsymbol{\varphi} \cdot \boldsymbol{C} e^{-t/\tau_D} / x_1 \; ; \quad \tilde{\phi}_2 = -\boldsymbol{\varphi} \cdot \boldsymbol{C} e^{-t/\tau_D} / x_2; \tag{17.10b}$$

$$\partial_C \boldsymbol{J}_D / \boldsymbol{J}_D = -1/\tau_D. \tag{17.10c}$$

Apparently, τ_D plays the role of

a) coefficient in the diffusional part of the HD distribution;

b) relaxation time in the diffusional part of the kinetic distribution;

c) quasi-relaxation time for the diffusion current;

it is clearly comparable to τ_μ and τ_λ defined in (7.13).

From ch. 14 onward, we have only considered the special case of a Maxwellian mixture. As in the single component treatment, many results holding for a more general intermolecular potential in first approximation can be obtained from the exact result for the Maxwellian case by taking matrix elements of the general Ω_{ij}, in a representation of Maxwellian χ,

instead of eigenvalues of the Maxwellian Ω_{ij}. Arguing in this way, it is easy to see which quantity takes over the role of the characteristic relaxation time: expressing $\tau_D = 1/w_1$ in w by (16.25a) and w in $\Omega_{12}^{(1,1)}$ by (15.16), we find:

$$\tau_D = \frac{3}{16nr\Omega_{12}^{(1,1)}} = \frac{3}{16n(x_1 M_1 + x_2 M_2)\Omega_{12}^{(1,1)}}. \tag{17.11}$$

For a binary Maxwellian mixture, this is exact; for other potentials it holds in first approximation. (17: 9, 11) show that τ_D is inversely proportional to the mass density ϱ, as well as to the temperature-averaged 1-2 cross-section.

Incidentally, the diffusion coefficient D can also be expressed in terms of τ_D, in the way (7.16) connects λ to τ_λ and μ to τ_μ:

$$D = kT/w = kTr\tau_D/\mu_{12}, \tag{17.12}$$

but this is not a very significant expression, because the x-dependent factors in r and in τ_D cancel.

Acknowledgement

This work forms part of the research program of the Foundation for Fundamental Research of Matter (F.O.M.), which is financially supported by the Organization for Pure Scientific Research (Z.W.O.).

It was carried out at the Institute for Theoretical Physics, University of Amsterdam.

REFERENCES

1. Offerhaus, M. J., Proc. Kon. Ned. Ak. v. Wetensch., Amsterdam, **B 64** (1961) 115. This, and the present article are contained in a thesis, University of Amsterdam (1961).
2. Chapman, S. and T. G. Cowling, The mathematical theory of non-uniform gases. Cambridge (1939, 1952).
3. Enskog, D., Kinetische Theorie der Vorgänge in mässig verdünnten Gasen, thesis Uppsala (1917).
4. Hellund, E. J. and E. A. Uehling, Phys. Rev. **56**, 818 (1939).
5. Hirschfelder, J. O., C. F. Curtiss and R. B. Bird, Molecular theory of gases and liquids. New York (1954).
6. Waldmann, L., Handb. d. Phys. **12**, 295–514 (1958).
7. Groot, S. R. de, Thermodynamics of Irreversible Processes. Amsterdam (1951).
8. Prigogine, I., Physica **15**, 272 (1949).
9. Wang Chang, C. S. and G. E. Uhlenbeck, report M 999, Eng. Res. Inst., Univ. of Michigan (1952).

List of symbols

(Missing symbols are explained near to the place where they are used. Superscripts and subscripts are mentioned separately at the bottom. In the equations quoted, the symbol is defined, first mentioned, or best elucidated.)

(10.36)	$A^{(\varkappa)}$	coefficient in $\phi^{(1)}$
(15.2)	$a_i^{(\varkappa)}$	coefficient in $A_i^{(\varkappa)}$
(13.30)	$a_i^{(r)}$	coefficient in $\bar{A}_i$
	$\mathbf{C}$	$\mathbf{c}-\mathbf{c}_0$
(14.12)	$\mathbf{C}$	$\mathbf{c}-\mathbf{v}$ (ch. 14 only)
(10.54c)	D_{ij}	multi-component diffusion coefficient
(10.54c)	D_{Ti}	multi-component thermal diffusion coefficient
(10.34)	$\mathbf{d}_i$	generalized concentration gradient
(10.39)	$G^{(\varkappa)}$	function of $\mathbf{C}$, LHS of integral equation
(14.12)	$\mathbf{G}_0$	$\mathbf{g}_0-\mathbf{v}$
(14.10b)	$\mathbf{g}$	velocity of relative motion: $\mathbf{c}_1-\mathbf{c}$
(14.10a)	$\mathbf{g}_0$	centre of mass velocity
(17.2)	$\mathbf{H}^{(j)}$	function of $\mathbf{C}$
(10.59)	k_{Ti}	multi-component thermal diffusion ratio
(15.5)	M_1, M_2	relative masses of 1-2-pair
	N	number of components in mixture
(14.21)	P, P_1	functions of ψ or χ
(15.6)	r	
	s	Sonine parameter
(10.46)	$\mathbf{u}$	average particle velocity
(14.12)	$\mathbf{v}$	constant vector
(10.24a)	W_{ij}	integral operator
(14.52)	$w_{ij}^{(lr)}$	eigenvalue of W_{ij}-operator
(16.7)	$w_k^{(lr)}$	eigenvalue of $w_{ij}^{(lr)}$-matrix
(15.7)	w	
(10.8)	x_i	relative number density of comp. i
(10.18a)	Y_{ij}	integral operator
(14.50a)	$y_{ij}^{(lr)}$	eigenvalue of Y_{ij}
(10.18b)	Z_{ij}	integral operator
(14.50b)	$z_{ij}^{(lr)}$	eigenvalue of Z_{ij}
(10.3)	α_{ij}	differential cross-section
(14.11)	β, β_1	roots of relative masses of i-j-pair
(10.47)	$\boldsymbol{\gamma}$	particle velocity relative to $\mathbf{u}$
(10.3)	ε	azimuth of $\mathbf{g}'$
(14.31)	θ	function of ψ or χ
(14.40)	ϑ	polar angle of $\mathbf{c}$ or $\mathbf{C}$
(10.60)	λ	heat conductivity coefficient in absence of diffusion currents
(10.54b)	λ'	heat conductivity coefficient in absence of concentration gradients
(10.54a)	μ	viscosity coefficient
(12: 12, 13)	μ_i	thermodynamic potential
(14.4)	μ_{ij}	reduced mass of i-j-pair

(16.9)	ν	number of different eigenvalues of $w_{ij}^{(lr)}$-matrix
(14.26)	σ	$s/(1-s)$
(17.9)	τ_D	diffusional relaxation time
(13.7)	$\tau^{(\varkappa)}$	transport coefficient
(14.40)	φ	azimuth of $\mathbf{c}$ or $\mathbf{C}$
(16.24)	$\boldsymbol{\varphi}_i$	coefficient in $\tilde{\phi}^{(1)}$
(16.2)	$\tilde{\varphi}_i^{(lmr)}$	coefficient in $\tilde{\phi}^{(1)}$
(16.6)	$\tilde{\varphi}_{ik}^{(lmr)}$	coefficient in $\tilde{\varphi}_i^{(lmr)}$
(10.3)	χ	angle between $\mathbf{g}$ and $\mathbf{g}'$
(14.46)	$\chi_i^{(lmr)}$	eigenfunction of Ω_{ij} for Maxwellian mixture
(10.5)	$\chi_i^{(0\lambda)}$	eigenfunction of Ω_{ij} at eigenvalue zero (collisional invariant)
(14.22)	ψ	$\frac{1}{2}(\pi-\chi)$
(10.9)	$\psi^{[\lambda]}$	moment of f
(10.19a)	Ω_{ij}	integral operator
(15.15)	$\Omega_{ij}^{(r,s)}$	average cross-section
(14.46)	$w_{ij}^{(lr)}$	eigenvalue of Ω_{ij}-operator
	i, j, k	e.g., f_i, x_i: indices of components i, j, k
(16.9)	k	e.g., $w_k^{(lr)}$: index of eigenvalues of $w_{ij}^{(lr)}$ matrix
(14.46)	(lmr)	e.g., $\chi_i^{(lmr)}$, $\tilde{\varphi}_i^{(lmr)}$: indices of eigenvalues of Ω_{ij}-operator for Maxwellian mixture
(13.7)	$(\varkappa)$	e.g., $X^{(\varkappa)}, J^{(\varkappa)}$: index of transport phenomenon ($=\mu, \lambda, 1, \ldots, N$)
(14: 8, 13)	$*$	e.g., $\mathbf{C}_i^*$: reduced (dimensionless) value
(10.26a)	$(\ )_i$	e.g., $(F_i, \chi_i)_i$: scalar product within component i
(10.26b)	$(\ )$	e.g., (F, χ): scalar product over all components
(14.56)	$(ii)^{(lr)}$	norm of $\chi_i^{(lmr)}$
(10.27)	$[\ ]$	e.g., $[A, A]$: matrix element of Ω- (or W-) operator
(10.8a)	$\bar{G}_i$	average of function $G_i(\mathbf{c})$ over component i
(10.8b)	$\bar{G}$	average of function $G_i(\mathbf{c})$ over all components
(13: 8, 9)		e.g., $\bar{\tau}$: approximation derived by variational method (ch. 13)
(10: 68, 69)	$\hat{}$	e.g., $\hat{X}, \hat{J}, \hat{L}$: independent X and J and corresponding L-coefficients
(12.19)	$'$	e.g., $\boldsymbol{\Gamma}', \mathbf{d}_i'$: alternative definitions of forces and currents

ON THE MECHANISMS UNDERLYING DE LANGE'S RESULTS

BY

F. VERINGA

(Communicated by Prof. G. W. RATHENAU at the meeting of January 28, 1961)

In a previous paper [1] more evidence was offered for the statement, made by DE LANGE [2, 3, 4], that linear low-pass filter action occurs in the visual system prior to non-linear processes. Moreover the successful interpretation by LEVINSON [5] of the experiments by BROWN and FORSYTH [6], based on Fourier-series, stresses the fact that the mechanism responsible for the fusion of on-off flicker behaves linearly.

It is now intended to show that this low-pass filter action, found by DE LANGE [2, 3, 4], as well as by other authors [7, 8], can be explained on the basis of a mechanism located inside the retinal receptor cells themselves. In doing so it is taken for granted that a photon absorbed by the visual pigment inside the rod or cone, produces, by photochemical reaction, a molecule (or ion, or radical, for that matter), which is specifically able to fire the receptor if and only if it reaches the wall of the cell. In that case the process bringing about the shifting of the molecule from the place where it is produced to the wall can be taken to be diffusion. On its way, however, the molecule may be rendered inactive by some reaction, which might be regenerative or recombinative. If the fraction of molecules lost by this reaction is important, i.e. if the quantum efficiency Q of the process described is low, or again, if the mean life of such a molecule is short as compared to the time it needs to diffuse to the wall, then clearly only molecules produced near the wall will have to be considered, and the shortest path to the wall will be favoured.

Apart from the fact, proved by other authors [9, 10, 11], that the overall quantum efficiency of the visual process is a few per cent only, it will be shown from DE LANGE's [4] data that the conditions described do apply. A reasonable model for calculating the mean behavior of a large number of receptor cells seems to be obtained by considering diffusion along a straight line from the place of production to a certain sensitive point, symbolizing the cell membrane, where the molecules under consideration are inactivated on arrival. For the sake of mathematical simplicity all photons are supposed to be absorbed at a distance x_0 from the wall, x_0 being smaller than the radius of a real receptor cell, perhaps considerably so. The value of the diffusion coefficient D for the kind of molecules expected (such as protein molecules) in the viscous cell mass will be

somewhere between 10^{-7} and 10^{-9} cm^2 sec.$^{-1}$; the characteristic time $\tau = \frac{x_0^2}{2D}$ of the process might be of the order of magnitude of 10^{-1} sec.

It is now desired to calculate the flux of molecules at the wall, which is $D\left(\frac{\partial}{\partial x} c\right)_{x=x_0}$, when the origin is taken in the absorption plane, the x-axis perpendicular to this plane and c represents the time- and space-dependent value of the concentration of travelling molecules.

The calculation has to be based on the diffusion equation

$$\varrho c = D \frac{\partial^2}{\partial x^2} c - \frac{\partial}{\partial t} c ;$$

ϱ describing the rate at which molecules are rendered inactive on their way. The boundary conditions are

$c_{x=x_0} = 0$ at the wall and $D\left(\frac{\partial}{\partial x} c\right)_{x=0} = 1 + Me^{j\omega t}$ in the absorption plane

when the retina is illuminated with sinusoidally modulated light at a frequency of $\omega/2\pi$ and a ripple ratio M.

The solution is

$$D\left(\frac{\partial}{\partial x} c\right)_{x=x_0} = \frac{1}{\cosh \sqrt{2\varrho\tau}} + \frac{M}{\cosh ax_0} e^{j\omega t},$$

where

$$ax_0 = \sqrt{\varrho\tau + \sqrt{\omega^2\tau^2 + \varrho^2\tau^2}} + j\sqrt{-\varrho\tau + \sqrt{\omega^2\tau^2 + \varrho^2\tau^2}}.$$

So the ripple ratio on the wall is $\frac{M \cosh \sqrt{2\varrho\tau}}{\cosh ax_0}$, and the reciprocal of the complex filter factor $Re^{j\psi} = \frac{\cosh ax_0}{\cosh \sqrt{2\varrho\tau}}$.

From this

$$\tan\psi = \tanh \sqrt{\varrho\tau + \sqrt{\omega^2\tau^2 + \varrho^2\tau^2}} \cdot \tan \sqrt{-\varrho\tau + \sqrt{\omega^2\tau^2 + \varrho^2\tau^2}}.$$

The amplitude of the ripple is diminished by a factor

$$R = \frac{\sqrt{\frac{1}{2}(\cosh 2\sqrt{\varrho\tau + \sqrt{\omega^2\tau^2 + \varrho^2\tau^2}} + \cos 2\sqrt{-\varrho\tau + \sqrt{\omega^2\tau^2 + \varrho^2\tau^2}})}}{\cosh \sqrt{2\varrho\tau}}.$$

This last result can at once be compared with De Lange's experimental points by plotting R as a function of $\omega\tau$ on log-log paper, taking $\varrho\tau$ for parameter. The experimental points [4] for 0.375 troland are then normalized to give $R = 1$ at $\omega = 0$, inserted in the graph and shifted in the $\omega\tau$-direction until a reasonable fit is obtained. They are found to agree best with the curve for $\varrho\tau = 10$.

From this the quantum efficiency Q, evidently being $\frac{1}{\cosh \sqrt{2\varrho\tau}}$, is found to be some $2\frac{1}{2}$ per cent, thus satisfying the condition for validity of the calculation. The precision of the $\varrho\tau$-determination is admittedly small, allowing a range of Q-values from some 7 per cent downward. The relation of this result to numerical values for the overall quantum efficiency will be an object of continued study.

Moreover, comparison of frequency scales shows $\tau = 0.37$ sec., yielding $\varrho = 27$ sec.$^{-1}$, thus fulfilling the condition $1/\varrho \ll \tau$.

When these values of ϱ and τ are inserted in the formula for $\tan\psi$ a prediction on phase-relation is obtained.

The reason for selecting the experimental points at the lowest luminance available in De Lange's [4] paper to determine parameters ϱ and τ is that at higher luminances an unknown non-linear mechanism diminishing the low-frequency response comes into play, thus causing the sensitivity maxima around 10 cps in De Lange's [4] other curves. The latter statement is justified by inspection of a plot of De Lange's [4] measurements with $\log L$ and $ML^{\frac{1}{2}}$ as axes and the frequency as parameter (L stands for luminance). Statistically optimal behaviour is represented by straight lines parallel to the $\log L$-axis; deviations from this are largely confined to the points for high luminances and low frequencies at the same time.

The said non-linear mechanism must have a complicated character, in view of the fact that low-frequency behaviour is strongly influenced by the luminance of the surrounds [12, 8]. It is presumably responsible for lack of fit in Rose's [9] plots, as well as for Broca–Sulzer's [13]. Brücke's [14] and related phenomena. Part of it might be attributed to or at least described as, a lengthening of the recovery time after firing a rod or cone as a function of the firing rate. Such a lengthening might be brought about by a bottle-neck in the energy supply necessary for rebuilding an electrical double layer.

Returning to the linear diffusion mechanism discussed here, a final remark may be made about the boundary condition $c_{x=x_0} = 0$ stating that stimulus-molecules are inactivated on reaching the wall.

From the solutions of the diffusion equation given above, the response R_δ to a δ-function at the input can be computed by means of Laplace-transforms. It is found to be $R_\delta = e^{-\varrho t} \cdot \frac{1}{4\tau} \cdot \vartheta_1'\left(0, \frac{\pi t}{2\tau}\right)$, where ϑ stands for the Jacobi ϑ-function, or again, using $\vartheta_1'(0, 1/k) = k^{3/2}\,\vartheta_1'(0, k)$,

$$R_\delta = e^{-\varrho t} \cdot \frac{1}{4\tau} \cdot \left(\frac{2\tau}{\pi t}\right)^{3/2} \vartheta_1'\left(0, \frac{2\tau}{\pi t}\right).$$

Using $\vartheta_1'(0, k) = 2\pi(r - 3r^9 + 5r^{25} \ldots)$ with $r = e^{-\pi k/4}$ and $k = \frac{2\tau}{\pi t}$, and considering that for $t > 0.25$ sec. $e^{-\varrho t} < 2.10^{-3}$, it is seen that for the deter-

mined values of ϱ and τ only the first term of the series need be considered to obtain a 1 per cent-approximation.

The result is

$$R_\delta \approx \sqrt{\frac{2\tau}{\pi}} \cdot t^{-3/2} \cdot e^{-\varrho t} \cdot e^{-\tau/2t}.$$

This is a well-known solution for the diffusion equation, which is obtained by neglecting the boundary condition $c_{x=x_0} = 0$.

This, of course, means that so few of the stimulus-molecules produced reach the wall that it does not matter much whether or not they are inactivated too.

Acknowledgements

The author wishes to thank Drs. H. den Hartog and F. A. Muller of this laboratory and Dr. L. H. van der Tweel of the Laboratory for Medical Physics of this University for discussing the present paper with him. It is a pleasure too to thank Prof. Dr. G. W. Rathenau, who generously spent time for the discussion of biophysical matters and generally stimulated the publication of this paper.

Natuurkundig Laboratorium der Universiteit van Amsterdam the Netherlands

REFERENCES

1. Veringa, F. JOSA **48**, 500 (1958).
2. Lange Dzn., H. de JOSA, **48**, 777 (1958).
3. ————, JOSA, **48**, 784 (1958).
4. ————, Thesis Delft, 1957.
5. Levinson, J., Bell Telephone Memorandum 24/6 1959.
6. Brown, C. R. and Forsyth, D. M. Science, **129**, 390 (1959).
7. Tweel, L. H. van der, Thesis Amsterdam 1956.
8. Kelly, D. H., JOSA, **49**, 730 (1959).
9. Rose, A., JOSA, **38**, 196 (1948).
10. ————, J. Soc. Motion Pict. Eng., **47**, 273 (1946).
11. Clark Jones, R., JOSA, **49**, 645 (1959).
12. Gon, J. J. Denier van der, Thesis Amsterdam 1959.
13. Broca, A. and Sulzer, D. C.R., **134**, 381 (1902) ibid. **137**, 944, 977, 1046 (1903).
14. Brücke, E., Sitzungsber. K. Akad. Wiss. Wien **49**[II], 128 (1864).

MIOGYPSINA IN HUNGARY

BY

C. W. DROOGER

(Communicated by Prof. G. H. R. VON KOENIGSWALD at the meeting of Febr. 25, 1961)

Abstract. The discovery of *Miogypsina septentrionalis* in northern Hungary, together with other foraminiferal species more or less characteristic of the Chattian, justifies the assumption of some direct way of marine connections between Hungary and northern Germany during the Late Oligocene.

INTRODUCTION

In order to clarify the position of the Chattian-Aquitanian boundary in their country, Hungarian paleontologists started a detailed investigation of a continuous sedimentary series near Novaj, some 10 km from Eger in northern Hungary (fig. 1). This boundary has been a constant problem in this part of Europe, as may readily be seen from the wealth of papers on this subject, for instance those of FUCHS (1894), SZÖTS (1956) and CSEPREGHY–MEZNERICS (1960).

The lower part of the investigated series consists of sandy marls, the microfauna of which is a *Clavulinoides szabói* association. Such associations are generally considered to be of Middle Oligocene (Rupelian) age. Overlying these marls, glauconitic, clayey sands occur, which in their

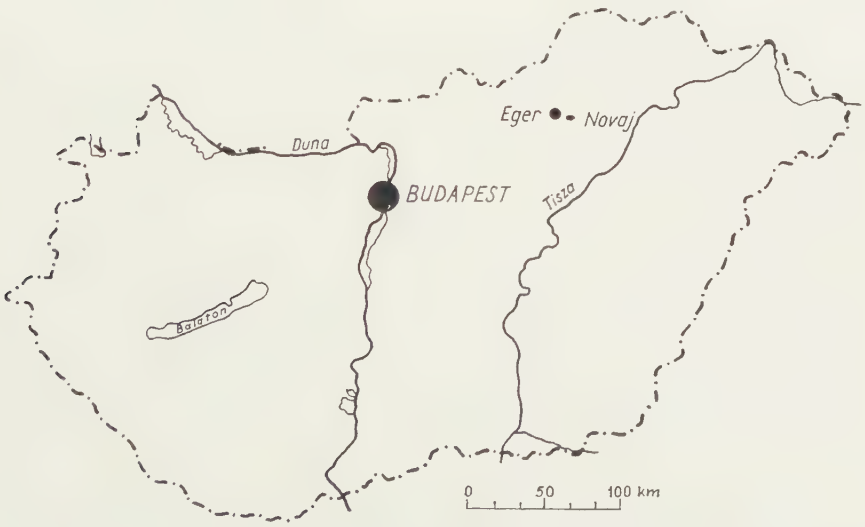

Fig. 1. Sketch map of Hungary showing the location of Novaj and Eger (after R. M. NYIRÖ).

higher part contain a level with indurated limestone lenses with Lepidocyclinids. Still higher in these sands, towards the top of the unit, a sample from the vineyard Nyárjas was found to contain a number of Miogypsinids. On top of the glauconitic sands the series continues with a grey marine clay (for instance that of the brickworks Wind), which in turn is overlain by sandy deposits, partly of continental origin. With rhyolitic tuffs, covering these sands, the series of Novaj comes to an end (fig. 2).

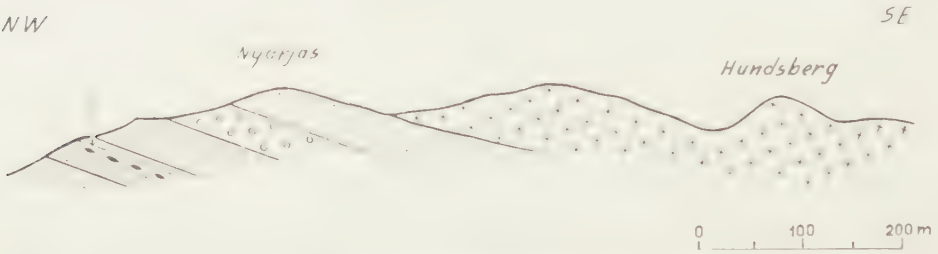

Fig. 2. Schematic section of the sedimentary series near Novaj (after T. BÁLDI). The arrow indicates the position of the *Miogypsina*-bearing sample.

Rhyolitic tuffs.

Grey, limonitic sandstone with plant remains.

Coarse sand with gravel, micaceous.

Grey, more or less limonitic clay with molluscs (Wind brickworks).

Glauconitic, clayey sands with limestone lenses.

Sandy marls with *Clavulinoides szabói* association (Rupelian).

A detailed publication on the stratigraphy and fauna of these deposits near Eger is to be expected in the near future in the Annals of the National Museum of Natural History of Hungary (T. BÁLDI, a.o., 1961). The stratigraphy and the molluscan fauna will be treated by TAMÁS BÁLDI, the smaller Foraminifera by RÉKA M. NYIRÖ, and the Lepidocyclinids by TIBOR KECSKEMÉTI. The author feels gratefully indebted to these Hungarian colleagues, and especially to Dr. NYIRÖ, for sending the Miogypsinids to Utrecht, and for kindly supplying him with stratigraphic and faunistic details for this publication.

THE MIOGYPSINIDS

Altogether some fifty specimens of *Miogypsina* were available. Most of them are small, consisting of only the embryonic and nepionic stages with but a few equatorial chambers.

Bigger specimens are roughly fan-shaped with a broadly rounded apical portion. These individuals are commonly unequally biconvex, in some instances one side being completely flat. The observed diameter of the test ranges from 0.7 mm to 2.4 mm, the corresponding thickness from 0.3 mm to 0.9 mm. The greatest thickness occurs at the place of the embryonic-nepionic stage. Pustules on the surface are distinct. In larger specimens they are fairly regularly distributed with the bigger ones over the thickest portion of the test. Their size range is from 35 to 200 μ.

Transverse sections of bigger specimens, five in total, show a nepionic spiral which is only slightly trochoid. The median layer was found to be strongly variable in height: 125–250 μ (internal diameter). This is mainly on account of the inflated character of the median chambers themselves. The side walls contain distinct lateral chambers, relatively few in number, and in section strongly different in size and shape. Their arrangement is variable, commonly very irregular and not in distinct layers or tiers. Their number between median layer and the surface of the test varies from place to place, from zero to four. The horizontal walls, especially those of the median chambers, are fairly thick and with distinct pores (fig. 3, 4).

For the first approximation of the specific characters twelve successful horizontal sections of macrospheric specimens could be used. They all show embryonic chambers of about equal size and a simple nepionic spiral of about $1\frac{1}{2}$ coil (fig. 5–7). The equatorial chambers are generally relatively few in number. A maximum of six rows of these were found. Their shape is arcuate to ogival, and the greatest observed dimensions are 175×250 μ. In some specimens the median layer has been damaged by burrowing organisms.

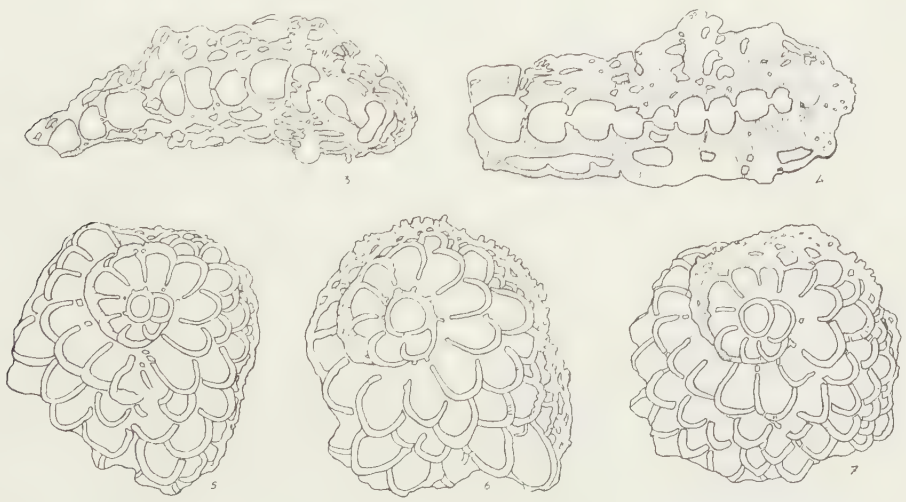

Fig. 3–7. *Miogypsina septentrionalis* Drooger. × 36. 3, 4, transverse sections; 5–7 median sections. Upper Glauconitic Sands, vineyard Nyárjas near Novaj, Hungary.

The features of the embryonic-nepionic apparatus of these twelve individuals are as follows:

Diameter protoconch: $R_I = 95–160\ \mu$; $M_I = 119\ \mu$; $\sigma_{M_I} = 4.8\ \mu$.

Diameter deuteroconch: $R_{II} = 90–140\ \mu$; $M_{II} = 118\ \mu$; $\sigma_{M_{II}} = 3.9\ \mu$. $M_{II}/M_I = 0.99$.

The angle between the apical-frontal line and the line connecting the centres of both embryonic chambers in the section: $R_\gamma = -340° - -180°$; $M_\gamma = -266°$; $\sigma_{M_\gamma} = 12.1°$.

The number of nepionic chambers: $R_X = 22–14$; $M_X = 17.8$; $\sigma_{M_X} = 0.6$.

The number of operculinid nepionic chambers (after which distinct equatorial chambers begin to develop) is in many specimens hard to decide. A second, distal stolon was evidently often present already in chambers adjoining the apical border of the test, each one giving rise to but a single, usually very small equatorial chamber. The probable number of operculinid chambers ranges from 9 to 3. $M = 5.4$; $\sigma_M = 0.4$.

In the sections the nepionic chambers usually increase fairly regularly in size, and the decrease afterwards is not abrupt either. An average value for the largest nepionic chamber had to be chosen in several of the specimens. This increase in size of the nepionic chambers occurs up to the 9th to 14th chamber (mean value 12.3; $\sigma_M = 0.6$). A number of three to seven chambers follow this largest chamber, before the spiral comes to an end.

Furthermore, some seven sections of specimens from the same locality had been made at Budapest. As far as their features are sufficiently clear, six of them are within the range of variation indicated above. The seventh, a slightly oblique section, is clearly beyond these limits with: diameter I and II both 200 μ; $\gamma = -70°$; $X = 10$; only one operculinid chamber, and increase in size up to the ninth chamber. It is unlikely that this specimen could have been reworked from older deposits, since its features represent rather those of a more advanced type. As yet it had better be regarded as an extreme variant of the population at hand.

Including all available sections, also two which were made later and again fall within the primarily found range, and also that of the individual with $X = 10$ (total $N = 18$ to 20), we obtain mean values for the enumerated features which differ by about one standard error from those given above. All combined values give shifts towards the individual values of the aberrant specimen.

A single microspheric individual was succesfully sectioned. Both its protoconch and deuteroconch are about 15 μ in diameter. $X = 27$; the number of operculinid chambers amounts to 14; increase in size occurs up to the 23d or 24th nepionic chamber; there are only two rows of mainly ogival equatorial chambers.

Finally we had at our disposal two specimens from the claypit of the brickworks Wind, near Eger, and derived from the basal part of the grey marine clay, which overlies the glauconitic sands. The sections are

not very good, but the number of nepionic chambers, the angle γ, and other visible features are comparable to those of the majority of the individuals from Nyárjas. For this reason these few specimens could have been reworked from the glauconitic sands, but for us there is no need for such an explanation. According to Dr. Nyirö reworking is unlikely because of the filling of the specimens by pyrite instead of by glauconite.

As to the specific determination of the Nyárjas assemblage, the outstanding point is the peculiar combination of a very high average number of nepionic chambers with the presence of distinct, though often poorly developed lateral chambers. Very similar assemblages were recently described from Chattian deposits in northwestern Germany as *Miogypsina* (*Miogypsina*) *septentrionalis* Drooger (1960, p. 41, pl. 1, fig. 1, 2, pl. 2, fig. 1–8). Comparison of the Hungarian and German assemblages shows distinct differences. Some of these differences are statistically very significant (diameter protoconch), others somewhat less, of the order of 2 σ to 3 σ, such as those for M_X, M_γ, and the mean number of operculinid chambers. In all these features the Hungarian assemblage is less advanced. The average diameters of I and II are smaller, the mean value of the angle γ is greater, on the average the nepionic spiral and its operculinid part are longer, and the maximum size of the nepionic chambers occurs slightly later. Regarding the principle of nepionic acceleration the Hungarian assemblage could be slightly older than those from Astrup and the Doberg in Germany. Just as it was shown for the latter, the Nyárjas population must be considered as closely related to the populations of *Miogypsina* (*Miogypsinoides*) *complanata* Schlumberger, which occurred in the more southern parts of the Mediterranean region.

Although statistically significant differences could be shown to exist between the Hungarian and the German assemblages, known so far, their exceptional combination of the very high M_X values and the beginning development of a system of lateral chambers, makes it certainly preferable to group them together in one species: *M. septentrionalis*.

SOME OTHER FAUNAL ELEMENTS

The microfauna accompanying the Miogypsinids at Novaj, could be evaluated from part of the original sample, kindly sent by Dr. Nyirö. Without entering into much detail (see R. M. Nyirö and T. Kecskeméti, in press), some of the species may be mentioned, which enable us to give an insight into the association, and which are considered to have some stratigraphic or paleogeographic value. Such value being considered doubtful, we did not try to determine specifically the accompanying species of *Amphistegina*, *Operculina* and *Heterostegina*. They merely stress the conclusion on environment that can be drawn from the *Miogypsina* species, which is open marine and at shallow depth, probably not exceeding 50 meters.

The few complete *Lepidocyclina* specimens of the sample are of moderate size; diameter 0.7 – 3.5 mm. Their central part is inflated and there is a thin flange which has usually been damaged. The centre has one or more pustules of considerable size (up to 150 μ); the remainder of the surface has very tiny pustules, it is smooth or it shows a meshwork of the lateral chambers' walls. Horizontal sections show that the individuals belong to the European *Nephrolepidina* lineage. Several specimens have been damaged by burrowing organisms. In five of the median sections the number of accessory auxiliary chambers on the deuteroconch could be counted (fig. 8, 9). In two individuals three such chambers were found, in the three others there are four. These numbers are considered to be primary features for specific determination. They would fit in best with the diagnosis of *Lepidocyclina morgani* Lemoine and R. Douvillé (1904, Soc. géol. France, Paléont., Mém. 32, p. 17, pl. 1, fig. 12, pl. 2, fig. 4, pl. 3, fig. 2; Drooger and Socin, 1959, Micropaleont., vol. 5, p. 420).

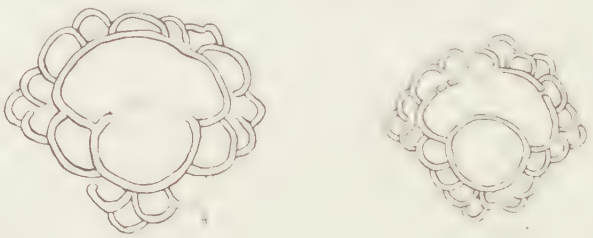

Fig. 8, 9. Embryonic-nepionic stage in median section of two specimens of *Lepidocyclina morgani* Lemoine and R. Douvillé. × 48. Upper Glauconitic Sands, vineyard Nyárjas near Novaj, Hungary.

The shape of the equatorial chambers is ogival to short spatulate-hexagonal. Their arrangement in concentric circles is not distinct at all ontogenetic stages. Several individuals show irregular growth, demonstrated by the intercalation of rings of too small chambers. Especially among the later equatorial chambers the diagonal stolons are not exactly in the same plane, though their distal ends often coalesce. Annular basal stolons were observed, but not as a regular feature. Van der Vlerk (1959) and Grimsdale (1959) in their recent studies of the Lepidocyclinidae stress the importance of the stolon pattern. Our species would belong to the Y lineage. Calculating the evolution factors, as advanced by Van der Vlerk (1959), we find a range of 35 to 44 for factor A, of 44 to 65 for factor B, and of 84 to 100 (average 91) for the total. These figures are again best comparable with those of *L. morgani*.

Some flattened fragments in the sample evidently belonged to very large *Lepidocyclina* specimens. Their surface shows a thickened meshwork of the lateral chambers' walls. In sections the shape of the equatorial chambers (fig. 10) is long-spatulate. The chambers are arranged in concentric rows. The thin diagonal stolons are clearly crossed and there

are equally distinct annular basal stolons. The thinness of the test and especially the shape of the equatorial chambers indicate that we are dealing with a species of the *Eulepidina* series. Probably we may determine these fragments as belonging to *Lepidocyclina dilatata* (Michelotti). Grimsdale (1952) has shown that most of the stated differences between described *Eulepidina* species are invalid for specific determination. Whether the European *L. dilatata* can really be differentiated from Grimsdale's *L. ephippioides* (Jones and Chapman) must be considered doubtful, if one accepts the wide variation he gives to the latter species.

Fig. 10. Horizontal section of part of the median layer of *Lepidocyclina dilatata* (Michelotti), showing crossed diagonal stolons and basal annular stolons between the equatorial chambers. × 48. Upper Glauconitic Sands, vineyard Nyárjas near Novaj, Hungary.

Among the smaller benthonic Foraminifera may be mentioned the presence of *Almaena osnabrugensis* (Roemer). This species was originally described from the Chattian deposits of western Germany. It has been reported from other European areas as well, and it is said to range into the Aquitanian, and in Central Europe even into the Burdigalian (Cicha, 1960). This upward extension of the range cannot be doubted, but so far the species has not been found together with *Miogypsina* species of Aquitanian or Burdigalian age.

Yet another interesting benthonic species of the Nyárjas sample is *Bulimina kasselensis* Batjes (1958, p. 127, pl. 5, fig. 4–6), also originally described from the German Chattian deposits. In all their details the Hungarian individuals are identical with Batjes's specimens. Nevertheless, not too much stratigraphic value can be given to this species, its range not yet being fully known. Similar forms occur in the Miocene of Germany (*B. dingdenensis* Batjes, 1958, p. 128, pl. 5, fig. 1–3) and in the Miocene of northern Italy. The latter may be closely related to the species *Tritubulogenerina dertonensis* Gianotti (1953, Riv. Ital. Pal. Strat., Mem. 6, p. 271, pl. 12, fig. 7) from the type Tortonian. Among the individuals from the Miocene of these countries, stored in the collections of the University of Utrecht, especially some of the smaller ones are not clearly different from the Chattian specimens.

In the Nyárjas sample representatives of the Globigerinidae are frequent, but mainly small (up to 200 μ). All belong to the genus *Globigerina* and probably no more than a single biological species is represented. The majority of the specimens are referable to *Globigerina globularis* (Roemer)

(Drooger and Batjes, 1959, p. 174, pl. 1, fig. 2). Adjacent types seem to be present, but their determination had to be based on very few specimens: *Globigerina* cf. *suteri* (Bolli), *G.* cf. *venezuelana* Hedberg, *G. obesa* (Bolli), *G. unicava* (Bolli, Loeblich and Tappan) and possibly *G. ciperoensis* Bolli (Bolli, 1957). This association resembles those of the German Chattian deposits, though it might be claimed to resemble those of other deposits of different age as well. The only distinct conclusion is that the character of the planktonic association, consisting of *Globigerina* types only, would better fit in with an Oligocene than with a Miocene age of the Nyárjas sample.

CONCLUSIONS

Considering the age of the fauna from Nyárjas, the joint occurrence of *Miogypsina septentrionalis* and *Lepidocyclina morgani* certainly supplies most of the evidence, since both species belong to rather well known evolutionary series. They have been found together in the deposits of the German localities Astrup and Doberg. The latter sediments are irrevocably of Chattian age.

The evolution of the European series of *Nephrolepidina* is not yet sufficiently known. As a consequence the occurrence of *L. morgani* does not give the restriction of a Chattian age.

However, the evolution pattern of the Miogypsinidae has been somewhat better established. Although the assemblage of *M. septentrionalis* of Nyárjas is considered less advanced than the German ones, the difference in age is probably slight. No arguments can be found in the faunal composition to suppose a Rupelian age. Also in the North Sea basin the difference between the faunas of the Rupelian and the Chattian deposits is strongly influenced by the change in facies, which makes the geologic time factor and the Rupelian-Chattian boundary practically elusive. On the other hand the Miogypsinids preclude a younger, Aquitanian age of the Nyárjas sediments. The equivalent of *M. septentrionalis* in the Aquitaine basin is *M. complanata*, which occurs in distinctly pre-Aquitanian sediments of this region. In the typical Aquitanian it had been replaced by the more highly developed species of the same stock: *M. gunteri* and *M. tani*. It cannot be accepted as probable that the Hungarian stock of *M. septentrionalis* remained unchanged for a long time, reaching into the Aquitanian. The occurrence of a population in Slovakia, which is morphologically intermediate between the two Aquitanian species *M. gunteri* and *M. tani* (Papp, 1960; Cicha, 1960), makes it very likely that also in the Hungarian Slovakian area the Miogypsinidae had a development, comparable to that in other regions.

The conclusion of a Chattian age is supported with more or less weight by the encountered *Globigerina globularis* association, and by the presence of *Almaena osnabrugensis* and *Bulimina kasselensis*. As has been shown,

none of these additional elements gives conclusive evidence, but they strengthen the comparison with the Chattian deposits of Germany.

The presence of an *Eulepidina* species at Nyárjas opens up possibilities for comparison in southern direction. In the pre-Aquitanian deposits of southwestern France (Saint–Géours, Saint-Étienne d'Orthe, etc.) *L. ephippioides* occurs together with *L. morgani*, *M. complanata* and *A. osnabrugensis*, only the last species of which has been claimed recently to be still present in younger deposits of this area. In itself *Eulepidina* (*L. dilatata* or *L. ephippioides*) is not a proof of Chattian age. Representatives have been found in Early Miocene deposits of the Mediterranean area.

About a year ago it could be concluded from the discovery of *Miogypsina* and *Lepidocyclina* in the Chattian deposits of Germany, that at least one wave of these larger Foraminifera had succeeded in penetrating from the Mediterranean area into the North Sea basin. One of the groups, the Miogypsinids, was considered to have developed a somewhat aberrant northern offshoot, *M. septentrionalis*, but still well comparable to the Mediterranean stock of *M. complanata*. The assemblages of the latter species from Christus (SW. France) and from the Bric del Duca (N. Italy) were mentioned as closely comparable, though already slightly more highly developed in their nepionic features. One may not expect, not even in an area such as the Mediterranean, in a narrow sense, that the change from *Miogypsinoides* into *Miogypsina* s.str. took place at but one level of nepionic development. Local deviations certainly occurred. Nevertheless, it is striking that the German *M. septentrionalis*, which in this respect is highly aberrant, is found again, and still more deviating in Hungary. Of course, one might assume that the German and the Hungarian *M. septentrionalis* populations had developed completely independently of one another from a similar stock, but then one might expect differences in minor features. The fact that they nicely fit into a single evolving lineage, added to the consideration that the separate rise of so very similar aberrant populations not very far from one another looks very unlikely, makes it much more plausible that both population groups were closely related.

This conclusion immediately requires some idea about the marine north-south connections during the Late Oligocene. The more so, if not only *L. morgani*, but also *A. osnabrugensis* and *B. kasselensis* of the German Chattian are considered to be immigrants from the south. The more or less classical solution, which assumes a connection from the Kassel area and the Mayence basin, along the Rhine depression and the Swiss Molasse basin towards the Lower Rhone area, has lost much of its attraction. One reason is that in the Swiss Molasse foredeep non-marine conditions prevailed during the Chattian (age based on mammals), resulting in the "Untere Süsswassermolasse". This blocks marine connections to the south in between the zones of the present Alps and Jura Mountains.

It is well known that the Oligocene marine faunas of Upper Bavaria very closely resemble those of Hungary (Hagn and Hölzl, 1952), and a direct marine connection between these two areas may be considered as well established. Admittedly, the distance from Bavaria to Kassel and Mayence is not great, but it is difficult to bridge this gap, since marine sediments of Oligocene age are not continuous. They are at the least very indistinct. One might think of some short-time marine connection from Upper Bavaria in the direction of Basel and from there northwards along the Rhine depression and Alsace, but the indications are not very clear (see for instance Oertli, 1956). Part of the fully marine sediments of this strip may still be present, buried under younger deposits, but another part of them has probably been removed by later erosion. It is certainly worth while to compare again the faunas of both ends to see whether such a connection could more easily explain the geographic distribution of still other species.

Whether the marine connections from Hungary to the more southern Mediterranean area during the Late Oligocene went directly south cannot be decided either. Miogypsinids are known to occur, together with *L. morgani*, in northern Yugoslavia (Papp, 1954, 1955). They belong to *M. complanata* s.l., but their nepionic stage is more highly developed than that of *M. septentrionalis*. Further evidence has to be awaited. Recalling the discoveries of Miogypsinids in Slovakia, Austria (Papp, 1960) Hungary and Germany during the last few years, it becomes evident that this group was fairly well distributed in and along the northern parts of the Alpine area. Further discoveries may therefore certainly be expected.

REFERENCES

Báldi, T., T. Kecskeméti, R. M. Nyirö and C. W. Drooger, Neue Angaben zur Grenzziehung zwischen Chatt und Aquitan in der Umgebung von Eger. Ann. Hist. Nat. Mus. Nat. Hung., 53, (1961, in press).

Batjes, D. A. J., Foraminifera of the Oligocene of Belgium. Verh. Kon. Belg. Inst. Natuurw., 143 (1958).

Bolli, H. M., Planktonic Foraminifera from the Oligocene-Miocene Cipero and Lengua formations of Trinidad, B.W.I. of U.S. Nat. Mus., Bull. 215, 97–123 (1957).

Cicha, I., Kurze Übersicht der Entwicklung der Mikrofauna des unteren und mittleren Miozäns der alpin-karpatischen Becken im Verhältnis zum Oberhelvet-"Karpatien". Verh. Comité Néogène méditerranéen, Vienna, 67–74 (1960).

Csepreghy-Meznerics, I., Das marine Neogen Ungarns in seiner Beziehung zum Wiener Becken. id., 87–91 (1960).

Drooger, C. W., Miogypsina in northwestern Germany. Proc. Kon. Ned. Ak. Wetensch., ser. B, 63, 38–50 (1960).

——— and D. A. J. Batjes, Planktonic Foraminifera in the Oligocene and Miocene of the North Sea basin. id., 62, 172–186 (1959).

Fuchs, Th., Tertiaerfossilien aus den kohlenführenden Miocaenablagerungen der Umgebung von Krapina und Radaboj und über die Stellung der sogenannten "Aquitanischen Stufe". Mitth. Jahrb. Kön. Ung. Geol. Anstalt, **10**, 163–175 (1894).

Grimsdale, T. F., Cretaceous and Tertiary Foraminifera from the Middle East. Bull. Brit. Mus. Nat. Hist., **1**, no. 8 (1952).

———, Evolution in the American Lepidocyclinidae (Cainozoic Foraminifera): an interim review. Proc. Kon. Ned. Ak. Wetensch., ser. B, **62**, 8–33 (1959).

Hagn, H. and O. Hölzl, Geologisch-paläontologische Untersuchungen in der subalpinen Molasse des östlichen Oberbayerns zwischen Prien und Sur mit Berücksichtigung des im Süden anschlieszenden Helvetikums. Geologica Bavarica, no. 10 (1952).

Oertli, H. J., Ostrakoden aus der oligozänen und miozänen Molasse der Schweiz. Schweiz. Pal. Abh., **74**, (1956).

Papp, A., Miogypsinidae aus dem Oligozän von Zagorje. Geologija, Razprave in poročila, **2**, 168–178 (1954).

———, Lepidocyclinen aus Zagorje und Tuhinjska dolina, östlich von Kamnik (Slowenien). id., **3**, 208–215 (1955).

———, Das Vorkommen von Miogypsina in Mitteleuropa und dessen Bedeutung für die Tertiärstratigraphie. Mitt. Geol. Ges. Wien, **51**, 219–228 (1960).

Szöts, E., Les problèmes de la limite entre le Paléogène et le Néogène et les étages Chattien et Aquitanien. Acta geol., **4**, 209–219 (1956).

Vlerk, I. M. van der, Problems and principles of Tertiary and Quaternary stratigraphy. Quart. Jour. Geol. Soc., **115**, 49–64 (1959).

———, Modification de l'ontogénèse pendant l'évolution des Lépidocyclines (Foraminifères). Bull. Soc. géol. France, ser. 7, **1**, 669–673 (1959).

SOME "VOLCANO-TECTONIC" DEPRESSIONS OF SUMATRA, THEIR ORIGIN AND MODE OF DEVELOPMENT

BY

H. TH. VERSTAPPEN [1])

(Communicated by Prof. F. A. VENING MEINESZ at the meeting of February 25, 1961)

CONTENTS:

1. Introduction.
2. Lake Kerintji.
3. Lake Singkarak.
4. Lake Toba.
   a) Critical considerations on the supposed "Batak tumor".
   b) The Toba graben.
5. Summary.
6. References.

1. *Introduction*

"Volcano-tectonic" depressions are a much discussed subject of volcanic geomorphology. The name of these, often rather irregularly shaped, depressions indicates that they are supposedly the result of both volcanic and tectonic phenomena. They are consequently considered as an intermediate category between the more symmetrical calderas formed by pure-volcanic collapse on the one hand, and the normal tectonic features graben, down warped basins and the like on the other. The leading thought is that blowing off or outflow of the magma results in the collapse of the roof of the magma chamber, which process results in the formation of graben and downwarped basins. The volume of the issued volcanic products generally is much less than the volume of the depression concerned and the latter then apparently are partly due to other, tectonic, causes (v. BEMMELEN, 1949, p. 212). The relative importance of both these factors should be carefully studied for every individual case. The tendency exists, in the author's opinion, to emphasize especially the role of volcanism in the collapse mechanism.

Many "volcano-tectonic" depressions have been the scene catastrophic eruptions of the Katmaian type. Fiery tuff-flows issued from fissures on those occasions and the huge amounts of deposited ignimbrites now form extensive plateaux, first described from New Zealand by MARSHALL (1935).

[1]) Geomorphologist, International Training Centre for Aerial Survey, Delft, The Netherlands. Formerly: Geographical Institute, Indonesian Topographical Survey, Djakarta.

The island of Sumatra is the classical area of these "volcano-tectonic" depressions. A great number of larger and smaller features of this type exist, the largest one being the Lake Toba depression. They were described as such by VAN BEMMELEN (1929, 1939, 1949) who introduced the "emptying out-and-caving in" hypothesis. He also emphasized the existence of associated "volcano-tectonic" uparching of the earth' crust, caused by the rising magma of a near-surface batholith. The so-called "Batak-tumor", since is known as the largest and clearest example of this phenomenon. The Lake Toba "volcano-tectonic" depression was formed in a later stage, according to VAN BEMMELEN. The vast ignimbrite sheets of Sumatra have been described by WESTERVELD (1947, 1953).

The author, on behalf of the Geographical Institute, Djakarta, carried out four larger geomorphological field investigations in the Barisan Mountains of Sumatra in 1954 and 1955, the results of which will be published soon. Special attention was paid automatically to the "volcano-tectonic" depressions, because of their conspicuous occurrence throughout the island. The Kerintji, Singkarak, and Toba depressions were studied in greater detail and the author's opinions therefore, are based primarily on his observations in these areas. The general conclusions regarding their origin, included in this paper, deviate considerably from the established ideas on the nature of these depressions. They may prove of some value for the study of similar features elsewhere. Unfortunately, the coverage of aerial photographs is negligible for the areas under consideration, and the study is based almost exclusively on field observations.

2. *Lake Kerintji*

The Kerintji plain forms part of the longitudinal graben of the Barisan Mountains in the southernmost part of Central Sumatra. The area was visited by the author in 1954 (VERSTAPPEN, 1955). It is a wedge-shaped complex graben lying at an altitude of approximately 800 metres above sea level. The plain is bordered by steep fault-scarps, having a height of about 400 metres and converging towards the north west. Consequently the narrowest and highest part of the graben is located there. The plain becomes broader and lower lying towards the south-east and it reaches its maximum width of about nine kilometres in the extreme south-eastern end where the "volcano-tectonic" lake of the same name, having a maximum depth of 110 metres, is situated. The narrow north western apex of the graben becomes more conspicuous due to the occurrence of two splinters in the northern part of the graben, which converge even more than the two main faults. The graben finally terminates at the North-Kerintji granite and quartz diorite massif, where the further continuation of the faults can be ascertained only with difficulty in the field. The impression gained is that the North Kerintji massif influenced the younger tectonic events of the region, which is reflected in the poor

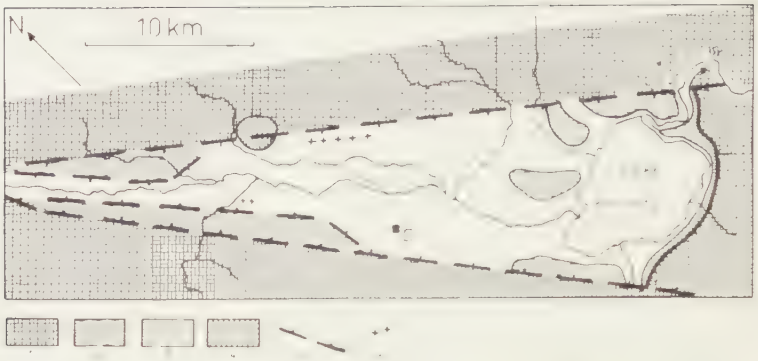

Fig. 1. Geomorphic map of the wedge shaped Kerintji graben.
Key: 1. Areas adjacent to the graben. — 2. Splinters in the graben. — 3. Tuff cone of lake Kerintji. — 4. Rhyolite plug. — 5. Fault-scarps. — 6. Hot springs. — S = Sungaipenuh.

development of the northern part of the Kerintji graben. Similar situations were observed in several other parts of the Barisan Mountains.

The Kerintji "volcano-tectonic" depression is only a comparatively small one. The volume of the tuffs issued can be roughly estimated at 4 km³, and the volume of the depression, as deduced from a lake survey carried out by the author in 1954, amounts to approximately 1,75 km³. It should be emphasized that the tuffs were deposited in the graben. The remainders of the tuff cone which originally surrounded the lake, are still present in the plain and form hills of considerable size, for instance the Kotapetai hill. Thus it is evident that the eruption took place in the pre-existing Kerintji graben. The drainage of the graben was not altered by the volcanic event: the main river enters the depression in its narrow north western end, and breaks through the eastern fault-scarp in the extreme south east. It leaves the graben nowadays at exactly the same locality as before the eruption and it has incised its course there in Kerintji tuffs deposited in its pre-eruption valley. The depression apparently is almost exclusively of a tectonic nature. No "volcano-tectonic" uparching can be traced either.

The river was dammed temporarily by the ejected tuffs and thus the graben was flooded. The water rose to about 90 metres above the present lake level, but it was lowered rapidly due to the quick incision of the river in the tuffs, and the plain ran dry again. A few terrace levels now indicate the subsequent stages of the lowering in lake level. The volcanic eruption and the flooding of the plain are registered in local folk tales and thus the event seems to have occurred in historic times. Another volcanic feature is the occurrence, along the eastern fault-scarp, of a rhyolite plug, a tholoid, which also was formed after the graben came into being. Earthquakes and young scarplets point to recent tectonic movements along the existing fault lines.

3. *Lake Singkarak*

This characteristically steep sided and flat bottomed "volcano-tectonic" lake is about 20 kilometres in length and its maximum width is 7 km. It is located in the Central Sumatran section of the Barisan median graben, approximately 200 kilometres to the north-west of Lake Kerintji. It lies at an altitude of 362 metres above sea level and reaches a maximum depth of 268 metres. The relevant sheets of the topographic map of Central Sumatra, reveal that this lake evidently occurs also in the very lowest part of this section of the graben.

The Solok plain, located further to the south-east, is only slightly higher lying than the level of Lake Singkarak (362 m). Its altitude ranges from 387 metres above sea level in the north-west to about 450 metres in the south-east. The greater height is more conspicuous, however, if the depth of Lake Singkarak (268 m) is taken into consideration: the altitude of the Solok plain above the lake bottom is between 293 and 356 metres. The floor of the graben rises rather abruptly to the south-east of the Solok plain and reaches a height of approximately 1,500 metres above sea-level in the surroundings of the lakes Baruh and Atas, at some 35–40 kilometres distance from the southern shore of Lake Singkarak. The rise of the graben floor to the north-west of the lake is even more rapid. A height of 1,180 metres above sea level is reached at a distance of 19 kilometres from the north western end of the lake, where between the Merapi and Singgalang volcanoes, a broad saddle is formed in the young volcanic products.

This saddle is important as a graben-watershed. The terrain to the north of it gradually slopes down towards the ignimbrite plateau of Bukittinggi, about 900 metres above sea level. The southward flowing rivers once entered Lake Singkarak. They were captured, however, in comparatively recent times, by the Anai river and since drain towards the Indian Ocean in the west. The pirate Anai river is deeply incised in a narrow gorge. The capture occurred near the town of Padang Pandjang, and the present, almost imperceptible divide between the Anai branches and the beheaded lower river courses still flowing towards the lake, lies at about 770 metres above sea level.

The rivers of the remainder of the graben section just described, including the Solok plain and as far south as Lake Baruh, flow towards Lake Singkarak, which is drained eastward by the Umbilin river. This situation only came into being rather recently, however. Van Valkenburg (1921) mentions the existence of a dry river valley to the east of the town of Solok. Evidently the Solok plain once drained eastwards via this nowadays deserted valley and the Lasi-Pumuatan river, which river debouches in the Umbilin river, many kilometres further downstream. The height of the dry valley is about 410 metres above sea level and equals the height of the higher terraces at the Umbilin outlet of Lake Singkarak. Obviously, both passages have been in use simultaneously.

The present north-west drainage of the Solok plain towards Lake Singkarak can only be explained by assuming a recent subsidence of the graben section between Solok and the lake. Several geomorphic features evidence the extremely young faulting movements occurring in this particular part of the graben structure.

Fig. 2. Longitudinal profile of the Singkarak section of the median graben.

The geomorphic development sketched above is essentially due to tectonic causes. Some volcanic activity was affiliated to the faulting movements, however. Young, whitish, volcanic tuffs are present *in the graben* to the north of Solok. They are not related to any young volcanic cone, but they originated from a fissure eruption at the eastern side of the graben, which accompanied the recent collapse of this section of the median graben, to which reference was made above. The tectonic movements continued after the fissure eruption and a number of well-preserved young scarplets can be traced in the tuffs. The Sumani river locally breaks through the tuffs in the central and eastern parts of the graben, even though an easy course through the flat and lower lying westerly zone seems indicated. This points to a continued tectonic subsidence, witnessed by the western side of this critical graben section.

The fault bordering the eastern side of Lake Singkarak also acted as a volcanic vent. The tuffs were deposited to the east of the fault-scarp and they form a surface with a gentle easterly slope (fig. 3) between the Umbilin river and Mt. Batu Baragung. Another, smaller flow occurs to the south of this mountain. A third tuff deposit is a tuff cone *in the graben* and enclosing the northern side of the lake (fig. 3).

The deposition of the tuffs in the graben to the north and south of

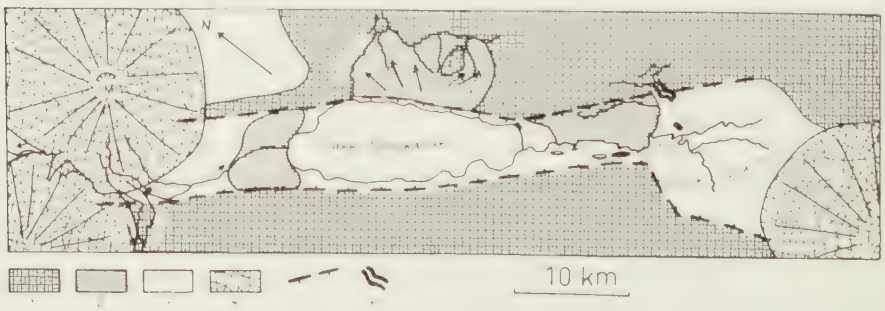

Fig. 3. Geomorphic map of the Singkarak section of the median graben.

Key: 1. Areas adjacent to the graben. — 2. Tuff deposits (partly in slightly higher graben sections). — 3. Plains. — 4. Volcanic cones. — 5. Fault-scarps. — 6. Dry river valley. — M = Merapi — S = Singgalang — T = Talang — B = Batubaragung — P = Padang Pandjang — Si = Singkarak — So = Solok

the lake justifies a conclusion that this graben also existed prior to the volcanic events. The eastward directed tuff flows occurring to the east of the lake similarly indicate the pre-existing relief. It is beyond doubt that the volcanic (fissure) eruptions, geomorphologically speaking, were of comparatively little importance. They only occasionally accompany the intense faulting movements, provided that a batholith is present at shallow depth. They are definitely not the cause of the depression.

The Kerintji and Singkarak depressions evidently do not fit VAN BEMMELEN'S definition of "volcano-tectonic depressions". Either this definition should be modified into "tectonic depressions with occasional volcanic activity along faults", or the term should not be applied at all. VAN BEMMELEN (1949, p. 684) lists 7 "volcano-tectonic" depressions in southern Sumatra, an area he studied in more detail. The formation by volcano-tectonic collapse of two of these depressions, viz. the Suoh and Gedongsurian depressions, is rejected by WESTERVELD (1953). He explains the Gedongsurian depression by tectonic causes with subsequent erosion, and considers the Suoh depression as a graben where acid lavas occur along fault-zones. WESTERVELD'S views on these features are rather similar to those developed by this author concerning the Kerintji and Singkarak depressions in Central Sumatra. The question arises whether volcano-tectonic uparching and collapse, in the sense of VAN BEMMELEN, exists at all in Sumatra. In seeking an answer to this question, it seems relevant to study the "classical example" of this type of phenomenon viz. Lake Toba, located in Northern Sumatra.

4. *Lake Toba*

A. Critical considerations about the supposed "Batak-tumor"

VAN BEMMELEN claims that the Toba cauldron is formed on top of a huge "tumor" formed by volcano-tectonic uparching and measuring 275×150 km. He states that the outline of the "tumor" is marked by the contour lines of 100 and 1,000 metres. The basement complex in the top part of the "tumor" reaches a height of more than 2,000 metres above sea-level as can be derived from the topographic maps (VAN BEMMELEN, 1949, 1a, p. 687).

However, a few objections are to be raised against this conception. The contour lines, to start with, are without significance to outline the assumed "tumor" because they indicate the slope of the ignimbrite plateau and *not* the pre-volcanic surface. It is established by borings that near the town of Tebingtinggi, some 70 kilometres from the lake, the ignimbrite sheet is still 80 metres thick (v. d. MAREL, 1948). Closer to the lake a thickness of several hundreds of metres is reached. If one takes the thickness of the ignimbrite sheet into consideration, the contour lines do not indicate an exceptional width of the Toba section of the Barisan Mountains. One could say that the parts adjacent to the Toba

area are exceptionally narrow. The width of the Toba section may be slightly above the average, but this is readily explained by the somewhat complicated structure of this part of the Barisan Mountains viz. the occurrence of the Toba graben to the east of the main longitudinal graben.

Furthermore, the height of the basement complex in the Toba area is not an extreme value. Similar heights are reached further to the south in the Barisan Mountains near Panjabungan and Hutanopan (Mt. Sopo Untjin, 2,199 m). Further to the North heights of 3,000 metres and more occur (Mt. Bandahara, 3,030 m; Mt. Leuser, 3,381 m).

The present topography certainly does not appear to justify the assumption of a "Batak-tumor". Warped lake terraces, formed in the Toba tuffs and occurring along the eastern shore of Lake Toba, were studied by the author (p. 12). It is evident from these geomorphic observations that after the Toba eruption(s) parts of the area were further uplifted, locally as much as 250–350 metres. Immediately after the eruption the topography thus was even less in line with the "tumor"-hypothesis.

The post-volcanic relief actually is not at all crucial in this relation, but only the topography before the ignimbrite eruptions counts. It does not seem imperative that a "tumor" should still prevail after the "emptying-out-and-collapse" phase. Van Bemmelen emphasizes on the one hand the existence at present of the Batak "tumor", whereas he states on the other that the "tumor" of the much larger Strait Sunda dome, cannot be traced nowadays. He claims that in this latter case "the field of gravitational stresses was too strong for the bearing-power of the crust, so that it collapsed" (van Bemmelen, 1949, 1a, p. 633), without any proof, however. The evidence of the Lake Ranau "tumor", Southern Sumatra, is not very convincing. The coastal features of the nearby part of the Indian Ocean, mentioned in this connection (Van Bemmelen, 1949, 1a, p. 680) have no certain relationship to the Lake Ranau eruption, neither in space nor in time.

The original, pre-volcanic topography of the Toba-area is, of course, very hard to establish due to the ignimbrite cover and because of the important tectonic events that occurred. The existence of a radial drainage pattern at that time, seems likely, if a dome or "tumor" has been present. It was observed by the author that the drainage of the Karo Highlands, situated to the northwest of Lake Toba prior to the eruption, was directed towards the lake. A radial drainage evidently did not exist there. It is, in view of the above considerations, rather unlikely that the assumed Batak "tumor", which cannot be traced at present, has ever existed at all.

B. The Toba graben

This "volcano-tectonic" lake, the largest one of Sumatra, measures approximately 87 kilometres in a northwest-southeast direction and its maximum width is about 26 kilometres. The graben itself is still somewhat

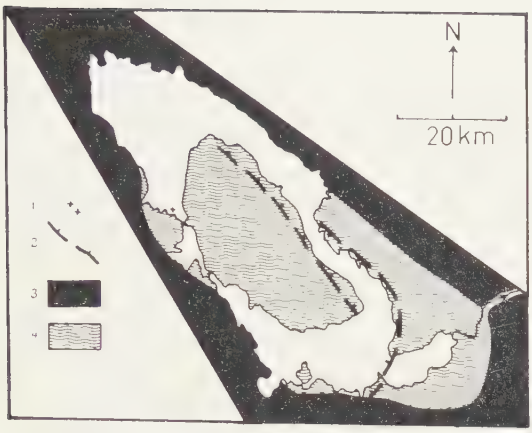

Fig. 4. Tectonic sketch of the wedge shaped Toba graben.

Key: 1. Hot springs. — 2. Fault-scarps within the main graben. — 3. Areas adjacent to the graben. — 4. Blocks/splinters within the main graben.

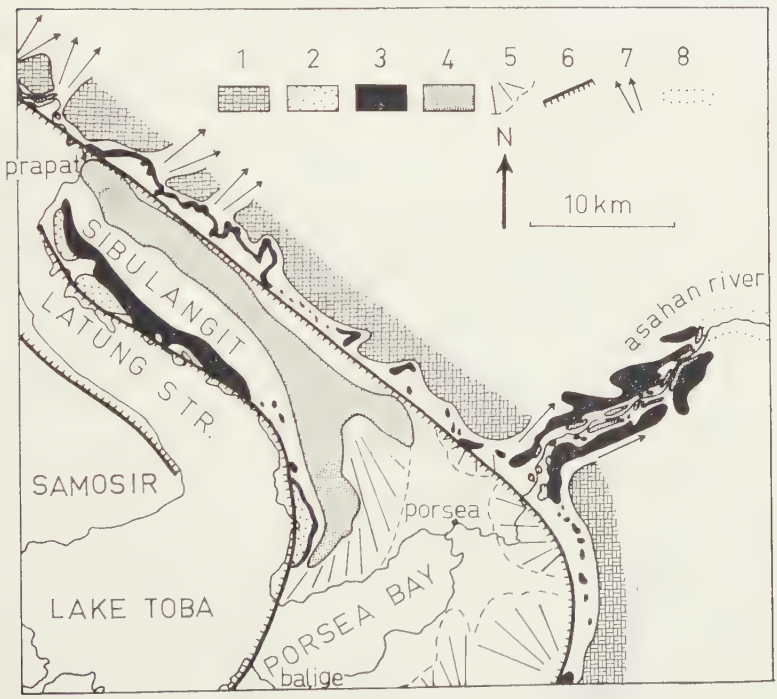

Fig. 5. Geomorphic map of the SE part of the Toba graben.

Key: 1. Pre-Toba rocks emerging from the tuff cover. — 2. Areas emerging from 1st Toba terrace. — 3. 1st Toba terrace. — 4. 2nd Toba terrace. — 5. Multi-cycle alluvial fan. — 6. Fault-scarp. — 7. Overflow of Toba tuffs. — 8. Escarpment of Asahan amphitheatre.

larger, viz. 100×31 km and it is bordered by steep fault-scarps, many hundreds of metres high. The island of Samosir is an important feature in the lake which finds its counterpart in the Sibulangit or Uluan peninsula located between Prapat and Porsea. The greatest depth of the lake is 529 metres and as the present lake level is at 906 metres; the deepest part of the graben lies at 377 metres above sea level.

The origin of the Toba trough is a much discussed problem, which centres on the question whether it was a graben existing prior to the Toba eruption, or whether it originated after the volcanic events by volcano-tectonic collapse. Of the older investigators Wing Easton (1894, 1896) is in favour of the graben hypothesis. Westerveld (1947, 1953) is among the modern scientists holding similar views. He maintains, with good right, in the present author's opinion, that a "shallow acid magma-chamber underlying a *pre-existing tectonic depression*, of which the bordering fault-fissures furnished the eruption channels" accounts for the phenomena observed.

Volz (1899, 1909) dates the graben as a post-eruption phenomenon. Van Bemmelen (1929, 1939, 1949) advocates the volcano-tectonic origin of the trough, which assumption also implies that the trough basically was formed after the eruption. Van Bemmelen, however, is not very consistent about this matter. He states (v. Bemmelen, 1949, 1a, p. 212) that "the Lake Toba area was probably already a graben, drained by the Asahan river, before the eruption took place". He then continues "it is difficult, if not impossible, to estimate which part of the volume of the present Toba-depression belongs to the pre-Toba graben, and which part is due to the over-deepening by the eruption". He concludes: "Because the Toba cauldron was formed partly by the doming up of the Batak tumor, which caused tensional stresses in the top area and the subsidence of a graben, and partly by the blowing out of the contents of the underlying shallow-seated, granite batholith, it may be called a "volcano-tectonic depression". Van Bemmelen thus admits that the graben, at least in part, existed prior to the eruption. He expresses a quite contradictory view on p. 691, however: "No investigator who has set eyes on the imposing precipitous escarpments surrounding the Toba cauldron, will ever contend that this trough existed already before the outburst". Also, no pre-existing graben is indicated in his schematic cross sections (p. 695) of the various stages of development of the Toba area.

It should be emphasized that Lake Toba actually is located in a wedge shaped graben having its apex in the north west. The southern end of the lake is formed by an E W directed escarpment, which is most likely another fault scarp. The graben is drained at its broadest southern end by the east-ward flowing Asahan river to the Malacca Straits. Westerveld (1947) pointed out that the Asahan already drained the graben before the Toba eruption occurred, a view shared by the present author. Even the oldest products of the Toba volcanic vents penetrate far downstream

in the pre-existing valley carved mainly in pre-tertiary rocks (Fryling, H., 1925). These deposits consequently now form a tongue shaped valley fill where the river re-incised its course in a narrow gorge. The older, consolidated, tuffs at present can be traced as far as 18 km to the east of the eastern Toba fault-scarp.

The fact that the wedge-shaped Toba graben always drained at its broadest south-eastern end indicates that this area was also, most probably, the deepest part of the graben. It should be mentioned in this context that at least the more recent Toba volcanic activity centered mainly in the SE (v. d. Marel, 1947, 1948a). There is evidently a certain degree of similarity between the Kerintji and the Toba graben structures: Both are wedge-shaped features with their apex pointing towards the NW and drained eastward at their broadest and lowest lying south eastern parts, where volcanic events occurred. This similarity was even more pronounced formerly, when the Karo highlands, located to the NE of the lake, still drained towards lake Toba in much the same way as the Siulak river at present still enters the Kerintji graben at its NE extremity. The Karo river system was beheaded by a branch of the Renun river system, after being pounded up by Toba tuffs and as a result of the increased vertical erosion of the Renun river system due to further subsidence of the Renun graben. The problem will be discussed at some length in a forthcoming publication of the author on the geomorphology of Sumatra.

Van Bemmelen (1949, 1a, p. 689, 691) also is of the opinion that the Asahan river already existed before the Toba eruption. Because of his views that the formation of the Toba trough mainly occurred after the volcanic events, it is inevitable for him to consider the Asahan valley as a relic of a river system that became beheaded by the downbreak of the Toba cauldron. The headwaters of this "proto-Asahan", according to him, were located in the western part of the present Lake Toba in between the Renun and Batang Toru catchment areas. The great thickness of the Toba tuffs deposited in the Asahan valley would not appear to support this hypothesis.

These tuffs reach a height of 1,160 metres above sea level at the entrance of the Asahan gorge to the east of Porsea. This tuff terrace slopes down downstream and is at 750 metres above sea level near the well-known Tangga falls at approximately 15 km from the eastern Toba fault scarp. The oldest, consolidated tuffs outcrop, according to the map of Fryling (1925) near the base of the Tangga falls. This outcrop is at a height of about 250 metres above sea-level and the total thickness of the tuffs at that locality consequently amounts to at least 500 metres. The bedding of the tuffs is approximately parallel to its surface and one may therefore safely assume that the thickness of the tuffs at closer range to the lake is at least the same and possibly more. The height above sea level of the Asahan valley bottom underneath the tuffs thus

amounts to 1,160 – 500 = 660 metres or less, near Porsea. It will appear from the author's observations on the terraces around Lake Toba, that possibly the Porsea area has been uplifted some 110 metres after the eruption occurred. The height of the Asahan valley bottom immediately after the eruption then was only 550 m above sea level at the most. The greatest depth in the southern part of the lake occurs to the north of Balige and amounts to 428 metres (VAN BEMMELEN, 1939), or in other words 906 – 428 = 478 metres above sea level. Evidently this part of the lake bottom is only slightly lower-lying than the valley bottom of the pre-eruption Asahan river. One may object that the present lake bottom is not representative due to deposition of Toba tuffs in the graben and as a result of post-eruption tectonic movements. It is more justified therefore to state that the original Asahan valley bottom is located approximately 1,500 metres below the highest parts of the edge of the eastern Toba fault-scarp. Collapse of the Toba graben as a result of – and thus after – the eruption, is obviously of a negligible order, if it existed at all. It is beyond doubt that the Asahan river, before the eruption, drained the already existing Toba graben.

VOLZ (1899, 1909) based his views of a post-eruption age of the Toba graben on the consideration that otherwise the graben would have been filled up completely with ejected tuffs. A detailed knowledge of the Katmaian type of eruption is necessary to account for the limited deposition of tuffs in the graben. It is suggested by the author that the – comparatively small amounts of – tuffs occurring on the bottom of each of the three "volcano-tectonic" depressions described in this paper, were deposited during the less violent phases of eruption, whereas the tuffs were deposited in the higher lying surroundings during the paroxysmal parts of the eruption.

A study of the pre-existing relief alone is not sufficient to estimate the influence of volcano-tectonics in the Toba area. The crustal movements which occurred posterior to the eruption also should be considered. Such young tectonic movements are rather important, as appears from the author's observations, and thus even less space is left for the assumed volcano-tectonic events at the end of the eruption period(s).

The Toba graben is a complex feature. A few faults of secondary importance and splinters occur along the western lake shore. The most striking features, however, are the south westerly tilted Samosir block and the Sibulangit (Uhuan) block, which are separated from each other by the Latung Strait. The fault-scarp bordering the Sibulangit block to the west can be traced in a southerly and south-westerly direction across the Porsea Bay and to the west of Balige. The Porsea Bay itself, in the author's opinion, is to be considered as a drowned part of the original Asahan valley.

RUTTNER (1935) reported the occurrence of lacustrine (diatom) deposits on the island of Samosir as high as 1,360 metres above sea-level and – as

he leaves young tectonic movements out of consideration – he claims that the lake formerly had a level about 500 metres higher than nowadays and that it was drained southward by the Batang Toru river. The 1,400 m contour does not close around Lake Toba, a fact which led to RUTTNER's assumption of a regional tilt. WESTERVELD (1947), who shares RUTTNER's opinion about the 1,400 metres lake level, tries to overcome part of the difficulty by supposing a considerable retrogressive erosion in the tuffs. However, this is geomorphologically not justified, as only narrow gorges are formed in the tuffs which cannot account for the broad gaps in the 1,400 m contour. A former southerly drainage of the lake seems to be out of the question, after a thorough field study of the author. No dry river valley/gorge can be traced there.

VAN BEMMELEN (1939) certainly is correct in assuming that the highest lake level is indicated by the upper tuff terrace near Porsea. This terrace is at present located at 1,160 metres above sea-level. The author agrees with VAN BEMMELEN that only young tectonic movements can explain the high location of the former lake deposits. V. D. MAREL (1948a.) maintains that the higher lying deposits are formed in small ponds and not in Lake Toba itself. The author in 1955 found an extensive lake deposit in eastern Samosir at not less than 1,600 metres above sea-level, which certainly was not formed in a small pond. The deposit contained, apart from sponge needles, a rather large number of the following diatoms:

Melosira distans (Ehr.) Kütz var. robusta Manguin
Melosira granulata (Ehr.) Ralfs var. valida Hustedt
Cyclotella stelligera Cl. & Grun.

This combination points to a littoral-pelagic freshwater deposit, f.i. along the shores of a large lake [1]). The author is thus inclined to reject V. D. MAREL's hypothesis, which opinion is further strengthened by a study of the lake terraces.

The Toba lake terraces are mentioned by several authors, but they are never studied in detail. The terraces are not preserved everywhere around the lake because the surf action in the lake was not vigourous enough to form terraces where hard rocks occur, and furthermore because slumping – a common phenomenon in the diatom deposits – destroyed the terraces in other localities. Recent emergence due to young tectonic movements is another possible cause for the scarcity of terrace remnants (Samosir f.i.). The best preserved terraces occur in the extensive tuff deposits in the south eastern part of the graben. These were investigated by the author. The study of the Toba terraces is complicated by the frequent occurrence of sub-horizontal rocks, where structural (pseudo) terraces are formed,

---

1) Determination by A. v. d. WERFF, bio-geologist, Geological Survey, Haarlem, The Netherlands on the request of Prof. Dr. J. WESTERVELD, Amsterdam. The author is greatly in debt for their kind cooperation.

which are without any significance for our purpose. Many older observations therefore had to be rejected, as being incorrect.

Two main terrace levels were distinguished. The highest one is represented by the 1,160 metres level at the entrance of the Asahan valley near Porsea. This tuff terrace corresponds with the upper level of the tuff terraces found along this river (p. 10). This terrace (I) was observed almost uninterrupted along the eastern fault-scarp to the south of Prapat and some scattered remains were found along the southern side of the graben to the east of Balige. It is also developed on the Sibulangit peninsula, where only a few small areas emerge from it, representing former islands. A second important terrace (II) is best developed along the road Prapat-Porsea, between the remnants of terrace I on the peninsula and along the eastern fault-scarp. Its height, near Porsea, is 1,050 metres. The strong tilt of these terraces can easily be seen in the field, even with the naked eye. Important post-eruption tectonic movements, resulting in terrace warping, occurred between Prapat and Porsea, as indicated in fig. 6. The height of the 1,160 m terrace varies from 1,070 to 1,420 metres. It is possible that this terrace —and thus the maximum lake level— was originally about 1,050 metres above sea-level and that the Porsea section was afterward uplifted some 110 metres (p. 438), thus forcing the Asahan river to increased vertical erosion. The uparching demonstrated by the terraces evidently occurred after the eruption and thus can not be explained by a "tumor-hypothesis" (except one connected to a future eruption). Small remnants of a number of lower terraces also occur, which have their counterpart in the multicycle alluvial fans formed in the lower parts of the tuff deposits.

It is important to note that the Toba lake terraces can be correlated to structural terraces formed in the Toba tuffs/ignimbrites along the

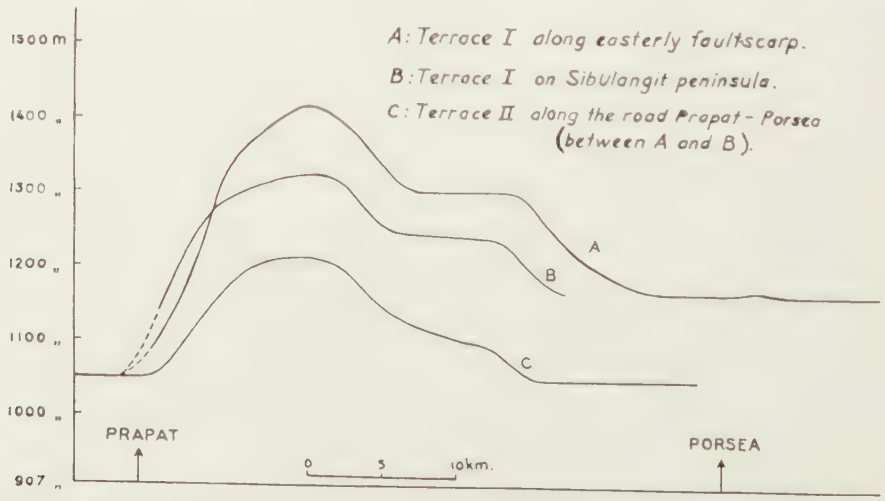

Fig. 6. Warped lake terraces along the eastern shore of lake Toba between Prapat and Porsea.

Asahan valley. The intermittent lowering of the lake level is readily explained by the different rate of incision of the Asahan river in the various subsequent volcanic strata. Every hard bed in the valley corresponds with a lake terrace. Two more lake terraces will be formed when the Siguragura (Wilhelmina) and Tangga falls of the Asahan river, which are both due to resistant beds. will have reached the lake as a result of retrogressive erosion. The stratification of these older Toba products points to the fact that a number of eruptions have occurred instead of the one or two (v. d. Marel) assumed so far.

The important post-eruption tectonic events on and near the Sibulangit peninsula make it likely that the nearby island of Samosir witnessed a similar development. No terraces can be traced there, however. This can only in part be due to destruction of such terraces by the slumping phenomena in the diatom deposits. The author is inclined to assume that the island was almost completely submerged after the eruption and only emerged afterward. The fault/flexure bordering Samosir in the east, the general westward tilt of even the youngest deposits and the diatom deposit at 1,600 metres altitude, point in the same direction.

The northern part of Lake Toba was probably rather stable after the eruption, as no terrace warping was observed there. The young crustal movements evidently centre in the Sibulangit peninsula and on Samosir. Extremely young faults were observed by the author in the north-western part of Samosir. This area may, at present, well be the most unstable part of the Toba graben.

The above considerations lead to the conclusion that the development of the Toba graben is basically tectonic and is spread over a considerable period. It is accompanied by occasional violent volcanic outbursts. It does not appear to be justified to attribute the depression or cauldron to volcano-tectonic processes in the sense of van Bemmelen's "emptying-out-and-breaking down" hypothesis.

5. *Summary*

The three "volcano-tectonic" lakes studied, viz. the Lakes Kerintji, Singkarak and Toba, are evidently formed in a pre-existing graben structure. The longitudinal graben of the Barisan Mountains is more or less like a guirlande, with "volcano-tectonic depressions" formed mostly in the lowest and broadest parts. The latter is probably due to the fact that the faults there also are best developed and reach the greatest depth. Thus they have a better chance to reach a near-surface batholith, if such a batholith is present underneath the area concerned. No "volcano-tectonic uparching" prior to the eruption, was observed, but in the case of Lake Toba important young tectonic movements could be proved.

The view here expressed is just the opposite of van Bemmelen's "emptying-out-and-caving-in" hypothesis on the origin of such depressions according to which the cauldrons are formed as a result of and thus after

a volcanic eruption, occurring preferably in a culmination or "tumor" of the mountains. The term "volcano-tectonic depression" should be abandoned according to the author, or its definition should be altered into "tectonic depression with occasional volcanic activity along faults".

6. REFERENCES

Bemmelen, R. W. van, On the origin of lake Toba (N. Sumatra) Proceedings 4th Pacific Sci. Congress IIa, 115–126 (1929a).

———, Het caldera probleem. De Mijningenieur, **10**, 101–112 (1929b).

———, Toelichting bij blad 6 (Kroë). Geologische kaart van Sumatra 1:200.000. Dienst v. d. Mijnbouw Ned. Ind. (1933).

———, Vulkano-tektonische depressies op Sumatra. 25e Ned. Natuurw. en Geneesk. Congres, Leiden, (1935).

———, The volcano-tectonic origin of lake Toba (Northern Sumatra). De Ingenieur in Ned. Ind., **6**, 126–140 (1939).

———, The Geology of Indonesia, 2 Vols. (1949).

Collings, H. D., Pleistocene site in the Malay peninsula. Nature, **142**, 575–576 (1938).

Cotton, C. A., Volcanoes as landscape forms. 2nd edition (1952).

Escher, B. G., On the formation of calderas. Proceedings IVth, Pacific Sci. Congress, IIb, 571–589 (1929).

Erb, J., Beiträge zur Geologie und Morphologie der südlichen Westküste von Sumatra. Ztschr. d. Ges. f. Erdkunde, Berlin, 251–281 (1905).

Frijling, H., Geologisch-mijnbouwkundig onderzoek in de omtrek van de Asahanen Koeala-rivieren (Toba landen, Oost Sumatra). Jrb. Mijnw. Ned. Ind. Verh. II, 153 (1925).

Klein, W. C., De oostoever van het Toba-meer in Noord-Sumatra. Jrb. Mijnw. Ned. Ind., **46**, Verh. I, 136–187 (1917).

Marel, H. W. v. d., Diatomeenaarde afzettingen in de omgeving van het Tobameer. De Ingenieur in Ned. Ind., **59**, Afd. Mijnb., 58–63 (1947).

———, Het Tobameer. Geol. en Mijnb., **10**, 80–89 (1948a).

———, Volcanic glass, allanite and zircon as characteristic minerals of the Toba rhyolite tuff at Sumatra's East Coast. J. of Sed. Petr., **18**, 24–29 (1948b).

Marshall, P., Acid rocks of the Taupo-Rotorua volcanic district. Trans. Royal Soc. of Nw. Zealand, **64**, 323–366 (1935).

Ruttner, F., Hydrographische und hydrochemische Beobachtungen auf Java, Sumatra und Bali. Archiv. f. Hydrobiologie, VIII, Tropische Binnengewässer, 197–454 (1931).

———, Seenstudien in Niederl. Indiën. Mitt. Geogr. Ges. Wien, **75**, 114–146 (1932).

———, Kieselgur und andere lakustrische Sedimente im Tobagebiet; Ein Beitrag zur Geschichte des Tobasees in Nordsumatra. Archiv. f. Hydrobiologie, XIII (Suppl.) Tropische Binnengewässer, V, 399–461 (1935).

Stehn, Ch. E., Die semivulkanischen Explosionen des Pematang Bata in der Socoh-Senke (Süd Sumatra) im Jahre 1933. Nat. Tijdschr. Ned. Ind., **94**, 46–69 (1934).

———, De nieuwe dieptekaart van het Tobameer (Noord Sumatra) van Drost en Beckering. De Ingenieur in Ned. Ind., 6, section IV, 121–126 (1939).

Valkenburg, S. van, Geomorphologische beschouwingen over de Padangse bovenlanden. Jaarverslag Top. Dienst, 76–103 (1921).

Verbeek, R. D. M., Nota over het ontstaan van het Tobameer. Tijdschr. Ind. T. L. en V. kunde, XXXI, 383–384 (1886).

Verstappen, H. Th., Geomorphic notes on Kerintji (Central Sumatra). Madjalah Ilmu Alam u. Indonesia (Indon. J. Nat. Sci., **11**, 166–177 (1955).

Volz, W., Beiträge zur geologischen Kenntniss von Nord Sumatra. Ztschr. D. Geol. Ges., **50**, 1–61 (1899).

————, Zur Geologie von Sumatra; Nord-Sumatra, Bd. I, Die Batakländer (1909).

Westerveld, J., On the origin of the acid volcanic rocks around lake Toba, North Sumatra. Verh. Kon. Ned. Akad. v. Wetensch., Afd. Natuurk., IIe sectie., **43**, 1–51 (1947).

————, Eruptions of acid pumice tuffs and related phenomena along the great Sumatran fault through system. Proceedings VIIth. Pacific Sci. Congr., II, 411–438 (1953).

Wing Easton, N., Een geologische verkenning in de Tobalanden. Jrb. Mijnwezen Ned. Ind., Wetensch. Ged., 99–164 (1894).

————, Der Tobasee, ein Beitrag zur Geologie von Nord Sumatra. Ztschr. d. D. Geol. Ges., 435–467 (1896).

CONTENTS

Geology

KUENEN, PH. H. and W. G. PERDOK: Frosting of quartz grains, p. 343.

VERSTAPPEN, H. TH.: Some "volcano-tectonic" depressions of Sumatra, their origin and mode of development. (Communicated by Prof. F. A. VENING MEINESZ), p. 428.

WAARD, D. DE: Tectonics of a metagabbro laccolith in the Adirondack Mts., and its significance in determining top and bottom of a metamorphic series, p. 335.

Mechanics

ALBLAS, J. B.: On the diffraction of sound waves in a heat-conducting viscous medium. (Communicated by Prof. C. J. BOUWKAMP), p. 351.

Paleontology

DROOGER, C. W.: Miogypsina in Hungary. (Communicated by Prof. G. H. R. VON KOENIGSWALD), p. 417.

Physics

OFFERHAUS, M. J.: Theory of transport and relaxation phenomena in a gas mixture. I. (Communicated by Prof. J. DE BOER), p. 368.

OFFERHAUS, M. J.: Theory of transport and relaxation phenomena in a gas mixture. II. (Communicated by Prof. J. DE BOER), p. 381.

OFFERHAUS, M. J.: Theory of transport and relaxation phenomena in a gas mixture. III. (Communicated by Prof. J. DE BOER), p. 392.

VERINGA, F.: On the mechanisms underlying de Lange's results. (Communicated by Prof. G. W. RATHENAU), p. 413.

Physical Chemistry

LANGE, R. G. DE and W. G. BURGERS: Stress release in plastically deformed silverchloride by annealing, p. 346.

PRINTED IN THE NETHERLANDS
DRUKKERIJ HOLLAND N.V., AMSTERDAM